

Sex-specific Computational Models of Blood Pressure Regulation

by

Jessica Leete

Graduate Program in Computational Biology and Bioinformatics
Duke University

Date: _____

Approved:

Anita T. Layton, Advisor

Susan B. Gurley

Timothy E. Reddy

Dennis O. Frank-Ito

Dissertation submitted in partial fulfillment of the
requirements for the degree of Doctor of Philosophy
in the Graduate Program in Computational Biology and Bioinformatics
in the Graduate School of
Duke University

2020

ABSTRACT

Sex-specific Computational Models of Blood Pressure
Regulation

by

Jessica Leete

Graduate Program in Computational Biology and Bioinformatics
Duke University

Date: _____

Approved:

Anita T. Layton, Advisor

Susan B. Gurley

Timothy E. Reddy

Dennis O. Frank-Ito

An abstract of a dissertation submitted in partial fulfillment of the
requirements for the degree of Doctor of Philosophy
in the Graduate Program in Computational Biology and Bioinformatics
in the Graduate School of
Duke University

2020

Copyright by
Jessica Leete
2020

Abstract

Hypertension is a global health challenge: it affects one billion people worldwide and is estimated to account for >60% of all cases or types of cardiovascular disease. Due to our partial understanding of sex differences in blood pressure regulation mechanisms, fewer hypertensive women achieve blood pressure control compared to men, even though compliance and treatment rates are generally higher in women. Furthermore, concurrent use of typical antihypertensive treatments such as a diuretic, a renin-angiotensin system (RAS) inhibitor, and a non-steroidal anti-inflammatory drug (NSAID) significantly increases the risk of acute kidney injury (AKI). This phenomenon is known as “triple whammy” AKI. Diuretics and RAS inhibitors are often prescribed in tandem for the treatment of hypertension, whereas some NSAIDs, such as ibuprofen, are available over the counter. As such, concurrent treatment with all three drugs is common.

Thus, the objective of this study is to identify which factors contribute to the sexual dimorphism in response to antihypertensive therapies targeting the RAS. We also aim to better understand the mechanisms underlying the development of triple whammy AKI and to identify physiological factors that may increase an individual’s susceptibility.

To accomplish these goals, we develop sex-specific models of blood pressure regulation in humans. Model components include variables describing the heart and circulation, kidney function, sodium and water reabsorption in the nephron, and the RAS. Sex differences in the RAS, baseline aldosterone level, and the reactivity of renal sympathetic nervous activity (RSNA) are represented.

Model results suggest that the main source of sexual dimorphism in treatment efficacy is how the effects of the bound RAS receptors differ between males and fe-

males – specifically the feedback mechanisms of the angiotensin II type 1 receptor on renin secretion and the effects of the angiotensin II type two receptor on renal resistance. In regards to triple whammy AKI, model simulations suggest that individual variations in water intake or the myogenic response as well as high dosages of these drugs may predispose patients with hypertension to develop triple whammy AKI.

These proposed models hold great potential for extensions to study other components of blood pressure regulation, such as the interconnectedness of K^+ regulation and Na^+ regulation. We present a model of K^+ regulation including the aldosterone and renal function feedback controls, as well as the feedforward control stimulated by dietary K^+ intake. Model results suggest that the feedforward effect is necessary for increased urinary K^+ excretion during digestion and that muscle-kidney cross talk can accelerate recovery following perturbations in extracellular K^+ concentration.

For Owen, my support and inspiration.

Contents

Abstract	iv
List of Figures	xi
List of Tables	xiii
List of Abbreviations	xiv
Acknowledgements	xvi
1 Introduction	1
1.1 Regulators of blood pressure	1
1.2 History of computational models	7
2 Sex Differences in the Rat Renin-Angiotensin System	12
2.1 Introduction	12
2.2 Methods	16
2.2.1 Model equations	16
2.2.2 Model parameters	18
2.3 Model results	21
2.3.1 Parameter identification	21
2.3.2 Parameter sensitivity study	22
2.3.3 ACE inhibitors	29
2.3.4 Angiotensin receptor blockers	32
2.3.5 Effect of feedback	33
2.4 Discussion	34
3 Sex-specific Long-term Blood Pressure Regulation: Modeling and Analysis	40

3.1	Introduction	40
3.2	Materials and methods	42
3.2.1	Blood pressure regulation model	42
3.2.2	Renin-angiotensin system model	44
3.2.3	Effects of RAS on blood pressure	46
3.2.4	Sex-specific parameters	49
3.3	Results	51
3.3.1	Responses to angiotensin infusion	51
3.3.2	Responses to various hypertensive stimuli	53
3.3.3	Explaining sex differences in response to hypertensive stimulus	55
3.3.4	Hypertensive drug treatments	57
3.4	Discussion	59
4	Triple Whammy AKI	64
4.1	Introduction	64
4.2	Methods	66
4.2.1	Water and sodium intake	66
4.2.2	Renal tubular water reabsorption and urine flow	68
4.2.3	Blood volume	69
4.2.4	Macula densa feedback	69
4.2.5	Simulating administration of ACEI	71
4.2.6	Simulating administration of furosemide	71
4.2.7	Simulating administration of NSAIDs	72
4.2.8	Simulating impaired autoregulation	73
4.3	Results	74

4.3.1	Response to hypertensive stimuli	74
4.3.2	Response to drug treatments	75
4.3.3	Risk factors for AKI	77
4.4	Discussion	80
5	Potassium Homeostasis	87
5.1	Introduction	87
5.1.1	Overview of K^+ regulation	87
5.2	Methods	91
5.2.1	Internal K^+ balance	91
5.2.2	Kidney function	94
5.2.3	Aldosterone	98
5.3	Results	101
5.3.1	Acute response to K^+ intake	101
5.3.2	Response to K^+ loading	101
5.3.3	Response to K^+ depletion	104
5.4	Discussion	105
6	Conclusion	110
6.1	Future directions	112
A	Determining Sex-specific Human RAS Parameters	113
B	Full Model Equations	115
B.1	Renal hemodynamics	115
B.2	Sodium	117
B.3	Water	121

B.4	The cardiovascular system	122
B.5	Feedback systems	125
B.6	Renin-angiotensin system model	127
	Bibliography	136
	Biography	160

List of Figures

1.1	Schematic diagram depicting the renin-angiotensin system reaction cascade with sex differences	4
2.1	Schematic diagram depicting the RAS reaction cascade.	13
2.2	ACEI and ARB treatment results	30
2.3	Effect of feedback on ACEI and ARB treatment	35
3.1	Schematic diagram of blood pressure regulation	43
3.2	Schematic diagram of the renin-angiotensin system	44
3.3	Predicted percent change from control due to Ang I and Ang II infusion.	52
3.4	Change in selected variables from various causes of hypertension	54
3.5	Predicted blood pressure in baseline male and female and three instances of male model with one trait set to female value	56
3.6	Change in MAP following ACEI and ARB administration on hypertensive models	58
4.1	Flowchart of the blood pressure regulation model.	67
4.2	Effects of furosemide and NSAIDs on renal blood flow and renin secretion.	70
4.3	The myogenic response	74
4.4	Effect of drug treatments on renal and cardiovascular function	76
4.5	Effect of drug combinations on renal and cardiovascular function of the male and female hypertensive models under aggravating conditions	79
5.1	Flowchart depicting K^+ homeostasis model	92
5.2	Variable values before and while digesting a 35mEq K^+ meal	102

5.3	Model response to K^+ loading with muscle-kidney cross talk	104
5.4	Model response to K^+ depletion with muscle-kidney cross talk	106

List of Tables

2.1	Rat RAS hormone levels and enzymatic activity	21
2.2	Calculated kinetic parameters for four cohorts of rats	22
2.3	Parameter sensitivity analysis for male normotensive rat	24
2.4	Parameter sensitivity analysis for female normotensive rat	25
2.5	Parameter sensitivity analysis for male hypertensive rat	26
2.6	Parameter sensitivity analysis for female hypertensive rat	27
3.1	Human RAS hormone levels.	49
3.2	Reaction rate constants for male and female normotensive humans . .	50
5.1	Parameter values for K^+ model equations	99
5.2	Variable values for K^+ model equations at steady state	99
A.1	Sex-specific RAS reaction rate constant ratios.	114
B.1	Parameter values for model equations	130
B.2	Variable values at steady state	132

List of Abbreviations

ACE	angiotensin converting enzyme
ACEI	angiotensin converting enzyme inhibitor
ADH	antidiuretic hormone
AGT	angiotensinogen
AKI	acute kidney injury
ALD	aldosterone
Ang I	angiotensin I
Ang II	angiotensin II
Ang (1-7)	angiotensin (1-7)
Ang IV	angiotensin IV
ANP	atrial natriuretic peptide
ARB	angiotensin receptor blocker
AT1R - bound Ang II	angiotensin type 1 receptor bound angiotensin II
AT2R - bound Ang II	angiotensin type 2 receptor bound angiotensin II
DRI	direct renin inhibitor
GFR	glomerular filtration rate
K ⁺	potassium
MAP	mean arterial pressure
Na ⁺	sodium
NEP	neutral endopeptidase
NSAID	nonsteroidal anti-inflammatory drugs
PRA	plasma renin activity
PRC	plasma renin concentration
RAS	renin-angiotensin system

RSNA	renal sympathetic nervous activity
SHR	spontaneously hypertensive rats
SNGFR	single nephron glomerular filtration rate

Acknowledgements

There are many people without whom this dissertation would not have been possible. First, I would like to thank my advisor, Anita T. Layton, for her guidance, teachings, and support. I have learned so much from her.

Next, I would like to thank my committee members, Susan Gurley, Tim Reddy, and Dennis Frank-Ito, who have guided me through this project, provided insights, and challenged me to dig deeper and be more exact in my methods.

I would like to thank the co-authors on my papers, specifically Susan Gurley for contributing her knowledge of the renin-angiotensin system and feedback on chapter 2 and Francisco J. López-Hernández for contributing his insight into triple whammy AKI and feedback on chapter 4.

I would like to thank Sameed Ahmed for working with me to prepare the code for chapter 4 for publication and working to make it applicable to rats as well as humans.

Finally, I would like to thank my parents, Ann and Brian Leete, for their support throughout my education. And to my husband, Owen Leete, for his unvarying support, encouragement, and belief in me.

Chapter 1

Introduction

¹Cardiovascular disease is the number one cause of death in American adults [163] and is the number one risk factor for global disease [12]. Hypertension is the single largest risk factor for cardiovascular mortality and effected an estimated 116.4 million American adults over 20 years of age in 2013–2016 [12] and an estimated 1.39 billion adults worldwide in 2010 [12]. The elimination of hypertension could reduce cardiovascular disease mortality by 30.4% among males and 38.0% among females [12]. Cardiovascular disease effects both men and women; however, there are substantial sex differences in its progression, severity, and treatment success.

Sex differences in prevalence and severity of hypertension have been reported in a number of mammalian and avian species [201]. In both spontaneously hypertensive rats (SHR) and Dahl salt-sensitive rats [171], males develop earlier and more severe hypertension than females. Women tend to have lower rates of hypertension than men before menopause, but higher after menopause [83, 197, 12]. Men are at higher risk for cardiovascular and renal diseases [115, 240]. In general, death rates attributable to high blood pressure is higher for males than females [12].

1.1 Regulators of blood pressure

Hypertension is a multifactorial disease, with causes including arterial stiffening, impaired renal sodium (Na^+) handling, stimulation of the renal sympathetic nervous

¹Parts of this introduction were previously published in [3].

system, and stimulation of the renin-angiotensin system (RAS). Many of these systems interact with each other, meaning that identifying a single cause of hypertension is difficult or impossible. This also leads to multiple targets for treating hypertension. The interactions between these three main components – the kidney, the RAS, and renal sympathetic nervous activity (RSNA) – as well as sex differences and treatments targeting these are described in this section.

The kidney. The kidney is a collection of nephrons, each beginning with a glomerulus where blood is filtered. Large proteins, such as hemoglobin are kept within the body, while water and solutes such as Na^+ and potassium flow into the lumen. The afferent and efferent arterioles bring blood to and away from the glomerulus, respectively, and control the glomerular filtration rate (GFR) through changing diameter to restrict blood flow and control pressure within the glomerulus. If the pressure is too high, indicated by an high GFR, it may damage the delicate capillaries of the glomerulus, rendering the filter unusable. Too low GFR, and cells may not get the blood flow they need to survive. As the luminal fluid leaves the glomerulus and passes through the nephron, solutes and water are reabsorbed or secreted according to the needs of the body. Finally, the concentrated urine then exits to the bladder. By controlling what is reabsorbed versus secreted, the kidney effects blood volume and thus blood pressure.

Kidney function is a key determinant of blood pressure [236]. This is evident through transplantation studies, where hypertension “goes with” the kidney; transplanting a kidney from a hypertensive rat into a normotensive rat causes hypertension in the recipient [13]. The main regulator of blood pressure is the pressure-natriuresis effect, whereby increases in renal perfusion pressure cause greater amounts of Na^+ to be excreted through the urine [162]. This also causes a greater excretion of water,

lowering blood volume and thus blood pressure.

While essential for blood pressure control in both sexes, the pressure-natriuresis curve is shifted leftward in females, meaning that the same renal perfusion pressure leads to higher levels of Na^+ excretion [87, 110]. Females tend to also have smaller kidneys, in rats females can have kidneys half the size of males [144, 198]. In humans, men's kidneys weigh 23% more than women's [182]. The main measure of kidney function, GFR, differs in males versus females. In rats, single nephron GFR is lower in females [164, 192]. In humans, women have lower total GFR, but whether differences in GFR lead to overall differences in urine flow is undetermined. When adjusted for body size, both female rats and humans have similar urinary output to their male counterparts [148, 198]. How mammals have sex differences in size and GFR without differing in body size adjusted urinary output may indicate that other sex difference may pick up the slack. Transporter abundance varies along the nephron [234] and may be why urinary output can be similar while size and GFR differs.

Antihypertensive therapies targeting the kidney include diuretics, which seek to reduce blood volume through increasing urine flow. In this dissertation, we focus on furosemide, a loop diuretic, which inhibits NKCC2 transporters in the thick ascending limb of the Loop of Henle [47, 165], thus decreasing Na^+ reabsorption. The changed osmotic gradient then decreases water reabsorption, leading to increased urine flow.

The RAS. The RAS controls blood pressure through adjusting GFR as well as Na^+ and water reabsorption in the nephrons, thus controlling urine flow and blood volume. Angiotensinogen (AGT) is produced in the liver and proximal tubules of the kidney and circulates throughout the body where it is cleaved by renin, produced in the juxtaglomerular apparatus, to produce angiotensin I (Ang I). As Ang I circulates through the body, it is cleaved into many other forms of angiotensin, including Ang

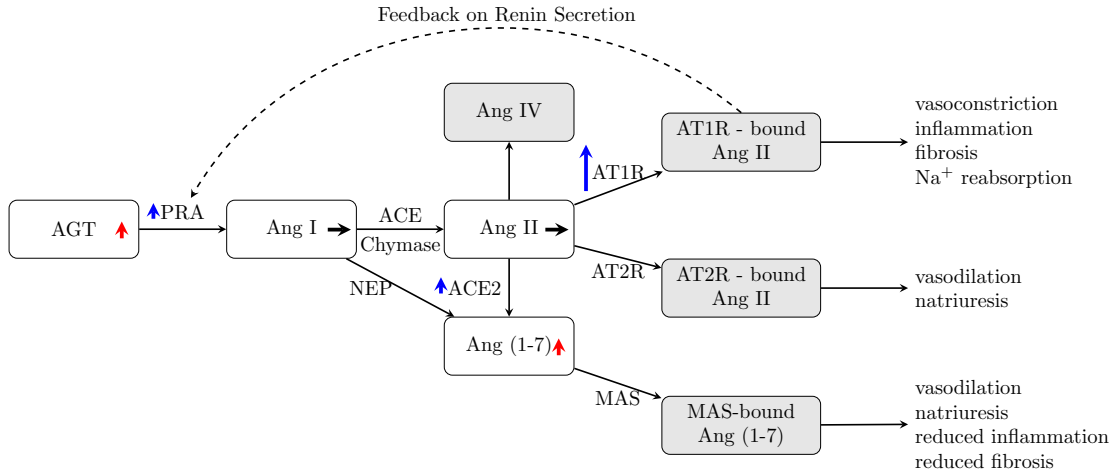


Figure 1.1: Schematic diagram depicting the renin-angiotensin system reaction cascade. Blue and red arrows indicate higher abundance in males and females, respectively. Size of arrows roughly corresponds to abundance ratio between the two sexes, based on human and rat studies [36, 176, 194, 205, 210]. Gray nodes indicate a lack of sex-specific data. Published in [3].

II, Ang IV, and Ang (1-7), each of which have their own effects on the body. A flowchart of the RAS, including sex differences indicated by arrows can be found in Fig. 1.1.

The most well studied pathway is where Ang I is cleaved by either angiotensin converting enzyme (ACE) or chymase into Ang II, which then binds to the angiotensin type 1 receptor (AT1R). AT1R-bound Ang II stimulates Na^+ reabsorption by increasing aldosterone secretion. AT1R-bound Ang II also stimulates renal vasoconstriction, inflammation, and fibrosis [24]. All of these contribute to raising blood pressure.

However, Ang II can also bind to the angiotensin type 2 receptor (AT2R), which causes vasodilation and natriuresis to lower blood pressure [24]. A third pathway in the RAS is through Ang (1-7), produced from neutral endopeptidase (NEP) activity on Ang I or ACE2 activity on Ang II. Ang (1-7) can bind to the MAS receptor, causing vasodilation, natriuresis, reduced inflammation, and reduced fibrosis [24, 25]. Other forms of angiotensin are known, but here we focus on those most well studied.

²Sex differences in the circulating and intrarenal concentrations of the various forms of angiotensin and of the receptors are becoming increasingly well studied [56, 89, 243]. Here, we focus on a few key differences. Sex hormones influence many parts of the RAS. Generally, in males, the ACE/ANG II/AT1R pathways are enhanced, whereas in females, the balance is shifted toward the ACE2/ANG (1-7)/MAS receptor and AT2R pathways. In humans, estrogen causes females to have greater levels of circulating AGT [56], while also decreasing circulating renin [205], ACE [61], AT1R density, and aldosterone production [115]. In rats, estrogen has been found to increase renal AT2R expression and to decrease renal AT1R synthesis [9, 157, 172, 205]. On the other hand, in rats, testosterone increases renal AGT, AT1R, and renin expression [31, 51, 100, 105]. These effects of sex hormones likely lead to the greater AT1R:AT2R ratio found in male rats [16, 201, 243]. Male rats also have greater ACE2 activity, while female rats have higher levels of ANG (1-7) [176].

The sex differences in the RAS are not limited to peptide concentrations, as there are also differences in how the body reacts to changes within the RAS. Changes in ANG II level produce significantly smaller changes in blood pressure in female rats than in male rats [56, 201], and ANG II infusion reduces renal perfusion significantly more in women than in men [62]. The latter may be attributable to the fact that during ANG II infusion, GFR is maintained in men, while it drops in women [155].

The RAS is a common target for antihypertensive therapies. Direct renin inhibitors (DRI) block renin, stopping the enzymatic cascade at the earliest opportunity. Angiotensin converting enzyme inhibitors (ACEI) block the conversion of Ang I into Ang II by ACE. Angiotensin receptor blockers (ARB) are AT1R antagonists and stop the binding of Ang II to AT1R. The goal of all of these drugs is to reduce

²The following two paragraphs have been published in [3].

the amount of AT1R-bound Ang II, thereby stopping its blood pressure increasing effects. However, their effects on the other arms of the RAS, such as AT2R-bound Ang II and the bound MAS receptor differ and are not as well studied.

Interaction between the kidney and the RAS is two-way, with signalling from the kidney controlling upstream components of the RAS, and downstream components of the RAS adjusting GFR as well as Na⁺ and water reabsorption in the nephrons. Signalling from the kidney to the RAS occurs at the juxtaglomerular apparatus, which is responsible for controlling GFR. Low GFR triggers a release of AGT and renin, increasing RAS activity and blood pressure to drive more blood to the kidney. High GFR has the opposite effect.

RSNA. The RAS is not the only regulator of kidney function. RSNA stimulates contraction of the afferent arteriole and renin secretion, lowering GFR and urine flow both directly and through RAS activity. In females, RSNA is less easily excitable and more easily repressed [90]. Renal denervation is a tool for fighting hypertension, where the nerves responsible for contracting the afferent arteriole are blocked, resulting in higher GFR and urine flow.

Despite these sex differences in the systems controlling blood pressure, men and women are treated identically when it comes to blood pressure control, leading to fewer women (45%) achieving blood pressure control compared to men (51%), even though compliance and treatment rates are higher in women [72]. Even drugs that target similar pathways in the RAS, such as ACEI and ARB, can have substantially different success rates in treating men and women. Women have been found to have better survival rates when taking ARBs rather than ACEIs [94], while ACEIs reduce blood pressure more in male SHR than in female SHR [190]. Understanding the

mechanisms whereby physiological sex differences cause differences in drug treatment efficacy is key to developing and prescribing proper treatment for individuals.

1.2 History of computational models

To investigate how physiological sex differences translate into differences in drug treatment efficacy, we use computational models to describe the systems that control blood pressure. Models describing both the RAS and blood pressure separately and together have been previously designed and used (see below). Here we describe some of the major contributions to the field.

RAS models. A number of computational models of the RAS have been published (see below). However, to our knowledge, none of these have been sex specific, and many only focus on the ACE/ANG II/AT1R pathway. ³Takahashi et al. [219] modeled this ACE/ANG II/AT1R pathway along with bradykinin's interactions with ACE and blood pressure. Their goal was to understand how ACE inhibitors can lower blood pressure, even when genetic variation in ACE and AGT expression does not substantially change blood pressure. They included blood pressure as an explicit variable, while other models below only used upstream ANG II levels as an indicator of drug treatment efficacy. With their model they were able to find that small changes in ACE and AGT, such as those caused by genetic differences, can be offset by bradykinin levels, so that ANG II levels stay the same. However, with ACE inhibition, the system deviates sufficiently far from baseline, such that bradykinin can no longer offset the drastic reduction in ANG I. As a result, ANG II levels, and thus blood pressure, are reduced.

³The following four paragraphs have been published in [3].

To compare ACEI with DRI, Hong et al. [91] developed a pharmacodynamic model for renin, ANG I, and ANG II, together with a pharmacokinetic component describing the effects of aliskiren, a DRI. They found that aliskiren was best described with a two-compartment model with nonlinear capacity-limited distribution and elimination kinetics. Their model was able to show the greater increase in active renin from aliskiren treatment as compared with ACEI or ARB. They also discovered that there is a limit to the amount of RAS blockade available from increasing doses of aliskiren. They presented a reduced model that does not rely on ANG II measurements, which can be difficult to attain.

Ramusovic and Laeer [189] also modeled this ACE/ANG II/AT1R axis to compare and contrast the effects of a single dose of ACEI, ARB, and DRI. Even without the inclusion of circadian rhythm parameters as used in Hong et al. [91], Ramusovic and Laeer were able to achieve a sufficiently good fit for the plasma ANG I and ANG II levels following aliskiren treatment. Notably, model responses were matched to a range of dosages rather than just a single dosage.

Lo et al. [141] developed a more comprehensive model of the RAS containing AGT, ANG I, ANG II, ANG (1–7), ANG IV, AT1R, and AT2R. They validated the model using angiotensin infusion experiments and compared the effects of ACEI, ARB, and DRI. They extended their model to include not only the circulating plasma hormone concentrations, but intrarenal RAS as well. Using this more complete and detailed model of the RAS, they were able to measure the effects of drug treatments by monitoring AT1R-bound ANG II levels, which is the actual effector of changes in the body, rather than plasma renin activity (PRA), which is the quantity commonly measured in clinical experiments. Although these models provide insight for understanding the RAS and guiding RAS-targeted antihypertensive therapy, none of them capture sex differences in the RAS or in men and women’s differing response to RAS

inhibitors.

Blood pressure regulation models. In 1972, Guyton and Coleman pioneered the field of computational models of physiological systems with their seminal circulation model [78]. Their model has components that describe cardiovascular function, circulatory dynamics, renal hemodynamics, kidney function, respiratory function, neurohormonal feedback, autonomic nervous system activity, and electrolyte balance. Their simulation results indicate that kidney function was of paramount importance in how the balance of Na^+ and water retention and secretion controls blood volume and thus blood pressure. Over the years the Guyton model has been rigorously studied and validated as it has been extended and built upon to answer a variety of questions.

Thomas et al. [222] adopted the Guyton model and incorporated Ikeda et al.'s [95] representation of body fluid regulation as well as a detailed model of the kidney. Describing these detailed mechanisms of body fluid homeostasis allowed them to model long- and short-term blood pressure regulation. Guillaud and Hannaert [73] then built on Thomas et al.'s model [222] and developed the first blood pressure regulation model that incorporates the RAS. Guillaud and Hannaert chose to include AGT, Ang I, Ang II, and their effects on vascular resistance and ALD. This extension allowed the modelling of hypertensive and cardiovascular renal disease patients, including those caused by salt-sensitivity, polymorphisms, and pharmacotherapeutics.

In 2005, Karaaslaan et al. took the Guyton model in another direction when they adopted some of its major components and added the effect of RSNA on tubular Na^+ reabsorption and renin secretion [103]. They applied the resulting model to study the consequences of long-term RSNA activation and impairment on hypertension [103]. In 2014, Hallow et al. built on their model and contributed a detailed RAS submodel

to more accurately simulate the effects of RAS-targeting antihypertensive therapies [80].

While many agree with the Guyton's conclusion that pressure-natriuresis is the main drive of blood pressure regulation, not all do. Averina et al. [7] proposed that sympathetic nerve activity, not the pressure-natriuresis curve, was the determinant of blood pressure and that the pressure-natriuresis curve could instead be replicated simply from Na^+ intake. This approach led to a model that could investigate causes of hypertension separate from kidney dysfunction.

Beard et al. [11] also diminished the kidneys' role in blood pressure regulation, and put greater importance on the baroreflex arc and the RAS. They focused on developing a model where all data, variables, parameters, and equations are clear to the reader. Their model is useful for gaining insight and building a basic knowledge of the systems involved, even if reproducing certain clinically interesting variables or scenarios is not possible.

Kidney models. A review of computational models of kidney function can be found in Refs. [119, 125, 120, 128, 127, 223].

Our contributions. While the aforementioned models provide valuable insights into the many different facets of blood pressure regulation, none of these models are sex specific, and in many instances are based on data pulled only from male patients or male experimental animals. This dissertation represents the first approach to using sex-specific computational models to understand sex differences in blood pressure regulation.

To investigate sex differences in blood pressure regulation, we begin with the sex-specific computational models of the RAS in rats described in Chapter 2. Rats

show many of the sex differences that are qualitatively similar to humans, and sex-specific data is more abundant in rats. This chapter was previously published in *Computers & Chemical Engineering* [136]. In Chapter 3, we re-parameterize the RAS submodel using human data and incorporate it into a larger circulation model based on the models by Karraaslaan et al. and Hallow et al. [80, 103]. In addition, we incorporate sex differences outside the RAS, such as RSNA and how bound RAS receptors effect the body, to investigate the mechanisms behind sex differences in antihypertensive drug efficacy. This chapter was previously published in *Computers in Biology and Medicine* [137]. In Chapter 4, we expand our model to represent the effects of diuretics and non-steroidal anti-inflammatory drugs (NSAID) to investigate risk factors for “triple whammy” acute kidney injury (AKI), whereby triple treatment with ACEI/ARB, diuretics, and NSAIDs can cause AKI in a significant portion of patients. This chapter has been submitted for publication [138]. In Chapter 5, we present a model of potassium homeostasis, that can be combined with our model of blood pressure regulation to investigate how the ratio of potassium to Na^+ intake affects blood pressure.

Chapter 2

Sex Differences in the Rat Renin-Angiotensin System

2.1 Introduction

¹The renin-angiotensin system (RAS) is an important regulator of blood pressure. The RAS consists of an enzymatic cascade that produces the bioactive peptide angiotensin II (Ang II)[211]. The cascade starts with angiotensinogen (AGT), which is cleaved by renin and later angiotensin converting enzyme (ACE) and neutral endopeptidase (NEP) into different forms of angiotensin (see Fig. 2.1) [211, 24, 25]. The enzyme renin catalyzes the first reaction in the RAS and is often thought as the driving force in the cascade. The products of the RAS are major biologically active products includes angiotensin (1-7) (Ang (1-7)) and Ang II. These bind to receptors and impact the brain, heart, kidney, vasculature, and immune system [211]. Ang II has two different types of receptors. When bound to angiotensin II type 1 receptor (AT1R), Ang II stimulates renal vasoconstriction, raises sodium reabsorption, and promotes inflammation and fibrosis [24]. When bound to angiotensin II type 2 receptor (AT2R), Ang II induces vasodilation and natriuresis. Ang (1-7) binds to the angiotensin type 7 receptor (AT7R), also known as the MAS receptor, to cause vasodilation and natriuresis and increase production of nitric oxide to reduce inflammation and fibrosis [24, 25].

¹This chapter was published as [136]. Susan Gurley contributed insights into the biology and edited the final draft. Anita T. Layton contributed with model and simulation design, edits, and

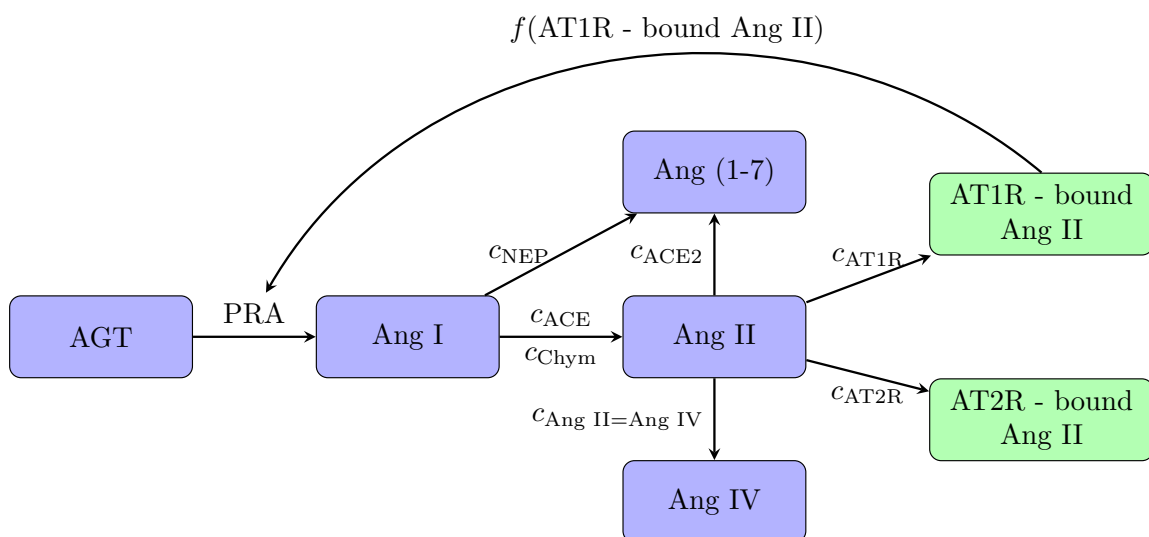


Figure 2.1: Schematic diagram depicting the RAS reaction cascade.

AT1R-bound Ang II regulates overall blood pressure via its effects on the kidney. The kidney is responsible for filtering blood into urine to remove waste from the body. Through the glomerulus, blood is filtered leaving all proteins, such as hemoglobin, behind in the body. Attached to the glomerulus is the nephron, which is the kidney's functional unit and is responsible for reabsorption and secretion. As the filtrate travels through the nephrons, essential solutes and water are reabsorbed or secreted. In particular, the reabsorption of sodium by the nephron is critical for blood pressure regulation [78]. AT1R-bound Ang II regulates blood pressure by increasing sodium and fluid reabsorption in the proximal tubule, which is a key segment of nephron that normally reabsorbs about 2/3 of the filtered salt and water [211].

The relation between the RAS and the kidney is two-way with the kidney influencing the RAS by providing the first two essential components of the RAS: AGT and renin. The proximal tubule, as well as the liver, are the primary places of production for AGT, whereas renin is produced in the juxtaglomerular apparatus, a microscopic

revisions.

structure in the kidney. When blood pressure is low, renal blood flow decreases and kidney function may become impaired. To compensate, the kidney elevates renin production, causing an increase in AT1R-bound Ang II, which raises blood pressure.

Because of its central role in fluid homeostasis, the RAS, in particular ACE and AT1R, are often targeted in hypertensive treatments. Given that AT1R-bound Ang II causes vasoconstriction and higher blood pressure, antihypertensive drug treatments seek to lower the amount of Ang II bound to AT1R. Given also that ACE converts Ang I into Ang II, by lowering the level of ACE activity through ACE inhibitors (ACEI), the total amount of Ang II that is available to bind to AT1R can be reduced. Angiotensin receptor blockers (ARB) are AT1R antagonists that reduce vasoconstriction by preventing the binding of vasoactive peptides (i.e. Ang II).

The RAS is similar in mammals, as are the sex differences. Females have been shown to have lower blood pressure than males in humans, rats, dogs, and birds [201]. Major sex differences in the RAS have been identified, including how much substrate is produced and how angiotensin interacts with receptors. For example, in both rats and humans, females have greater circulating levels of AGT [56], causing an overall greater amount of angiotensin to be flowing through the system. Also, male rats have been shown to have greater Ang II levels [201] while female rats have greater levels of Ang (1-7) [243]. However, a greater level of ACE2 activity (which converts Ang II to Ang (1-7)) has been measured in male rats [243].

Interestingly, males and females exhibit differing responses to Ang II. Changes in Ang II levels produce smaller changes in blood pressure in female rats [56, 201]. That discrepancy may be attributed to differences in receptor expression, inasmuch as male rats have greater AT1R expression and lower AT2R expression than female rats [16, 201, 243]. Estrogen also reduces the half life of AT1R-bound Ang II [224].

Given the above observations, it should come as no surprise that males and females

respond differently to antihypertensive treatments that target the RAS. In one study, women who were prescribed ARBs had better survival rates than women prescribed ACEIs, while the opposite was true in men [215]. Studies have provided evidence that the effectiveness of ACEIs in women decreases over time and offers less benefit to women as determined by total mortality [215]. While these trends have been observed in multiple studies, the underlying mechanisms are not well understood. Thus, the goal of this study is to obtain a better understanding of the RAS of the rat and the functional implications of the sex differences. To achieve that goal, we develop mathematical models of the RAS for four groups of rats: normotensive male, normotensive female, hypertensive male, and hypertensive female rats. The models are formulated using ordinary differential equations based on a published RAS model for normotensive humans, presumably males [141]. Other studies have modeled the RAS within the larger context of the circulatory system, but none of these have looked into how sex differences within the RAS affects the circulatory system and blood pressure [80, 73, 57]. A goal of this study is to identify individual parameter sets that correspond to the different types of rats (normotensive and hypertensive rats, male and female). Our focus on the rat is motivated by its role as one of the most commonly used animal models in experiments and drug trials. Following the successful determination of the model parameters, we apply the models to elucidate the mechanisms by which the known differences between the sexes contribute to the sex-specific responses to antihypertensive therapies. Since the rat and human share many of the known sex differences in the RAS, conclusions from this study should be applicable to humans.

2.2 Methods

2.2.1 Model equations

A schematic diagram that depicts the RAS reaction cascade can be found in Fig. 2.1. As previously discussed, AGT is catalytically cleaved by renin to produce Ang I. The rate of change of $[AGT]$ is given by the production rate k_{AGT} , the conversion to Ang I catalyzed by renin, and the decay based on its half life h_{AGT} :

$$\frac{d[AGT]}{dt} = k_{AGT} - \text{PRA} - \frac{\ln(2)}{h_{AGT}}[AGT] \quad (2.1)$$

where PRA denotes plasma renin activity. PRA is assumed to follow Michaelis-Menton kinetics, characterized by the maximum rate V_{\max} [141]. The Michaelis constant is taken to be the $[AGT]$ value at which PRA reaches half of its maximum value (denoted $[AGT]_{EQ}$). PRA also depends on the feedback effect of AT1R-bound Ang II [80].

$$\text{PRA} = \frac{V_{\max}[AGT]}{[AGT] + [AGT]_{EQ}} * f([\text{AT1R-bound Ang II}]) \quad (2.2)$$

$$f = \left(\frac{[\text{AT1R-bound Ang II}]_{EQ}}{[\text{AT1R-bound Ang II}]} \right)^{B_{AT1}} \quad (2.3)$$

Because the exponent B_{AT1} is taken to be positive (0.95), when $[\text{AT1R-bound Ang II}]$ is above its equilibrium value ($[\text{AT1R-bound Ang II}]_{EQ}$), PRA decreases.

Ang I is converted into other forms through ACE, chymase, and NEP; the respective reaction rate constants are denoted c_{ACE} , c_{Chym} , and c_{NEP} . The rate of change of $[\text{Ang I}]$ is given by

$$\frac{d[\text{Ang I}]}{dt} = \text{PRA} - (c_{ACE} + c_{Chym} + c_{NEP})[\text{Ang I}] - \frac{\ln(2)}{h_{\text{Ang I}}}[\text{Ang I}] \quad (2.4)$$

where $h_{\text{Ang I}}$ denotes the half-life of Ang I.

Ang II is converted from Ang I through ACE and chymase and then converted into Ang (1-7) through ACE2 with the rate constant c_{ACE2} . Ang II also binds to the AT1R and AT2R with rate constants c_{AT1R} and c_{AT2R} , respectively. We assume that Ang II has a half life of $h_{\text{Ang II}}$. With this notation the rate of change of [Ang II] is

$$\begin{aligned} \frac{d[\text{Ang II}]}{dt} &= (c_{\text{ACE}} + c_{\text{Chym}})[\text{Ang I}] - (c_{\text{ACE2}} + c_{\text{Ang II}=\text{Ang IV}} + c_{\text{AT1R}} + c_{\text{AT2R}}) \\ &\quad \times [\text{Ang II}] - \frac{\ln(2)}{h_{\text{Ang II}}}[\text{Ang II}]. \end{aligned} \quad (2.5)$$

Ang II binds to AT1R with rate constant c_{AT1R} to produce AT1R-bound Ang II. AT1R-bound Ang II decays with a half life of h_{AT1R} , giving the rate of change of [AT1R-bound Ang II] as

$$\frac{d[\text{AT1R-bound Ang II}]}{dt} = c_{\text{AT1R}}[\text{Ang II}] - \frac{\ln(2)}{h_{\text{AT1R}}}[\text{AT1R-bound Ang II}]. \quad (2.6)$$

Ang II binds to the AT2R with rate constant c_{AT2R} to produce AT2R-bound Ang II. AT2R-bound Ang II decays with a half life of h_{AT2R} , giving the rate of change of [AT2R-bound Ang II] as

$$\frac{d[\text{AT2R-bound Ang II}]}{dt} = c_{\text{AT2R}}[\text{Ang II}] - \frac{\ln(2)}{h_{\text{AT2R}}}[\text{AT2R-bound Ang II}]. \quad (2.7)$$

Ang (1-7) is converted by NEP from Ang I and by ACE2 from Ang II, and it decays with a half life of $h_{\text{Ang (1-7)}}$. Thus the rate of change of [Ang (1-7)] is

$$\frac{d[\text{Ang (1-7)}]}{dt} = c_{\text{NEP}}[\text{Ang I}] + c_{\text{ACE2}}[\text{Ang II}] - \frac{\ln(2)}{h_{\text{Ang (1-7)}}}[\text{Ang (1-7)}]. \quad (2.8)$$

Ang IV is converted from Ang II with the rate constant $c_{\text{Ang II}=\text{Ang IV}}$ and decays with a half life of $h_{\text{Ang IV}}$, giving the rate of change of $[\text{Ang IV}]$ as

$$\frac{d[\text{Ang IV}]}{dt} = c_{\text{Ang II}=\text{Ang IV}}[\text{Ang II}] - \frac{\ln(2)}{h_{\text{Ang IV}}}[\text{Ang IV}]. \quad (2.9)$$

2.2.2 Model parameters

As previously noted, the goal of this study is to identify model parameters that characterize the RAS system in a normotensive male rat, a hypertensive male rat, a normotensive female rat, and a hypertensive female rat. To that end, we seek to identify parameters that yield hormone levels that are known to differ among these four types of rats. Notably, Ang I and Ang II levels have been observed to be substantially elevated in hypertensive males [176]. We seek parameter sets such that at steady state, Eqs. (2.1)–(2.9) yield the desired hormone levels for each type of rats, as follows:

1. We substitute the known hormone concentrations (shown in Table 2.1) into the steady-state formulation of the model equations (i.e., Eqs. (2.1), (2.4)–(2.9) with the time derivatives set to zero).
2. Half lives for each form of angiotensin, the steady state AGT and Ang IV concentrations, and the feedback function fitting constant B_{AT1} are assumed the same for all groups of rats. Half lives and B_{AT1} are assumed to be constant over time. The value for B_{AT1} is taken to be 0.95 [80].

3. AT1R-bound Ang II levels are determined from the measured [Ang II] in rats [176] and the ratio of [AT1R-bound Ang II] to [Ang II] in Ref. [141]. Similarly, AT2R-bound Ang II levels are determined from the measured [Ang II] in rats [176] and the ratio of [AT2R-bound Ang II] to [Ang II] in Ref. [141].
4. At steady state, $[AGT] = [AGT]_{EQ}$, and $[AT1R\text{-bound Ang II}] = [AT1R\text{-bound Ang II}]_{EQ}$. From Eq. (2.2), $f = 1$ and $PRA = V_{\max}/2$.
5. Given these assumptions, the unknowns are PRA, k_{AGT} , c_{ACE} , c_{Chym} , c_{NEP} , c_{ACE2} , $c_{Ang\ II=Ang\ IV}$, c_{AT1R} , and c_{AT2R} . This gives 7 linear equations (Eqs. (2.2) and (2.3) do not give additional constraints) and 9 unknowns.
6. To achieve a fully determined system of equations, we impose two additional constraints. One relates the reaction rate constant of ACE to chymase, since ACE is responsible for over 90% of the Ang I that is converted into Ang II [141].

$$c_{ACE} = 9 \times c_{Chym} \quad (2.10)$$

The second relates c_{ACE2} and c_{NEP} by

$$c_{ACE2} = \alpha_{ACE2,NEP} \times c_{NEP} \quad (2.11)$$

where $\alpha_{ACE2,NEP}$ is given by the experimentally determined enzymatic activity for ACE2 and NEP for the different types of rats (Table 2.1).

Given the above assumptions, we can formulate a linear system $Ax = b$ as shown in Eqs. 2.12 and 2.13.

$$A = \tag{2.12}$$

$$\begin{bmatrix} -1 & 1 & 0 & 0 & 0 & 0 & 0 & 0 & 0 \\ 1 & 0 & -[\text{Ang I}] & -[\text{Ang I}] & -[\text{Ang I}] & 0 & 0 & 0 & 0 \\ 0 & 0 & [\text{Ang I}] & [\text{Ang I}] & 0 & -[\text{Ang II}] & -[\text{Ang II}] & -[\text{Ang II}] & -[\text{Ang II}] \\ 0 & 0 & 0 & 0 & [\text{Ang I}] & [\text{Ang II}] & 0 & 0 & 0 \\ 0 & 0 & 0 & 0 & 0 & 0 & [\text{Ang II}] & 0 & 0 \\ 0 & 0 & 0 & 0 & 0 & 0 & 0 & [\text{Ang II}] & 0 \\ 0 & 0 & 0 & 0 & 0 & 0 & 0 & 0 & [\text{Ang II}] \\ 0 & 0 & 1 & -9 & 0 & 0 & 0 & 0 & 0 \\ 0 & 0 & 0 & 0 & \alpha_{\text{ACE2,NEP}} & -1 & 0 & 0 & 0 \end{bmatrix}$$

$$x = \begin{bmatrix} PRA \\ k_{\text{AGT}} \\ c_{\text{ACE}} \\ c_{\text{Chym}} \\ c_{\text{NEP}} \\ c_{\text{ACE2}} \\ c_{\text{Ang II}=\text{Ang IV}} \\ c_{\text{AT1R}} \\ c_{\text{AT2R}} \end{bmatrix} \quad b = \begin{bmatrix} \frac{\ln(2)}{h_{\text{AGT}}} [\text{AGT}] \\ \frac{\ln(2)}{h_{\text{Ang I}}} * [\text{Ang I}] \\ \frac{\ln(2)}{h_{\text{Ang II}}} * [\text{Ang II}] \\ \frac{\ln(2)}{h_{\text{Ang (1-7)}}} * [\text{Ang (1-7)}] \\ \frac{\ln(2)}{h_{\text{Ang IV}}} * [\text{Ang IV}] \\ \frac{\ln(2)}{h_{\text{AT1R}}} * [\text{AT1R} - \text{bound Ang II}] \\ \frac{\ln(2)}{h_{\text{AT2R}}} * [\text{AT2R} - \text{bound Ang II}] \\ 0 \\ 0 \end{bmatrix} \tag{2.13}$$

Table 2.1: RAS hormone levels and enzymatic activity. Values from Ref. [176] are for normotensive Lewis rats and hypertensive mRen(2).Lewis rats and were estimated from figures therein. Values from Ref. [20] are for Sprague-Dawley rats. Human values from Ref. [141] are applied to the rat when rodent data are not available.

Hormone	Unit	Normotensive		Hypertensive		Reference
		Male	Female	Male	Female	
AGT	fmol/ml	576000	576000	576000	576000	[20]
Ang I	fmol/ml	90	75	200	61	[176]
Ang II	fmol/ml	6	6	47	20	[176]
Ang 1-7	fmol/ml	50	25	31	162	[176]
Ang IV	fmol/ml	1.29	1.29	1.29	1.29	[141]
AT1R - bound Ang II	fmol/ml	20.46	20.46	160.29	68.21	
AT2R - bound Ang II	fmol/ml	6.82	6.82	53.43	22.74	
Enzyme Activity						
ACE2	fmol/mg/min	87.5	55	69	41	[176]
NEP	fmol/mg/min	412.5	975	300	920	[176]

2.3 Model results

2.3.1 Parameter identification

By solving the system $Ax = b$ (Eqs. 2.12 and 2.13), we obtain model parameters for normo/hypertensive male/female rats. Results are shown in Table 2.2. A notable difference between the reaction rate constants computed for the normotensive and hypertensive rats are the much higher c_{ACE} and lower $c_{Ang\ II=Ang\ IV}$ in the latter, for both male and female rats. This implies a higher Ang I-to-Ang II conversion rate and a lower Ang II-to-Ang IV conversion rate, which explains the substantially higher [Ang II] in hypertensive rats (Table 2.1).

Additionally, the model predicts substantial sex differences among *hypertensive* rats in c_{ACE} , c_{Chym} , c_{NEP} , and c_{ACE2} . In contrast, sex differences for these reaction rate constants are much smaller among normotensive rats. This result should be expected, given the more substantial sex differences in hormone levels among hypertensive rats

Table 2.2: Calculated kinetic parameters for four cohorts of rats.

Parameter	Unit	Normotensive		Hypertensive	
		Male	Female	Male	Female
V_{\max}	fmol/ml/h	16270.4	13705.8	40976	13962.4
PRA	fmol/ml/h	8135.2	6852.9	20488	6981.2
k_{AGT}	fmol/ml/h	48061	46778	60413	46906
c_{ACE}	1/h	5.81	6.96	17.15	24.88
c_{Chym}	1/h	0.65	0.77	1.91	2.76
c_{NEP}	1/h	0.76	0.46	0.20	3.63
c_{ACE2}	1/h	0.16	0.026	0.047	0.16
$c_{\text{Ang II=Ang IV}}$	1/h	17.88	17.88	2.28	5.37
c_{AT1R}	1/h	11.82	11.82	11.82	11.82
c_{AT2R}	1/h	3.94	3.94	3.94	3.94

(Table 2.1). Model results indicate that hypertensive females have an especially high level of NEP activity (3.63, compared to 0.2 and 0.76 for hypertensive and normotensive male). That, combined with their higher ACE2 rate constant compared to hypertensive male, means that much more angiotensin is being converted into Ang (1-7). These higher rate constants can explain the high Ang (1-7) levels observed experimentally. Similarly, the relatively lower ACE2 and NEP activities predicted for hypertensive male rats slows the conversion of Ang II and explains the higher Ang II levels seen in these rats.

2.3.2 Parameter sensitivity study

In the next set of simulations, we sought to assess the stability of the system and to determine the extent to which a perturbation in each parameter can affect model results. To achieve these goals, we conducted a local sensitivity analysis in which we varied each parameter by 10% and recalculated the steady state hormone levels by solving for the root of the nonlinear system. In addition, we assessed the impact of the feedback system (Eq. 2.3) by conducting the parameter sensitivity study with and

without feedback ($f = 1$ in the latter). Tables 2.3–2.6 show the results for the four groups of rats, given as the percentage changes in key hormone levels in response to a given parameter variation. Values in parentheses are for the system without feedback.

An overall observation is that adjusting a parameter causes each hormone to change in the same direction (albeit by different amounts) in all rats. In other words, the four rats behave qualitatively similarly, which is to be expected. In addition, with and without feedback, increasing a parameter by 10% causes the opposite response as decreasing it by 10%. Without feedback, each reaction rate constant is positively correlated with hormones downstream of it. For example, k_{AGT} is positively correlated with all variables while c_{AT1R} is only positively correlated with AT1R-bound Ang II. The hormone that is directly upstream of the reaction rate constant is negatively correlated, while hormones farther upstream are not effected. Hormones that are part of an alternate path than the path defined by the reaction rate constant are negatively correlated with the perturbed reaction rate constant, but have a much smaller effect size. With feedback some noise is introduced but the same patterns hold.

Our model supports the common description of PRA as the driving force of the RAS. V_{max} , $[\text{AGT}]_{\text{EQ}}$, and $[\text{AT1R-bound Ang II}]_{\text{EQ}}$ determine PRA and have strong effects on all hormones.

In the absence of feedback, V_{max} is the strongest determinant of all hormone levels, through its effect on PRA. c_{ACE} is the second strongest determinant of all downstream hormone levels except for $[\text{Ang (1-7)}]$. With feedback, c_{ACE} is a strong effector of all hormones save $[\text{AGT}]$. With or without feedback, $[\text{Ang (1-7)}]$, $[\text{Ang IV}]$, $[\text{AT1R-bound Ang II}]$, and $[\text{AT2R-bound Ang II}]$ are more strongly effected by c_{NEP} , $c_{\text{Ang II=Ang IV}}$, c_{AT1R} , and c_{AT2R} , respectively. A clinical implication of these results is

Table 2.3: Percent change in response to parameter perturbation for male normotensive rats. Values in parentheses are from the system without feedback function f .

	AT1R-bound					AT2R-bound		
	AGT	Ang I	Ang II	Ang (1-7)	Ang IV	Ang II	Ang II	PRA
$V_{\max}+10\%$	-0.97 (-1.83)	4.75 (8.98)	4.75 (8.98)	4.75 (8.98)	4.75 (8.98)	4.75 (8.98)	4.75 (8.98)	4.75 (8.98)
$V_{\max}-10\%$	1.02 (1.87)	-5.01 (-9.17)	-5.01 (-9.17)	-5.01 (-9.17)	-5.01 (-9.17)	-5.01 (-9.17)	-5.01 (-9.17)	-5.01 (-9.17)
$[AGT]_{EQ}+10\%$	0.48 (0.88)	-2.35 (-4.32)	-2.35 (-4.32)	-2.35 (-4.32)	-2.35 (-4.32)	-2.35 (-4.32)	-2.35 (-4.32)	-2.35 (-4.32)
$[AGT]_{EQ}-10\%$	-0.52 (-0.97)	2.54 (4.78)	2.54 (4.78)	2.54 (4.78)	2.54 (4.78)	2.54 (4.78)	2.54 (4.78)	2.54 (4.78)
$[AT1R-bound$ $Ang II]_{EQ}+10\%$	-0.92 (0)	4.50 (0)	4.50 (0)	4.50 (0)	4.50 (0)	4.50 (0)	4.50 (0)	4.50 (0)
$[AT1R-bound$ $Ang II]_{EQ}-10\%$	0.97 (0)	-4.77 (0)	-4.77 (0)	-4.77 (0)	-4.77 (0)	-4.77 (0)	-4.77 (0)	-4.77 (0)
$k_{AGT}+10\%$	11.48 (10.98)	2.75 (5.20)	2.75 (5.20)	2.75 (5.20)	2.75 (5.20)	2.75 (5.20)	2.75 (5.20)	2.75 (5.20)
$k_{AGT}-10\%$	-11.40 (-10.87)	-3.15 (-5.75)	-3.15 (-5.75)	-3.15 (-5.75)	-3.15 (-5.75)	-3.15 (-5.75)	-3.15 (-5.75)	-3.15 (-5.75)
$c_{ACE}+10\%$	0.74 (0)	-4.25 (-0.64)	4.37 (8.30)	-4.13 (-0.51)	4.37 (8.30)	4.37 (8.30)	4.37 (8.30)	-3.63 (0)
$c_{ACE}-10\%$	-0.84 (0)	4.82 (0.65)	-4.61 (-8.41)	4.69 (0.52)	-4.61 (-8.41)	-4.61 (-8.41)	-4.61 (-8.41)	4.15 (0)
$c_{Chym}+10\%$	0.09 (0)	-0.50 (-0.07)	0.50 (0.93)	-0.48 (-0.06)	0.50 (0.93)	0.50 (0.93)	0.50 (0.93)	-0.43 (0)
$c_{Chym}-10\%$	-0.09 (0)	0.50 (0.07)	-0.50 (-0.93)	0.49 (0.06)	-0.50 (-0.93)	-0.50 (-0.93)	-0.50 (-0.93)	0.43 (0)
$c_{NEP}+10\%$	-0.01 (0)	-0.05 (-0.08)	-0.05 (-0.08)	9.81 (9.77)	-0.05 (-0.08)	-0.05 (-0.08)	-0.05 (-0.08)	0.04 (0)
$c_{NEP}-10\%$	0.01 (0)	0.05 (0.08)	0.05 (0.08)	-9.82 (-9.78)	0.05 (0.08)	0.05 (0.08)	0.05 (0.08)	-0.04 (0)
$c_{ACE2}+10\%$	0 (0)	0.01 (0)	-0.01 (-0.02)	0.15 (0.14)	-0.01 (-0.02)	-0.01 (-0.02)	-0.01 (-0.02)	0.01 (0)
$c_{ACE2}-10\%$	0 (0)	-0.01 (0)	0.01 (0.02)	-0.15 (-0.14)	0.01 (0.02)	0.01 (0.02)	0.01 (0.02)	-0.01 (0)
$c_{AngII=AngIV}+10\%$	-0.17 (0)	0.85 (0)	-0.98 (-1.81)	0.83 (-0.03)	8.92 (8.01)	-0.98 (-1.81)	-0.98 (-1.81)	0.85 (0)
$c_{AngII=AngIV}-10\%$	0.18 (0)	-0.86 (0)	1.01 (1.88)	-0.83 (0.03)	-9.09 (-8.31)	1.01 (1.88)	1.01 (1.88)	-0.86 (0)
$c_{AT1R}+10\%$	0.77 (0)	-3.78 (0)	-4.94 (-1.21)	-3.80 (-0.02)	-4.94 (-1.21)	4.56 (8.67)	-4.94 (-1.21)	-3.78 (0)
$c_{AT1R}-10\%$	-0.90 (0)	4.40 (0)	5.69 (1.24)	4.42 (0.02)	5.69 (1.24)	-4.88 (-8.89)	5.69 (1.24)	4.40 (0)
$c_{AT2R}+10\%$	-0.04 (0)	0.19 (0)	-0.22 (-0.41)	0.18 (-0.01)	-0.22 (-0.41)	-0.22 (-0.41)	9.76 (9.55)	0.19 (0)
$c_{AT2R}-10\%$	0.04 (0)	-0.19 (0)	0.22 (0.41)	-0.18 (0.01)	0.22 (0.41)	0.22 (0.41)	-9.80 (-9.63)	-0.19 (0)

Table 2.4: Percent change in response to parameter perturbation for female normotensive rats. Values in parentheses are from the system without feedback function f .

	AT1R-bound					AT2R-bound		
	AGT	Ang I	Ang II	Ang (1-7)	Ang IV	Ang II	Ang II	PRA
$V_{\max}+10\%$	-0.82 (-1.57)	4.79 (9.13)	4.79 (9.13)	4.79 (9.13)	4.79 (9.13)	4.79 (9.13)	4.79 (9.13)	4.79 (9.13)
$V_{\max}-10\%$	0.87 (1.59)	-5.05 (-9.29)	-5.05 (-9.29)	-5.05 (-9.29)	-5.05 (-9.29)	-5.05 (-9.29)	-5.05 (-9.29)	-5.05 (-9.29)
$[AGT]_{EQ}+10\%$	0.41 (0.75)	-2.36 (-4.39)	-2.36 (-4.39)	-2.36 (-4.39)	-2.36 (-4.39)	-2.36 (-4.39)	-2.36 (-4.39)	-2.36 (-4.39)
$[AGT]_{EQ}-10\%$	-0.44 (-0.83)	2.56 (4.85)	2.56 (4.85)	2.56 (4.85)	2.56 (4.85)	2.56 (4.85)	2.56 (4.85)	2.56 (4.85)
$[AT1R-bound$ $Ang II]_{EQ}+10\%$	-0.78 (0)	4.54 (0)	4.54 (0)	4.54 (0)	4.54 (0)	4.54 (0)	4.54 (0)	4.54 (0)
$[AT1R-bound$ $Ang II]_{EQ}-10\%$	0.82 (0)	-4.80 (0)	-4.80 (0)	-4.80 (0)	-4.80 (0)	-4.80 (0)	-4.80 (0)	-4.80 (0)
$k_{AGT}+10\%$	11.25 (10.83)	2.70 (5.14)	2.70 (5.14)	2.70 (5.14)	2.70 (5.14)	2.70 (5.14)	2.70 (5.14)	2.70 (5.14)
$k_{AGT}-10\%$	-11.19 (-10.74)	-3.08 (-5.68)	-3.08 (-5.68)	-3.08 (-5.68)	-3.08 (-5.68)	-3.08 (-5.68)	-3.08 (-5.68)	-3.08 (-5.68)
$c_{ACE}+10\%$	0.62 (0)	-4.33 (-0.76)	4.28 (8.18)	-4.29 (-0.72)	4.28 (8.18)	4.28 (8.18)	4.28 (8.18)	-3.60 (0)
$c_{ACE}-10\%$	-0.71 (0)	4.92 (0.77)	-4.52 (-8.30)	4.88 (0.73)	-4.52 (-8.30)	-4.52 (-8.30)	-4.52 (-8.30)	4.12 (0)
$c_{Chym}+10\%$	0.07 (0)	-0.51 (-0.08)	0.49 (0.91)	-0.50 (-0.08)	0.49 (0.91)	0.49 (0.91)	0.49 (0.91)	-0.42 (0)
$c_{Chym}-10\%$	-0.07 (0)	0.52 (0.08)	-0.49 (-0.92)	0.51 (0.08)	-0.49 (-0.92)	-0.49 (-0.92)	-0.49 (-0.92)	0.43 (0)
$c_{NEP}+10\%$	0 (0)	-0.03 (-0.05)	-0.03 (-0.05)	9.93 (9.90)	-0.03 (-0.05)	-0.03 (-0.05)	-0.03 (-0.05)	0.02 (0)
$c_{NEP}-10\%$	0 (0)	0.03 (0.05)	0.03 (0.05)	-9.93 (-9.91)	0.03 (0.05)	0.03 (0.05)	0.03 (0.05)	-0.02 (0)
$c_{ACE2}+10\%$	0 (0)	0 (0)	0 (0)	0.05 (0.04)	0 (0)	0 (0)	0 (0)	0 (0)
$c_{ACE2}-10\%$	0 (0)	0 (0)	0 (0)	-0.05 (-0.04)	0 (0)	0 (0)	0 (0)	0 (0)
$c_{AngII=AngIV}+10\%$	-0.15 (0)	0.86 (0)	-0.97 (-1.82)	0.85 (-0.01)	8.93 (8.00)	-0.97 (-1.82)	-0.97 (-1.82)	0.86 (0)
$c_{AngII=AngIV}-10\%$	0.15 (0)	-0.87 (0)	1.00 (1.88)	-0.86 (0.01)	-9.10 (-8.30)	1.00 (1.88)	1.00 (1.88)	-0.87 (0)
$c_{AT1R}+10\%$	0.65 (0)	-3.81 (0)	-4.97 (-1.21)	-3.82 (-0.01)	-4.97 (-1.21)	4.53 (8.67)	-4.97 (-1.21)	-3.81 (0)
$c_{AT1R}-10\%$	-0.76 (0)	4.43 (0)	5.73 (1.24)	4.44 (0.01)	5.73 (1.24)	-4.85 (-8.89)	5.73 (1.24)	4.43 (0)
$c_{AT2R}+10\%$	-0.03 (0)	0.19 (0)	-0.22 (-0.41)	0.19 (0)	-0.22 (-0.41)	-0.22 (-0.41)	9.76 (9.55)	0.19 (0)
$c_{AT2R}-10\%$	0.03 (0)	-0.19 (0)	0.22 (0.41)	-0.19 (0)	0.22 (0.41)	0.22 (0.41)	-9.80 (-9.63)	-0.19 (0)

Table 2.5: Percent change in response to parameter perturbation for male hypertensive rats. Values in parentheses are from the system without feedback function f .

	AT1R-bound					AT2R-bound		
	AGT	Ang I	Ang II	Ang (1-7)	Ang IV	Ang II	Ang II	PRA
$V_{\max}+10\%$	-2.25 (-3.98)	4.39 (7.76)	4.39 (7.76)	4.39 (7.76)	4.39 (7.76)	4.39 (7.76)	4.39 (7.76)	4.39 (7.76)
$V_{\max}-10\%$	2.40 (4.18)	-4.68 (-8.16)	-4.68 (-8.16)	-4.68 (-8.16)	-4.68 (-8.16)	-4.68 (-8.16)	-4.68 (-8.16)	-4.68 (-8.16)
$[AGT]_{EQ}+10\%$	1.12 (1.95)	-2.18 (-3.80)	-2.18 (-3.80)	-2.18 (-3.80)	-2.18 (-3.80)	-2.18 (-3.80)	-2.18 (-3.80)	-2.18 (-3.80)
$[AGT]_{EQ}-10\%$	-1.21 (-2.15)	2.36 (4.18)	2.36 (4.18)	2.36 (4.18)	2.36 (4.18)	2.36 (4.18)	2.36 (4.18)	2.36 (4.18)
$[AT1R-bound$ $Ang II]_{EQ}+10\%$	-2.14 (0)	4.17 (0)	4.17 (0)	4.17 (0)	4.17 (0)	4.17 (0)	4.17 (0)	4.17 (0)
$[AT1R-bound.$ $Ang II]_{EQ}-10\%$	2.29 (0)	-4.45 (0)	-4.45 (0)	-4.45 (0)	-4.45 (0)	-4.45 (0)	-4.45 (0)	-4.45 (0)
$k_{AGT}+10\%$	13.49 (12.18)	3.19 (5.74)	3.19 (5.74)	3.19 (5.74)	3.19 (5.74)	3.19 (5.74)	3.19 (5.74)	3.19 (5.74)
$k_{AGT}-10\%$	-13.23 (-11.89)	-3.70 (-6.32)	-3.70 (-6.32)	-3.70 (-6.32)	-3.70 (-6.32)	-3.70 (-6.32)	-3.70 (-6.32)	-3.70 (-6.32)
$c_{ACE}+10\%$	1.52 (0)	-4.56 (-1.65)	4.03 (7.20)	-4.12 (-1.19)	4.03 (7.20)	4.03 (7.20)	4.03 (7.20)	-2.96 (0)
$c_{ACE}-10\%$	-1.73 (0)	5.14 (1.70)	-4.32 (-7.45)	4.65 (1.23)	-4.32 (-7.45)	-4.32 (-7.45)	-4.32 (-7.45)	3.38 (0)
$c_{Chym}+10\%$	0.18 (0)	-0.53 (-0.19)	0.46 (0.81)	-0.48 (-0.13)	0.46 (0.81)	0.46 (0.81)	0.46 (0.81)	-0.35 (0)
$c_{Chym}-10\%$	-0.18 (0)	0.54 (0.19)	-0.47 (-0.82)	0.49 (0.14)	-0.47 (-0.82)	-0.47 (-0.82)	-0.47 (-0.82)	0.35 (0)
$c_{NEP}+10\%$	0 (0)	-0.01 (-0.02)	-0.01 (-0.02)	9.47 (9.47)	-0.01 (-0.02)	-0.01 (-0.02)	-0.01 (-0.02)	0.01 (0)
$c_{NEP}-10\%$	0 (0)	0.01 (0.02)	0.01 (0.02)	-9.48 (-9.47)	0.01 (0.02)	0.01 (0.02)	0.01 (0.02)	-0.01 (0)
$c_{ACE2}+10\%$	0 (0)	0 (0)	0 (-0.01)	0.51 (0.51)	0 (-0.01)	0 (-0.01)	0 (-0.01)	0 (0)
$c_{ACE2}-10\%$	0 (0)	0 (0)	0 (0.01)	-0.51 (-0.51)	0 (0.01)	0 (0.01)	0 (0.01)	0 (0)
$c_{AngII=AngIV}+10\%$	-0.06 (0)	0.12 (0)	-0.16 (-0.28)	0.11 (-0.01)	9.82 (9.69)	-0.16 (-0.28)	-0.16 (-0.28)	0.12 (0)
$c_{AngII=AngIV}-10\%$	0.06 (0)	-0.12 (0)	0.16 (0.28)	-0.11 (0.01)	-9.86 (-9.75)	0.16 (0.28)	0.16 (0.28)	-0.12 (0)
$c_{AT1R}+10\%$	1.76 (0)	-3.43 (0)	-4.82 (-1.44)	-3.50 (-0.07)	-4.82 (-1.44)	4.70 (8.42)	-4.82 (-1.44)	-3.43 (0)
$c_{AT1R}-10\%$	-2.03 (0)	3.96 (0)	5.50 (1.48)	4.04 (0.08)	5.50 (1.48)	-5.05 (-8.67)	5.50 (1.48)	3.96 (0)
$c_{AT2R}+10\%$	-0.11 (0)	0.21 (0)	-0.28 (-0.48)	0.18 (-0.02)	-0.28 (-0.48)	-0.28 (-0.48)	9.70 (9.47)	0.21 (0)
$c_{AT2R}-10\%$	0.11 (0)	-0.21 (0)	0.28 (0.49)	-0.18 (0.03)	0.28 (0.49)	0.28 (0.49)	-9.75 (-9.56)	-0.21 (0)

Table 2.6: Percent change in response to parameter perturbation for female hypertensive rats. Values in parentheses are from the system without feedback function f .

	AT1R-bound					AT2R-bound		
	AGT	Ang I	Ang II	Ang (1-7)	Ang IV	Ang II	Ang II	PRA
$V_{\max}+10\%$	-0.84 (-1.59)	4.78 (9.12)	4.78 (9.12)	4.78 (9.12)	4.78 (9.12)	4.78 (9.12)	4.78 (9.12)	4.78 (9.12)
$V_{\max}-10\%$	0.88 (1.62)	-5.05 (-9.28)	-5.05 (-9.28)	-5.05 (-9.28)	-5.05 (-9.28)	-5.05 (-9.28)	-5.05 (-9.28)	-5.05 (-9.28)
$[\text{AGT}]_{\text{EQ}}+10\%$	0.41 (0.77)	-2.36 (-4.38)	-2.36 (-4.38)	-2.36 (-4.38)	-2.36 (-4.38)	-2.36 (-4.38)	-2.36 (-4.38)	-2.36 (-4.38)
$[\text{AGT}]_{\text{EQ}}-10\%$	-0.45 (-0.85)	2.55 (4.84)	2.55 (4.84)	2.55 (4.84)	2.55 (4.84)	2.55 (4.84)	2.55 (4.84)	2.55 (4.84)
$[\text{AT1R-bound Ang II}]_{\text{EQ}}+10\%$	-0.79 (0)	4.54 (0)	4.54 (0)	4.54 (0)	4.54 (0)	4.54 (0)	4.54 (0)	4.54 (0)
$[\text{AT1R-bound Ang II}]_{\text{EQ}}-10\%$	0.84 (0)	-4.80 (0)	-4.80 (0)	-4.80 (0)	-4.80 (0)	-4.80 (0)	-4.80 (0)	-4.80 (0)
$k_{\text{AGT}}+10\%$	11.28 (10.85)	2.70 (5.15)	2.70 (5.15)	2.70 (5.15)	2.70 (5.15)	2.70 (5.15)	2.70 (5.15)	2.70 (5.15)
$k_{\text{AGT}}-10\%$	-11.21 (-10.75)	-3.09 (-5.68)	-3.09 (-5.68)	-3.09 (-5.68)	-3.09 (-5.68)	-3.09 (-5.68)	-3.09 (-5.68)	-3.09 (-5.68)
$c_{\text{ACE}}+10\%$	0.52 (0)	-5.04 (-2.13)	3.51 (6.68)	-4.91 (-2.00)	3.51 (6.68)	3.51 (6.68)	3.51 (6.68)	-2.97 (0)
$c_{\text{ACE}}-10\%$	-0.60 (0)	5.73 (2.22)	-3.79 (-6.98)	5.59 (2.09)	-3.79 (-6.98)	-3.79 (-6.98)	-3.79 (-6.98)	3.43 (0)
$c_{\text{Chym}}+10\%$	0.06 (0)	-0.59 (-0.24)	0.40 (0.76)	-0.58 (-0.23)	0.40 (0.76)	0.40 (0.76)	0.40 (0.76)	-0.35 (0)
$c_{\text{Chym}}-10\%$	-0.06 (0)	0.60 (0.24)	-0.41 (-0.76)	0.58 (0.23)	-0.41 (-0.76)	-0.41 (-0.76)	-0.41 (-0.76)	0.36 (0)
$c_{\text{NEP}}+10\%$	-0.03 (0)	-0.17 (-0.32)	-0.17 (-0.32)	9.67 (9.51)	-0.17 (-0.32)	-0.17 (-0.32)	-0.17 (-0.32)	0.15 (0)
$c_{\text{NEP}}-10\%$	0.03 (0)	0.17 (0.32)	0.17 (0.32)	-9.70 (-9.57)	0.17 (0.32)	0.17 (0.32)	0.17 (0.32)	-0.15 (0)
$c_{\text{ACE2}}+10\%$	0 (0)	0.01 (0)	-0.01 (-0.02)	0.15 (0.14)	-0.01 (-0.02)	-0.01 (-0.02)	-0.01 (-0.02)	0.01 (0)
$c_{\text{ACE2}}-10\%$	0 (0)	-0.01 (0)	0.01 (0.02)	-0.15 (-0.14)	0.01 (0.02)	0.01 (0.02)	0.01 (0.02)	-0.01 (0)
$c_{\text{AngII=AngIV}}+10\%$	-0.05 (0)	0.30 (0)	-0.34 (-0.63)	0.29 (-0.01)	9.63 (9.30)	-0.34 (-0.63)	-0.34 (-0.63)	0.30 (0)
$c_{\text{AngII=AngIV}}-10\%$	0.05 (0)	-0.30 (0)	0.34 (0.64)	-0.29 (0.01)	-9.69 (-9.42)	0.34 (0.64)	0.34 (0.64)	-0.30 (0)
$c_{\text{AT1R}}+10\%$	0.65 (0)	-3.73 (0)	-5.06 (-1.38)	-3.75 (-0.02)	-5.06 (-1.38)	4.44 (8.48)	-5.06 (-1.38)	-3.73 (0)
$c_{\text{AT1R}}-10\%$	-0.76 (0)	4.34 (0)	5.82 (1.42)	4.36 (0.02)	5.82 (1.42)	-4.76 (-8.72)	5.82 (1.42)	4.34 (0)
$c_{\text{AT2R}}+10\%$	-0.04 (0)	0.22 (0)	-0.25 (-0.47)	0.21 (-0.01)	-0.25 (-0.47)	-0.25 (-0.47)	9.73 (9.49)	0.22 (0)
$c_{\text{AT2R}}-10\%$	0.04 (0)	-0.22 (0)	0.25 (0.47)	-0.21 (0.01)	0.25 (0.47)	0.25 (0.47)	-9.77 (-9.58)	-0.22 (0)

that ACEIs (which reduce c_{ACE}) have a potential for strongly influencing most RAS components and for regulating blood pressure via its effects on the concentration of [AT1R-bound Ang II]. However, blood pressure is positively influenced by [Ang (1-7)] and [AT2R-bound Ang II], which ACEIs suppress. [AT2R-bound Ang II] has been shown to have a greater influence in females, so this may explain why ACEI are less effective in females.

Without feedback, c_{AT1R} has a strong effect on [AT1R-bound Ang II], a smaller effect on [Ang II], [Ang IV], and [AT2R-bound Ang II], and a weak effect on other hormones. With feedback, c_{AT1R} has a weaker effect on [AT1R-bound Ang II], but a strong effect on other hormone levels. [Ang I] and [Ang (1-7)] exhibit the same percentage change as PRA, a result that suggests that their changes are driven by PRA. [Ang II], [Ang IV], and [AT2R-bound Ang II] change by a larger percentage than PRA, meaning that their change is driven by PRA and by the blockage or increase of flow from the change in c_{AT1R} . Taken together, these results indicate that the feedback stabilizes [AT1R-bound Ang II], i.e., the feedback mechanism keeps [AT1R-bound Ang II] close to its equilibrium value. A clinical implication of this result is that ARBs may regulate blood pressure by both lowering [AT1R-bound Ang II] and by adjusting the levels of other hormones such as [AT2R-bound Ang II].

Except for the cases of c_{NEP} and c_{ACE2} , [Ang I] and [Ang (1-7)] change by similar *percentages*. But notably, [Ang (1-7)] changes by a larger *amount* in female hypertensive rats relative to all other rats, while in all other rats [Ang I] increases by a larger amount. This is due to female hypertensive rats having a much higher baseline [Ang (1-7)] and the lowest [Ang I]: female hypertensive [Ang (1-7)] is more than triple that of the next highest (male normotensive) (Table 2.1). As neither ACEIs nor ARBs, the two drug treatments considered in this study, change c_{NEP} and c_{ACE2} , we can expect [Ang I] and [Ang (1-7)] to behave similarly in all drug simulations.

Except for the cases of c_{AT1R} and k_{AGT} , [AT1R-bound Ang II] changes by a similar *percentage* in all rats but by a much larger *amount* in male hypertensive rats, followed by female hypertensive rats, whereas normotensive rats show the least response and do not show a significant sex difference. This result stems from the fact that in our model the male hypertensive rat is assumed to have a much larger baseline [AT1R-bound Ang II], meaning that a given percentage change has a larger absolute effect.

2.3.3 ACE inhibitors

As previously noted, a major goal of this study is to better understand the mechanisms by which animals exhibit sex differences in their responses to pharmaceutical drugs used in the treatment for hypertension and congestive heart failure. We first considered ACEIs. To simulate their effects, we reduce c_{ACE} by a target level κ_{ACE} :

$$c_{\text{ACE}} = c_{\text{ACE}}^0 \times (1 - \kappa_{\text{ACE}}) \quad (2.14)$$

We modeled 50% and 90% inhibition of ACE (i.e., $\kappa_{\text{ACE}} = 0.5$ and 0.9) and assessed any sex differences in the responses of hypertensive rats. Results are shown in Fig. 2.2. The model predicted that a 90% reduction in c_{ACE} resulted in 60.0% and 54.5% reduction in [Ang II] in male and female hypertensive rats, respectively. This corresponds to a drop from 47 fmol/ml to 18.8 fmol/ml in male hypertensive rats and a drop from 20 fmol/ml to 9.1 fmol/ml in female hypertensive rats. Model predictions are consistent with experiments by Campbell et al., who found in male hypertensive rats that Ang II drops by 65.9% [20]. A 50% reduction in ACE resulted in a 25.7% and 22.8% reduction in [Ang II] in male and female hypertensive rats, respectively (Fig. 2.2d). While the percentages are similar, in male hypertensive rats exhibited a larger absolute reduction in [Ang II] (from 47 fmol/ml to 34.9 fmol/ml)

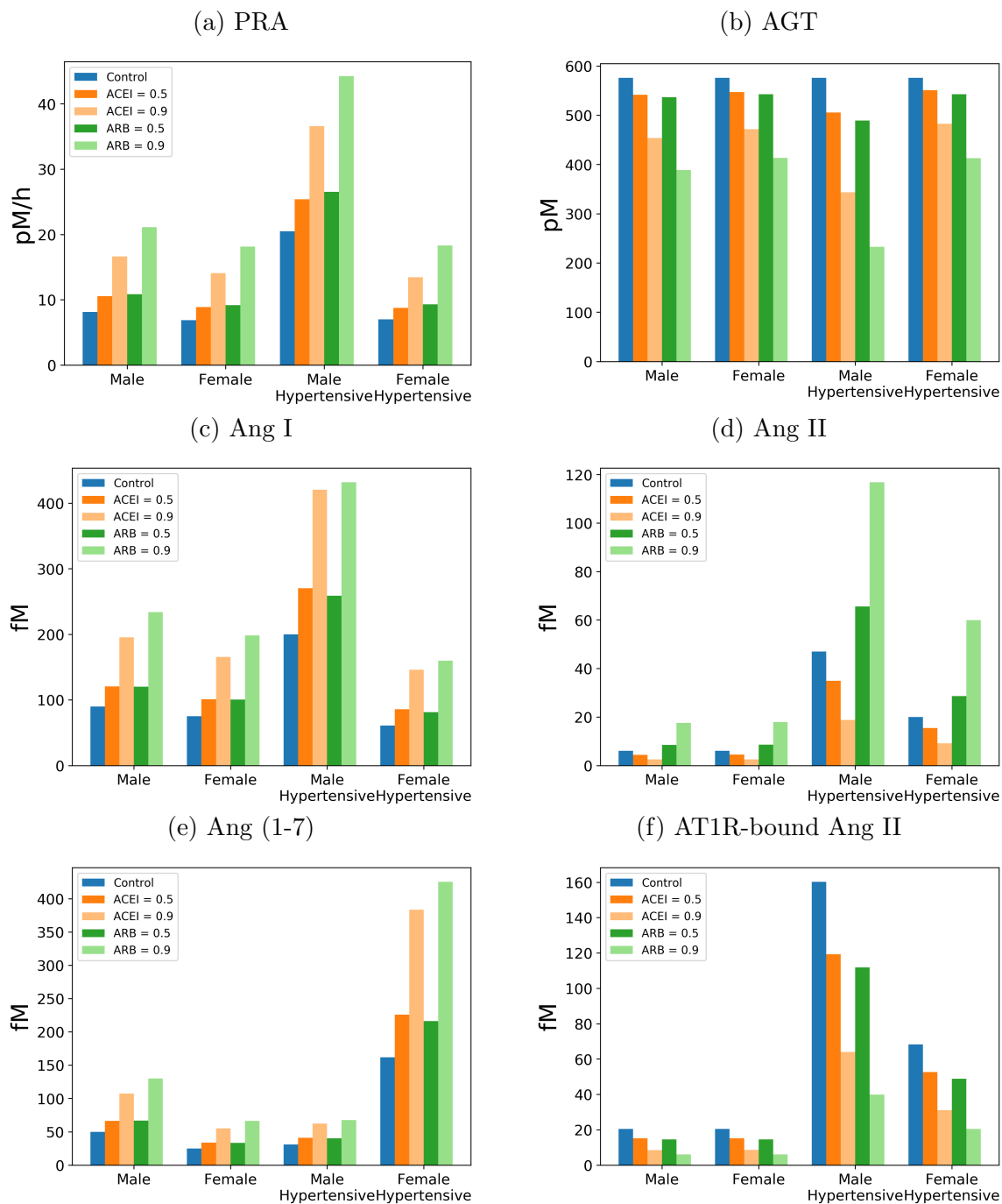


Figure 2.2: Simulated hormone concentrations after angiotensin converting enzyme inhibitors (ACEI) or angiotensin receptor blockers (ARB) treatment for virtual normotensive and hypertensive rats.

than its female counterpart (from 20 fmol/ml to 15.4 fmol/ml). Taken together, our model predicted a moderately larger percentage decrease and a much larger absolute decrease in male hypertensive [Ang II] levels than it does for female hypertensive rats. This result suggests that ACEIs may be more effective in lowering [Ang II] in males compared to females. Under ACE inhibition, [Ang IV], [AT1R-bound Ang II], and [AT2R-bound Ang II] all directly scale with [Ang II] in our model.

With 90% ACE inhibition our model predicted a 110.3% and a 139.5% increase in [Ang I] in male and female hypertensive rats, respectively (Fig. 2.2c). In male hypertensive rats, [Ang I] increased from 200 fmol/ml to 420.6 fmol/ml, whereas in females [Ang I] increased from 61 fmol/ml to 146.1 fmol/ml. A 50% reduction shows a smaller but qualitatively similar response for both sexes.

The model predicted that ACE inhibition induces similar percentage increases in [Ang (1-7)] between the two sexes. With 90% ACE inhibition, our model predicted a 101.6% and 136.7% increase in [Ang (1-7)] levels in male and female hypertensive rats, respectively. Due to their higher baseline [Ang (1-7)], the absolute increase is higher in female hypertensive rats than males (Fig. 2.2e). The larger increase in females may be explained, in part, by their higher c_{NEP} . Thus, as [Ang I] rises, more of the Ang I is converted by NEP to Ang (1-7) in females.

Model male hypertensive rats have a higher level of PRA, compared to females, with and without ACE inhibition. However, ACE inhibition results in a larger percentage increase in female hypertensive rats (Fig. 2.2a). With 90% ACE inhibition, male hypertensive rat's PRA increases by 78.6% while PRA increases by 92.6% in female hypertensive rats. This difference in PRA drives the sexes' different responses in [AGT]. Since the production rate of AGT is constant in our model, an increase in PRA decreases [AGT]. In male hypertensive rats we predict a drop of 40.3% while in female hypertensive rats we predict a drop of 16.2% (Fig. 2.2b).

2.3.4 Angiotensin receptor blockers

In the next set of simulations, we studied the effect of ARBs. To simulate their effects, we reduce c_{AT1R} by a target level κ_{ARB} :

$$c_{\text{AT1R}} = c_{\text{AT1R}}^0 \times (1 - \kappa_{\text{ARB}}) \quad (2.15)$$

We modeled 50% and 90% blockage of angiotensin receptors, i.e., $\kappa_{\text{ARB}} = 0.5$ and 0.9 . Model results are summarized in Fig. 2.2. With 50% inhibition of c_{AT1R} , our model predicted essentially the same *percentage* decreases (30.2% and 28.4%) in [AT1R-bound Ang II] in male and female hypertensive rats respectively (Fig. 2.2f). These percentage reductions correspond to an absolute decrease from 160.3 fmol/ml to 111.8 fmol/ml in hypertensive males, and a smaller decrease from 68.2 fmol/ml to 48.85 fmol/ml in hypertensive females. With 90% inhibition of c_{AT1R} , the model predicted a 75.13% and 70.01% decrease in [AT1R-bound Ang II] in male and female, respectively. In this case, [AT1R-bound Ang II] in male hypertensive rats decreased from 160.3 fmol/ml to 39.9 fmol/ml, and in female hypertensive rats, it decreased from 68.2 fmol/ml to 20.5 fmol/ml.

The lowered conversion rate to AT1R-bound Ang II elevated the concentrations of its precursors. Larger fractional increases in [Ang I] and [Ang II] were predicted in female hypertensive rats (162.1 and 199.9%, respectively) than in male hypertensive rats (116.1 and 148.7%, respectively), although male hypertensive rats had higher levels overall. In females, [Ang I] increased from 61 fmol/ml to 159.9 fmol/ml, and [Ang II] from 20 fmol/ml to 60 fmol/ml. In males, [Ang I] increased from 200 fmol/ml to 432.1 fmol/ml, and [Ang II] increased from 47 fmol/ml to 116.9 fmol/ml. Since Ang (1-7) is derived from Ang I and Ang II, its dynamics follow similar trends.

2.3.5 Effect of feedback

Our current model shows a 110.3% and 101.6% increase in Ang I and Ang (1-7), respectively, in male hypertensive rats in response to 90% ACE inhibition. These predicted changes are substantially smaller compared to the 766% and 1120% increases observed experimentally [20]. As discussed above (Sect. 2.3.2), through its action on PRA (Eq. 2.3), V_{\max} is one of the strongest effectors of RAS hormone levels. Thus, we hypothesize that increasing the sensitivity of the feedback function, f , would more acutely increase PRA during ACE inhibition, which would elevate Ang I level and may yield model results that accurately replicate experimental observed changes in Ang I and Ang (1-7). To test this hypothesis, we simulated drug treatments with 10 different values for B_{AT1} between 0 and 2 (baseline $B_{AT1} = 0.95$). Results are shown in Fig. 2.3. Values obtained without feedback ($B_{AT1} = 0$) are indicated by bars.

For both ACEI and ARB, a stronger feedback gain (i.e., larger B_{AT1}) keeps [AT1R-bound Ang II] closer to its equilibrium value shown in the blue bar (Fig. 2.3g). This result can be explained by the observation that with a larger B_{AT1} , a reduction in [AT1R-bound Ang II] would increase PRA by a larger amount. This negative feedback increases [Ang I], [Ang II], and thus [AT1R-bound Ang II].

As noted above, with ACE inhibition, PRA is higher when feedback is represented. Thus, more AGT is being converted into Ang I, but, with lower ACE, less Ang I is being converted into Ang II. Consequently, a higher B_{AT1} yields a higher [Ang I] (Fig. 2.3c); [Ang (1-7)] has a response similar to [Ang I]. Taken together, the competing factors of a higher [Ang I] and a slower conversion rate (with ACE inhibition) result in smaller reductions in downstream peptides [Ang II], [Ang IV], and [AT2R-bound Ang II] when feedback is stronger (larger B_{AT1}) (Fig. 2.3e).

When ARBs are administered in the absence of feedback, upstream peptides [Ang I] and [Ang (1-7)] are unaffected, whereas [Ang II], [Ang IV], and [AT2R-bound Ang II] increase. With feedback, all peptides except [AGT] monotonically increase with B_{AT1} .

2.4 Discussion

The goal of this study is to seek insights into the sex differences in the RAS of the rat, an animal that plays a major role in many experimental and clinical studies. To accomplish that goal, we have applied a previously published human RAS model [141], and identified parameter sets to simulate the RAS in normotensive and hypertensive rats, both male and female. In particular, we identified different parameter sets for the four types of rats to recapitulate the higher [Ang II] in hypertensive rats, especially in males. Analysis of model results suggests that the observed difference in hormone levels among the four types of rats may be attributable to the differing key reaction rate constants that characterize the conversion from Ang I to Ang II (see Table 2.2). For example, our model identified much higher k_{AGT} in male hypertensive rats than in any other group (k_{AGT} in male hypertensive rat is 28.8% higher than female). Similarly, PRA in male hypertensive rat is 193.5% higher than female. k_{AGT} and PRA are key players in the first reactions in this pathway and control the overall amount of angiotensin circulating through the system. Indeed, one reason male hypertensive rats can support a higher Ang II and AT1R-bound Ang II levels is simply because there is more angiotensin circulating through the system. The higher k_{AGT} and PRA values mean that male hypertensive rats can support more Ang II even when female hypertensive rats have higher ACE activity and thus a faster Ang I-to-Ang II conversion rate (a c_{ACE} level of 24.88 1/h in female hypertensive rats as

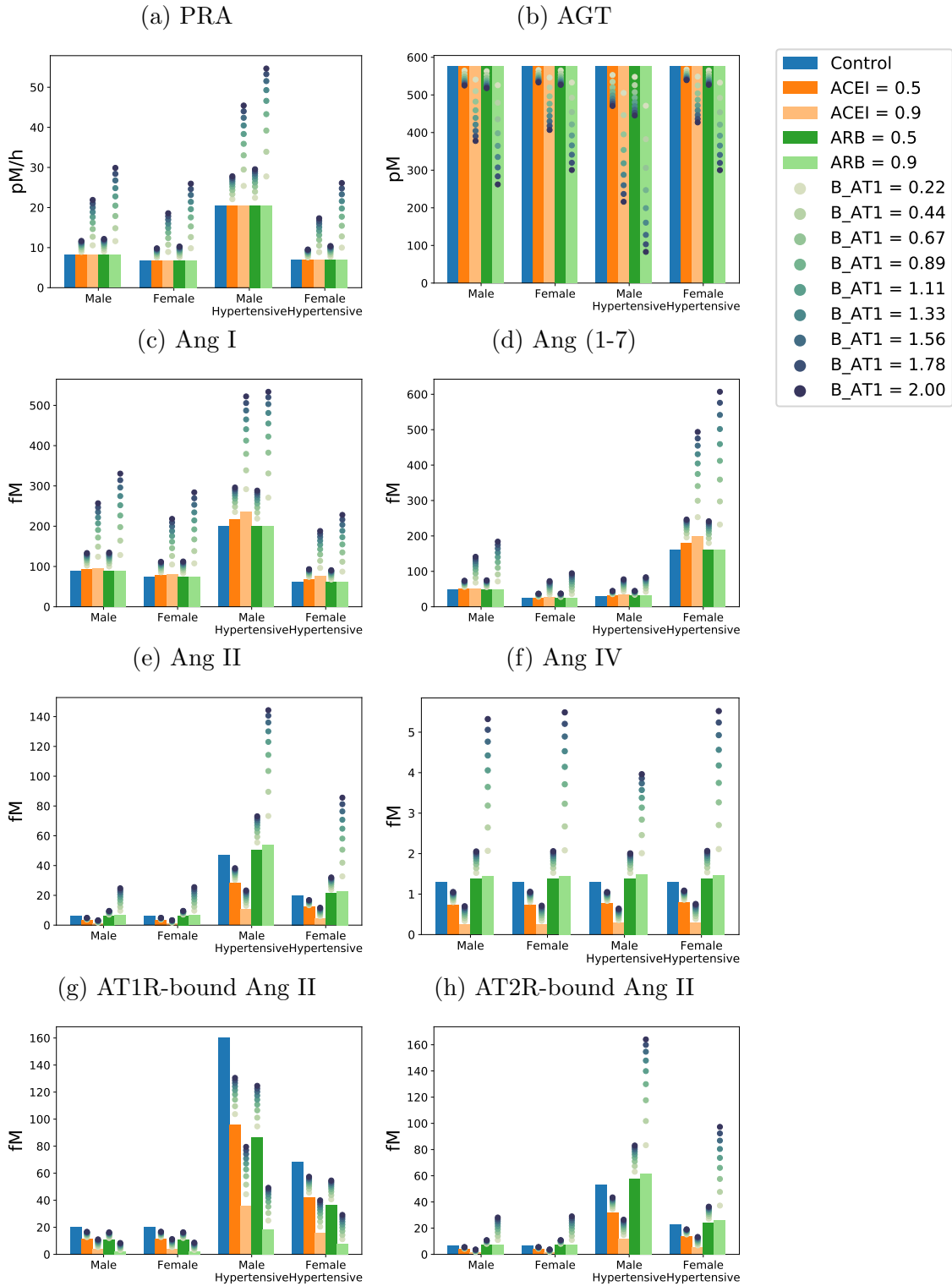


Figure 2.3: Hormone levels after drug treatment simulation with varying levels of feedback. Bars show the system with no feedback ($B_{AT1} = 0$).

compared to 17.15 1/h in male hypertensive rats).

Another of goal of this study is to better understand the sex-specific responses to antihypertensive treatments. To that end, we applied the model to simulate the effects of two major classes of hypertensive drugs: ACEIs and ARBs. Following ACE inhibition, the model predicts a significantly larger absolute decrease in [Ang II] in male hypertensive rats, relative to females. Given that Ang II induces vasoconstriction and raises blood pressure, our model result suggests that ACE inhibition may be more effective in lowering blood pressure in males than in females. That result is consistent with findings by Reckelhoff et al., who measured blood pressure in male and female spontaneously hypertensive rats (SHR) after treatment with ACEIs [190]. They found that the ACEIs reduced blood pressure in both genders of hypertensive rats but significantly more so in male SHR than females (63% versus 40–45%) [190].

Model simulation of ACE inhibition yielded changes that are in general agreement with experimental data [20, 190]. Nonetheless, some discrepancies can be noted. Campbell et al. reports that [Ang I] and [Ang (1-7)] increase by 766% and 1120%, respectively, in male normotensive rats following ACE inhibition [20]. Those observed increases are many folds higher than our model’s predicted increases of 110.3% and 101.6%. To reconcile that discrepancy, we increased the strength of the feedback function (Eq. 2.3). That has the effect of enhancing the model’s response to ACE inhibition, a result that suggests the feedback in the male normotensive rat may be stronger than the model’s baseline assumption. Alternatively, the fact that our model underestimates the changes in [Ang I] and [Ang (1-7)] may imply that the some of the animal’s responses to the drug treatment may be missing from the model.

Model simulation of ARBs indicates similar percentage decreases in [AT1R-bound Ang II] in hypertensive male and female rats, with a larger absolute decrease predicted in hypertensive males. To our knowledge, sex differences in the response of

AT1R-bound Ang II to ARB treatment have not been well characterized in experiments. Thus, we instead compare model predictions to measured blood pressure responses, assuming that high [AT1R-bound Ang II] corresponds to higher blood pressure. Yanes et al. found that following ARB treatment male SHR exhibit a larger blood pressure reduction than female (51.5% versus 39%) [241]. In contrast, Rodrigues et al. reported similar decreases in both sexes after 24 hours of ARB treatment [40]. The discrepancy may be attributed to differences in strains and experimental protocols. Also, comparing [AT1R-bound Ang II] to blood pressure does not take into account the vasodilatory effects of [AT2R-bound Ang II].

The feedback parameter B_{AT1} has a substantial impact on the animal's predicted response to drug treatment. A stronger feedback parameter lowers the percentage change of [AT1R-bound Ang II], indicating a potentially smaller blood pressure response (Fig. 2.3g). However, ACEIs and ARBs have different effects on AT2R-bound Ang II that are changed by varying B_{AT1} . This is worth noting as AT1R-bound Ang II and AT2R-bound Ang II are known to have opposing effects on the body, with AT1R-bound Ang II increasing blood pressure and AT2R-bound Ang II decreasing blood pressure. A stronger feedback function causes AT2R-bound Ang II to decrease less with ACEI and to increase more with ARB while a weaker feedback function causes AT2R-bound Ang II to decrease more with ACEI and to increase less with ARB. This suggests that the feedback function determines the balance in receptor responses to drug treatment. Since AT1R and AT2R receptors have opposing effects on the body, the balance between them could determine the difference between the animal's responses to ARB.

We offer two possible explanations for why ARBs may be more effective in women than ACEIs [191]. First, AT2R-bound Ang II may have a stronger effect on the body in women than in men. AT2R-bound Ang II causes vasodilation and ACEIs decrease

[AT2R-bound Ang II] by a similar percentage in hypertensive males and females but by a larger amount in hypertensive males. In both sexes the benefit from a drop in [AT1R-bound Ang II] outweighs the harm from a drop in [AT2R-bound Ang II] but more so in males than in females. Since we see a greater blood pressure reduction yet a larger absolute drop in [AT2R-bound Ang II] from ACEI in males, the difference must be in how the body responds to a drop in [AT2R-bound Ang II] in each sex. Second, women may have a stronger feedback loop than men. This would cause ACEIs to reduce [AT1R-bound Ang II] less in women than in men and thus cause less vasodilation (Fig. 2.3g). A stronger feedback loop in women would also mean that ARBs increase [AT2R-bound Ang II] in women more than in men (Fig. 2.3h). Thus women would have a stronger vasodilatory response. Both factors provide adequate explanation for why ARBs may be more effective in women than ACEIs while the opposite is true for men [215].

A limitation of the present model is that there is not sufficient data to fully characterize the system. For instance, because AT1R-bound Ang II and AT2R-bound Ang II levels have not been determined, the present model assumes that their values are proportional to the corresponding Ang II level. One consequence of this assumption is that c_{AT1R} and c_{AT2R} are identical among all groups of rats. However, normotensive females have been shown to have higher levels of AT2 receptors than normotensive males [243, 88] while hypertensive male have higher levels of AT1 receptors and a similar level of AT2R than hypertensive females [210]. Also, the present model predicts a higher c_{ACE2} (conversion from Ang II to Ang (1-7)) in hypertensive females compared to hypertensive males. However, experimental results point to higher ACE2 activity in normotensive and hypertensive males as compared to females [243]. Despite this discrepancy, our model still supports the higher expression of Ang (1-7) found in females [88] by predicting a much higher c_{ACE} in females (Table 2.2).

This model is not a complete diagram of the RAS. Instead it limits the number of model parameters (and the inevitable degree of uncertainty) by focusing on the more well studied components. The model does not include the conversion of Ang I to Ang (1-9) by ACE2 [154], Ang (1-7) to Ang (1-5) by ACE, or the binding of Ang (1-7) to its receptor. Our model contains a simplified conversion of Ang II to Ang IV by skipping the intermediate form of Ang III [24]. Despite not representing the influence of these reactions and hormones on blood pressure, our model still captures the actions and responses of the two major vasoactive hormones, Ang II and Ang (1-7), to antihypertensive treatment. Expanding our model to include Ang (1-7) receptors could be useful to explore other options for antihypertensive therapies. Ang (1-7) stimulation of vasodilation through the production of nitric oxide [24] suggests that drug treatments targeting NEP activity, ACE2 activity or Ang (1-7) receptors may be particularly effective for females in which Ang (1-7) is expressed at higher levels.

Chapter 3

Sex-specific Long-term Blood Pressure Regulation: Modeling and Analysis

3.1 Introduction

¹Hypertension is a global health challenge: it affects one billion people and is estimated to account for $> 60\%$ of all cases or types of cardiovascular disease. Interestingly, women have lower blood pressure than men before menopause but higher afterwards [83, 197]. Yet, hypertensive men and women are typically treated using the same approach. In part due to our insufficient knowledge regarding sex-specific blood pressure regulation mechanisms, fewer women achieve blood pressure control compared to men, even though compliance and treatment rates are higher in women [72]. These data highlight the critical need to better understand the mechanisms of blood pressure control in both sexes and cast doubt on the current “one size fits all” therapeutic approach.

Sex differences in blood pressure and the prevalence of hypertension have been reported in a number of mammalian and avian species [201]. In humans [240] and in genetic models of hypertension such as spontaneously hypertensive rats (SHR) and Dahl salt-sensitive rats [171], males develop earlier and more severe hypertension than females. To date, the mechanisms underlying male-female differences in blood pressure control remain incompletely understood.

¹This chapter was published as [137]. Anita T. Layton contributed with model and simulation design, edits, and revisions.

Hypertension is undoubtedly a multifactorial disease with contributions from and affecting multiple organs [38, 77, 68, 69, 17, 178]. In particular, the kidney is a key (albeit not sole) determinant of blood pressure and of sex differences in hypertension [236]. That role is evident in transplantation studies, where blood pressure “goes with” the kidney: transplanting a kidney from a hypertensive rat into a normotensive rat induces hypertension in the recipient [13]. Essential for the kidney’s long-term control of blood pressure is the pressure-natriuresis mechanism, whereby increases in renal perfusion pressure lead to increases in Na^+ excretion, which in turn lowers salt and water retention and reduces effective circulating volume. Under physiological conditions, females exhibit a leftward shift in the pressure-natriuresis relation relative to males, such that females excrete the same amount of Na^+ as males at a lower arterial pressure [87, 110]. Pressure-natriuresis responses encompass multiple levels of Na^+ transporter regulation [149, 150], and are substantially modulated by the renin-angiotensin system (RAS) [156]. The RAS is a non-sex hormonal system critical for maintaining blood pressure and effective circulating volume. For instance, one of the peptides angiotensin (Ang) II, through the angiotensin II type 1 receptor (AT1R), induces vasoconstriction and, via its effects on kidney function, enhance Na^+ and fluid retention. These vascular and tubular actions serve to maintain or raise blood pressure. However, Ang II can also bind to the angiotensin II type 2 receptor (AT2R) which induces vasodilation.

In the past few years, an explosion of data has emerged concerning sex differences in the RAS [145, 161, 89, 115], in kidney function [87, 30, 82], and in responses to anti-hypertensive therapies targeting the RAS. For instance, the benefits of chronic treatment of angiotensin converting enzyme inhibitors (ACEI) in women have been reported to lessen over time [52], while angiotensin receptor blockers (ARB) reduce blood pressure more in women than in men [22]. That observed stronger advantage

of ARB over ACEI in women relative to men may be attributed to the sex differences in intrarenal RAS components. To identify the physiological mechanisms underlying those differences, we develop *sex-specific* computational models of blood pressure control that include the kidney and the RAS. Our model is based on major components of the seminal computational model for long-term blood pressure regulation by Guyton et al. [78]; that model has since been revised and extended by a number of researchers [103, 80, 1, 95, 222]. However, none of these models are gender specific. Thus, the present *sex-specific models* are the first to capture the key sex differences in blood pressure regulation mechanisms. This distinguishing feature allows our models to identify the physiological mechanisms that lead to the sexual dimorphism in the pathophysiology of hypertension and discrepancies in men’s and women’s responses to ACEI and ARB.

3.2 Materials and methods

3.2.1 Blood pressure regulation model

The present models are an expansion of the long-term blood pressure regulation models by Hallow et al. [80] and by Karaaslan et al. [103], which are in terms based on the model by Guyton et al. [78]. These models describe, using a large system of coupled nonlinear algebraic differential equations, the interactions among the cardiovascular system, the renal system, the renal sympathetic nervous system, the endocrine (renin-angiotensin) system, and how these systems regulate blood pressure and respond to various perturbations. For instance, renal blood flow is adjusted, via renal autoregulatory mechanisms [208, 209], according to hormonal and nervous inputs; and renal blood flow determines, in part, Na^+ excretion, which impacts blood pressure. We

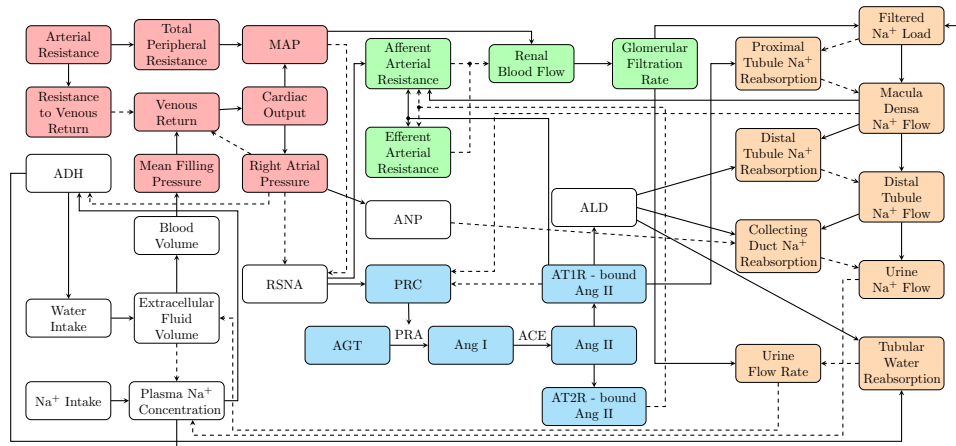


Figure 3.1: Schematic diagram of blood pressure regulation. Red nodes denote variables that describe cardiovascular function; green nodes, renal hemodynamics; orange nodes, renal Na⁺ handling and urine production; blue nodes, the RAS. ADH, antidiuretic hormone; MAP, mean arterial pressure; ANP, atrial natriuretic peptide; RSNA, renal sympathetic nervous activity; PRC, plasma renin concentration; PRA, plasma renin activity; AGT, angiotensinogen; Ang I, angiotensin I; Ang II, angiotensin II; AT1R-bound Ang II, angiotensin II type 1 receptor bound angiotensin II; AT2R-bound Ang II, angiotensin II type 2 receptor bound angiotensin II; ALD, aldosterone.

incorporate the RAS as done in [80] while keeping the single nephron model as done in [103].

A major goal of this study is to identify the mechanisms that underlie the stronger cardiovascular benefits of ARB over ACEI in women compared to men. To that end, we incorporate into the published blood pressure regulation models [80, 103] a detailed, sex-specific representation of the RAS, the target of ACEI and ARB. The RAS model is adopted from a rat RAS model previously published by us [136], with parameters refit separately for men and women (see below). Sex-specific model parameters are identified to represent the well-known sex differences in the RAS and in renal sympathetic nervous activity (RSNA; see below). A schematic diagram of the blood pressure regulation model is shown in Fig. 3.1. Model equations and parameters not described in detail here can be found in Ref. [103].

3.2.2 Renin-angiotensin system model

The present models are the first long-term blood pressure regulation models to include a sex-specific RAS component. It describes the reaction cascade from angiotensinogen (AGT) to Ang (1-7)/Ang II/Ang IV. A schematic diagram that depicts that reaction cascade is shown in Fig. 3.2. Below we describe the RAS model equations.

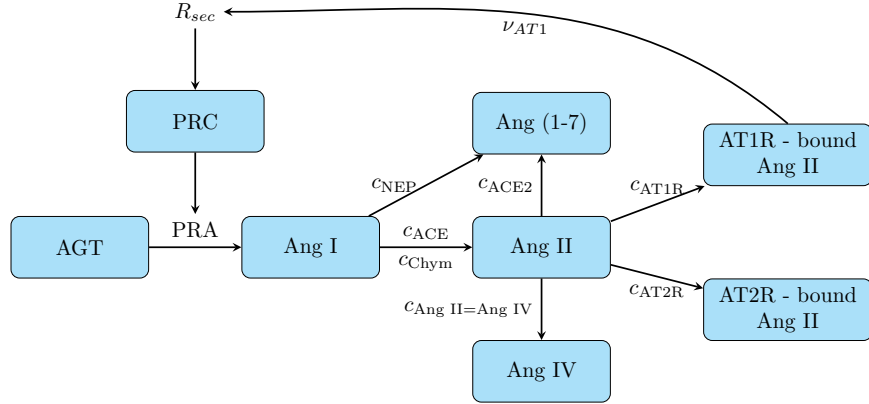


Figure 3.2: Schematic diagram of the renin-angiotensin system. Corresponds to the blue nodes in Fig. 3.1 with added details.

AGT is catalytically cleaved by plasma renin activity (PRA) to produce Ang I. The rate of change of $[AGT]$ is given by the production rate k_{AGT} , its conversion to Ang I, and the decay based on its half life h_{AGT} .

$$\frac{d[AGT]}{dt} = k_{AGT} - PRA - \frac{\ln(2)}{h_{AGT}}[AGT] \quad (3.1)$$

Renin is secreted at the rate R_{sec} . It has a baseline rate of N_{rs} and is dependent on the feedback from $[AT1R\text{-bound Ang II}](\nu_{AT1})$, where A and B are fitting constants taken from [80].

$$\nu_{AT1} = 10^{A-B \times \log_{10}\left(\frac{[AT1R-bound Ang II]}{[AT1R-bound Ang II]_{EQ}}\right)} \quad (3.2)$$

$$R_{sec} = N_{rs} \times \nu_{AT1} \quad (3.3)$$

The plasma renin concentration (PRC) is dependent on R_{sec} and decays with a half life of h_{renin} . PRA is related to [PRC] by a fixed constant of $X_{PRC-PRA}$ which was determined by [80] from the ratio of PRA to PRC in normotensive subjects in the absence of RAS-blocking therapies.

$$\frac{d[PRC]}{dt} = R_{sec} - \frac{\ln(2)}{h_{renin}}[PRC] \quad (3.4)$$

$$PRA = [PRC] \times X_{PRC-PRA} \quad (3.5)$$

Ang I is converted into other forms through angiotensin converting enzyme (ACE), chymase, and neutral endopeptidase (NEP) activity; the respective reaction rate constants are denoted c_{ACE} , c_{chym} , and c_{NEP} . The half life of Ang I is denoted $h_{Ang I}$.

$$\frac{d[Ang I]}{dt} = PRA - (c_{ACE} + c_{chym} + c_{NEP})[Ang I] - \frac{\ln(2)}{h_{Ang I}}[Ang I] \quad (3.6)$$

Ang II is converted from Ang I through ACE and chymase and then converted into Ang (1-7) through ACE2 at the rate c_{ACE2} . Ang II also binds to the AT1R and AT2R at rates c_{AT1R} and c_{AT2R} , respectively. We assume that Ang II, AT1R-bound Ang II, and AT2R-bound Ang II have half lives $h_{Ang II}$, h_{AT1R} , and h_{AT2R} ,

respectively.

$$\begin{aligned} \frac{d[\text{Ang II}]}{dt} &= (c_{\text{ACE}} + c_{\text{chym}})[\text{Ang I}] - (c_{\text{ACE2}} + c_{\text{Ang II}=\text{Ang IV}} + c_{\text{AT1R}} + c_{\text{AT2R}}) \\ &\quad \times [\text{Ang II}] - \frac{\ln(2)}{h_{\text{Ang II}}}[\text{Ang II}] \end{aligned} \quad (3.7)$$

$$\frac{d[\text{AT1R-bound Ang II}]}{dt} = c_{\text{AT1R}}[\text{Ang II}] - \frac{\ln(2)}{h_{\text{AT1R}}}[\text{AT1R-bound Ang II}] \quad (3.8)$$

$$\frac{d[\text{AT2R-bound Ang II}]}{dt} = c_{\text{AT2R}}[\text{Ang II}] - \frac{\ln(2)}{h_{\text{AT2R}}}[\text{AT2R-bound Ang II}] \quad (3.9)$$

Ang (1-7) is converted by NEP from Ang I and by ACE2 from Ang II, and it decays with a half life of $h_{\text{Ang (1-7)}}$.

$$\frac{d[\text{Ang (1-7)}]}{dt} = c_{\text{NEP}}[\text{Ang I}] + c_{\text{ACE2}}[\text{Ang II}] - \frac{\ln(2)}{h_{\text{Ang (1-7)}}}[\text{Ang (1-7)}] \quad (3.10)$$

Ang IV is converted from Ang II at the rate $c_{\text{Ang II}=\text{Ang IV}}$ and decays with a half life of $h_{\text{Ang IV}}$.

$$\frac{d[\text{Ang IV}]}{dt} = c_{\text{Ang II}=\text{Ang IV}}[\text{Ang II}] - \frac{\ln(2)}{h_{\text{Ang IV}}}[\text{Ang IV}] \quad (3.11)$$

3.2.3 Effects of RAS on blood pressure

The RAS regulates blood pressure and fluid balance primarily via its effects on the kidney. Specifically,

- ALD enhances Na^+ reabsorption along the distal tubule and the collecting duct;
- AT1R-bound Ang II enhances Na^+ reabsorption along the proximal tubule, and increases afferent and efferent arteriole resistance.

A less well-studied aspect is the blood pressure-lowering effects of AT2R-bound Ang II: it decreases afferent and efferent arteriole resistance (opposite effect of AT1R-bound Ang II) [243]. In general, males have a higher AT1R:AT2R ratio than females [243, 210]. In fact, in the kidney of the adult male rat, AT2R have been reported to be absent or only present at low levels [215]. Given these observations, it has been proposed that *AT2R-bound Ang II may play a significant role in the sex differences in blood pressure regulation and in patients' responses to ACEI and ARB.*

To test the validity of this hypothesis, we incorporate the vasodilatory effect of AT2R-bound Ang II into *only* the female blood pressure regulation model. The equations below present the interaction between AT2R-bound Ang II and renal vascular resistance. We adopt the following notations. Afferent arteriole resistance (R_{aa}) is the baseline resistance ($R_{aa-ss} = 31.67 \text{ mmHg min l}^{-1}$) multiplied by the effects of RSNA (β_{RSNA}), tubuloglomerular feedback (Σ_{TGF}), the myogenic effect (Σ_{myo}), AT1R-bound Ang II ($\Psi_{AT1R-AA}$) and AT2R-bound Ang II ($\Psi_{AT2R-AA}$). Efferent arteriole resistance (R_{ea}) is the baseline resistance ($R_{ea-ss} = 51.66 \text{ mmHg min l}^{-1}$) multiplied by the effects of AT1R-bound Ang II ($\Psi_{AT1R-EA}$) [80] and AT2R-bound Ang II ($\Psi_{AT2R-EA}$). β_{RSNA} and Σ_{TGF} are given by Karaaslan et al. [103] while $\Psi_{AT1R-AA}$ and $\Psi_{AT1R-EA}$ are given by Hallow et al. [80].

$$R_{aa} = R_{aa-ss} \times \beta_{RSNA} \times \Sigma_{TGF} \times \Sigma_{myo} \times \Psi_{AT1R-AA} \times \Psi_{AT2R-AA} \quad (3.12)$$

$$R_{ea} = R_{ea-ss} \times \Psi_{AT1R-EA} \times \Psi_{AT2R-EA} \quad (3.13)$$

We assume that $\Psi_{AT2R-AA}$ and $\Psi_{AT2R-EA}$ are linearly decreasing functions of [AT2R-bound Ang II], where [AT2R-bound Ang II]_{eq} denotes the equilibrium concentration of the bound peptide.

$$\Psi_{\text{AT2R-AA}} = \begin{cases} 0.025([\text{AT2R} - \text{bound Ang II}]_{\text{eq}} \\ \quad - [\text{AT2R} - \text{bound Ang II}]) + 1 & \text{in females} \\ 1 & \text{in males} \end{cases} \quad (3.14)$$

$$\Psi_{\text{AT2R-EA}} = \begin{cases} 0.021([\text{AT2R} - \text{bound Ang II}]_{\text{eq}} \\ \quad - [\text{AT2R} - \text{bound Ang II}]) + 1 & \text{in females} \\ 1 & \text{in males} \end{cases} \quad (3.15)$$

Afferent and efferent arteriole resistance together control the renal blood flow (ϕ_{rb}).

$$R_r = R_{aa} + R_{ea} \quad (3.16)$$

$$\phi_{rb} = \text{MAP}/R_r \quad (3.17)$$

The glomerular filtration rate (ϕ_{GFR}) is the product of the net filtration pressure (P_f) and a constant glomerular capillary filtration coefficient (C_{gcf}). The net filtration pressure (P_f) is in turn given by the difference between the glomerular hydrostatic pressure (P_{gh}) and the sum of the Bowman hydrostatic pressure (P_B) and the glomerular osmotic pressure (P_{go}). P_B and P_{go} are assumed known a priori. The glomerular hydrostatic pressure (P_{gh}) is calculated from the difference between MAP and the mean afferent arteriolar pressure, which is given by the product of ϕ_{rb} and R_{aa} .

$$\phi_{GFR} = P_f \times C_{gcf} \quad (3.18)$$

$$P_f = P_{gh} - (P_B + P_{go}) \quad (3.19)$$

$$P_{gh} = \text{MAP} - \phi_{rb} \times R_{aa} \quad (3.20)$$

3.2.4 Sex-specific parameters

Besides the effects of AT2R-bound Ang II, the models also represent sex differences in the RAS, baseline aldosterone (ALD) levels, and RSNA sensitivity.

The RAS To identify sex-specific RAS model parameters, we apply RAS hormone peptide levels from the literature (see Table 3.1 and description in Appendix A) and solve for sex-specific RAS reaction rate constants as done in Chapter 2. The goal is to determine the reaction rates in Eqs. 3.1–3.11. These RAS reaction rates, shown in Table 3.2, are used in the hypertensive simulations.

Table 3.1: Human RAS hormone levels.

Hormone	Normotensive		
	Unit	Male	Female
[AGT]	fmol/ml	483900[104]	512770 [205]
[Ang I]	fmol/ml	7.5[168]	7.5[36, 193]
[Ang II]	fmol/ml	4.75[168]	4.75[193]
[Ang (1-7)]	fmol/ml	14[26]	9.33 [216]
[Ang IV]	fmol/ml		
[AT1R - bound Ang II]	fmol/ml		
[AT2R - bound Ang II]	fmol/ml	5.4[141]	5.4[210]

Baseline ALD Males have higher levels of ALD than females [155]. For the male model, we keep the baseline level of 85 ng/l from [103]. For the female model, we

Table 3.2: Reaction rate constants solved for in the linear system for male and female normotensive humans.

Reaction Rate Constant	Unit	Male	Female
[PRC]	fmol/ml/min	17.72	17.72
PRA	fmol/ml/min	18.02	18.02
k_{AGT}	fmol/ml/min	577.04	610.39
c_{ACE}	1/min	0.88	1.41
c_{chym}	1/min	0.09	0.15
c_{NEP}	1/min	0.04	0.06
c_{ACE2}	1/min	0.0078	0.004
$c_{\text{AngII=AngIV}}$	1/min	0.25	0.04
c_{AT1}	1/min	0.17	0.03
c_{AT2}	1/min	0.07	0.04
[AT1R – boundAngII]	fmol/ml	13.99	3.78
[AngIV]	fmol/ml	0.86	1.36

use the ratio of male to female ALD reported in Ref. [155] to determine the female baseline ALD level to be 69.2 ng/l.

RSNA Females have less excitable and more easily repressed RSNA [90]. RSNA is affected by mean arterial pressure (MAP) and right atrial pressure (P_{ra}). Mathematically, RSNA is the baseline level ($N_{\text{rsna}} = 1$) multiplied by the effects of MAP (α_{map}) and the effects of P_{ra} (α_{rap}) as shown in Eqs. 3.21 and 3.22 and defined in Ref. [103]. To qualitatively model the female’s RSNA sensitivity, we introduce a new

step in the female model, Eq. 3.24.

$$\alpha_{\text{map}} = 0.5 + \frac{1.1}{1 + e^{(\text{MAP} - 100\text{mmHg})/15\text{mmHg}}} \quad (3.21)$$

$$\alpha_{\text{rap}} = 1 - 0.008(\text{mmHg})^{-1}P_{\text{ra}} \quad (3.22)$$

$$\text{rsna}_0 = N_{\text{rsna}} \times \alpha_{\text{map}} \times \alpha_{\text{rap}} \quad (3.23)$$

$$\text{rsna} = \begin{cases} \text{rsna}_0^{\frac{1}{\text{rsna}_0}} & \text{in females} \\ \text{rsna}_0 & \text{in males} \end{cases} \quad (3.24)$$

Note that the baseline value of rsna_0 is 1. Thus, the female rsna formula implies lower RSNA levels at higher levels of stimulation (i.e., slower increase in rsna for $\text{rsna}_0 > 1$), and higher RSNA levels with low stimulation.

3.3 Results

3.3.1 Responses to angiotensin infusion

Angiotensin infusion experiments are commonly done in both animals and humans to characterize the body's reaction. We simulate the Ang I and II infusion experiments in [2] by adding to Eqs. 3.6 and 3.7 infusion constants $k_{\text{I}} = 0.44833$ fmol/ml/min and $k_{\text{II}} = 0.3633$ fmol/ml/min, respectively to simulate the constant infusion rate of Ang I and II used in the study.

The key difference between the model's responses to Ang I and Ang II infusion is the direction of change in [Ang I] (Fig. 3.3a). Ang I infusion, naturally, increases [Ang I], but Ang II infusion decreases [Ang I]. The opposite responses can be explained as follows. Both Ang I and Ang II infusion raises [AT1R-bound Ang II]. By means of a feedback mechanism (depicted in Fig. 3.2 and Eq. 3.2), the higher [AT1R-bound

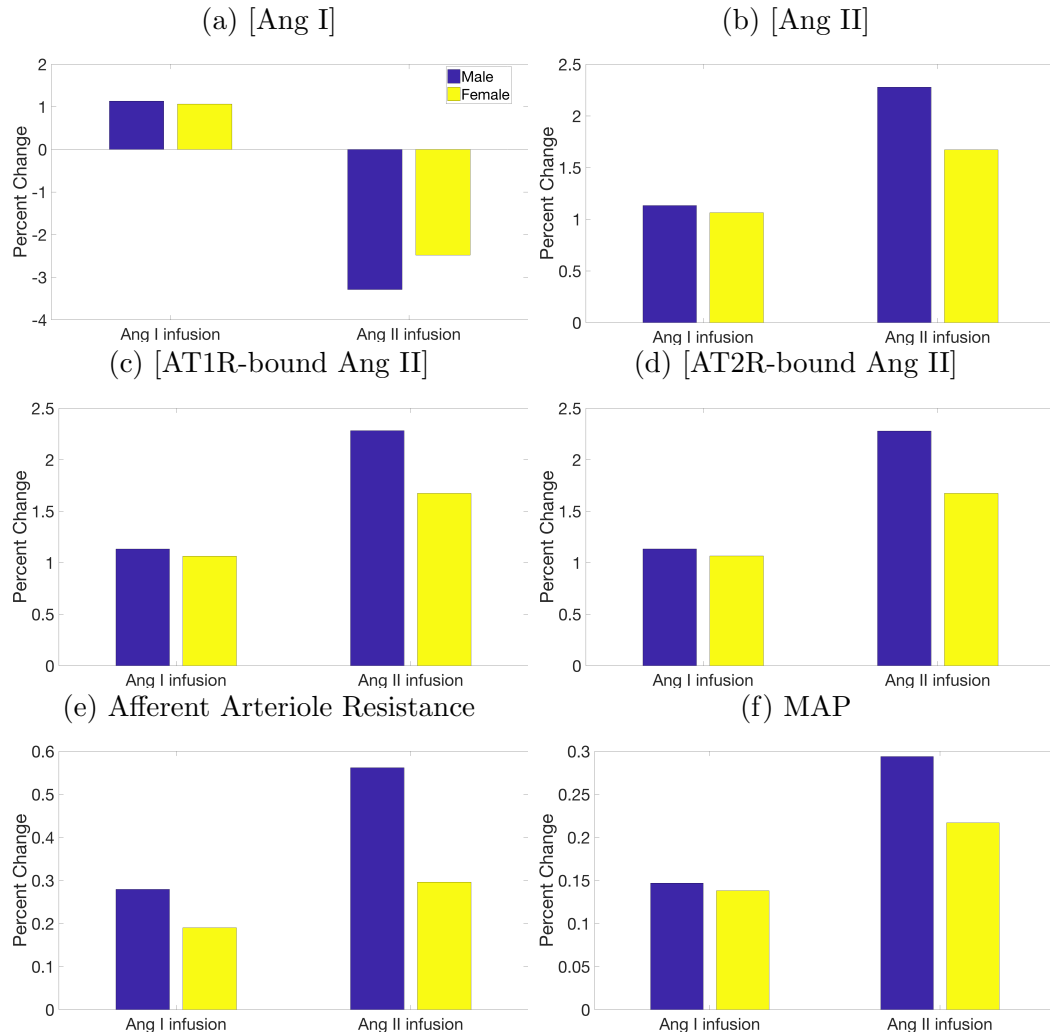


Figure 3.3: Predicted percent change from control due to Ang I and Ang II infusion.

Ang II] suppresses PRA. Taken in isolation, the lower PRA would decrease [Ang I] and [Ang II]. Indeed, this is what was observed with the *Ang II infusion* simulation. For the *Ang I infusion* simulation, however, the added Ang I overwhelms competing factors, resulting in an increase in [Ang I].

The predicted response to Ang II infusion shows a greater sexual dimorphism than Ang I infusion. This can be attributed to the significantly larger male-to-female difference between reaction rate constants in the Ang II reaction (Eq. 3.7) compared to Ang I (Eq. 3.6); see Table 3.2. As a result, a given stimulus generally yields smaller

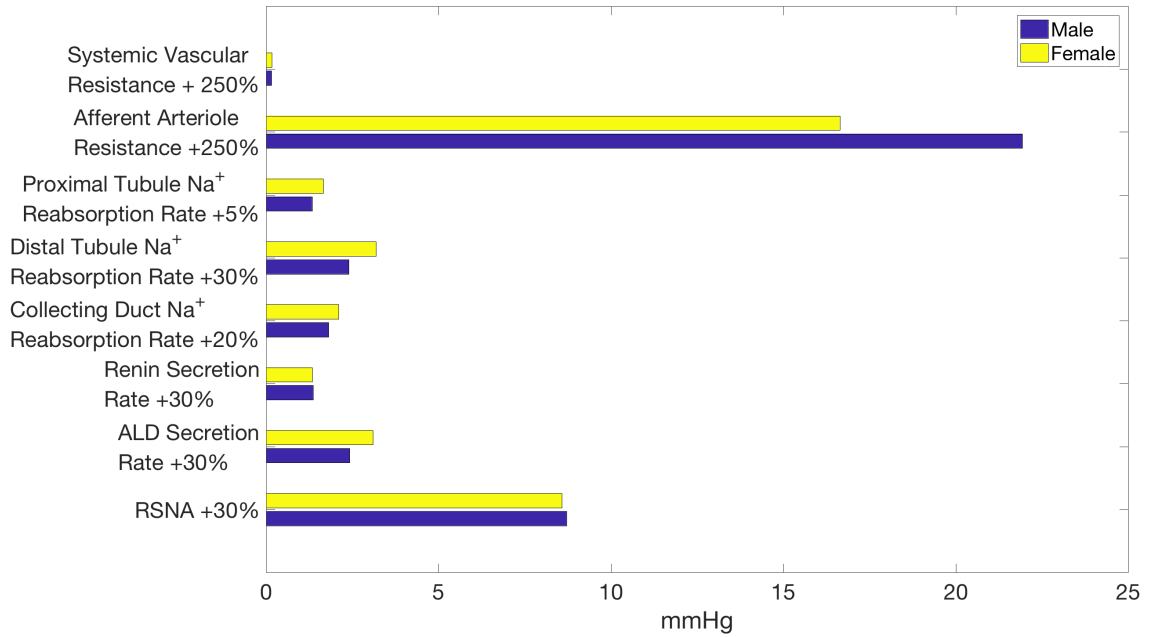
changes in [AT1R-bound Ang II] and [AT2R-bound Ang II] in females than in males (Figs. 3.3c and 3.3d). With both Ang I and Ang II infusion, the lower [AT1R-bound Ang II] in females cause smaller increases in MAP by elevating afferent arteriole resistance, Na^+ reabsorption in the proximal tubule, and Na^+ reabsorption in the distal tubule (through effects on ALD levels) by less than in the male model.

3.3.2 Responses to various hypertensive stimuli

Hypertension is a multifactorial disease, with causes including arterial stiffening, impaired renal Na^+ handling, and stimulation of the renal sympathetic nervous system. To assess the sensitivity of blood pressure to key contributors of hypertension, we induce hypertension, in both the male and female models, by individually increasing the following model parameters: systemic vascular resistance, afferent arteriole resistance, proximal tubule Na^+ reabsorption, distal tubule Na^+ reabsorption, collecting duct Na^+ reabsorption, renin secretion, ALD secretion, and RSNA (Fig. 3.4). The amount of increase for each parameter is selected to represent a large increase within physiological bounds.

Both the male and female models predict that increases in afferent arteriole resistance induce the largest increase in extracellular fluid volume and thus MAP (Fig. 3.4a). Other parameter changes (e.g., RSNA, ALD, etc.) yield smaller effects, in part, because of the activation of the autoregulatory response, which elevates renal blood flow, GFR, and eventually urine and Na^+ excretion, via the dilation of the afferent arteriole. That compensatory response is nullified in the case where afferent arteriole resistance is assumed *a priori* to be elevated. Indeed, increased afferent arteriole resistance lowers renal blood flow and GFR, whereas all other cases predict an opposite change in these variables. It is noteworthy that increased afferent arteriole

(a) Change in MAP.



(b) Change in Extracellular Fluid Volume.

(c) Change in Total Na⁺ Amount.

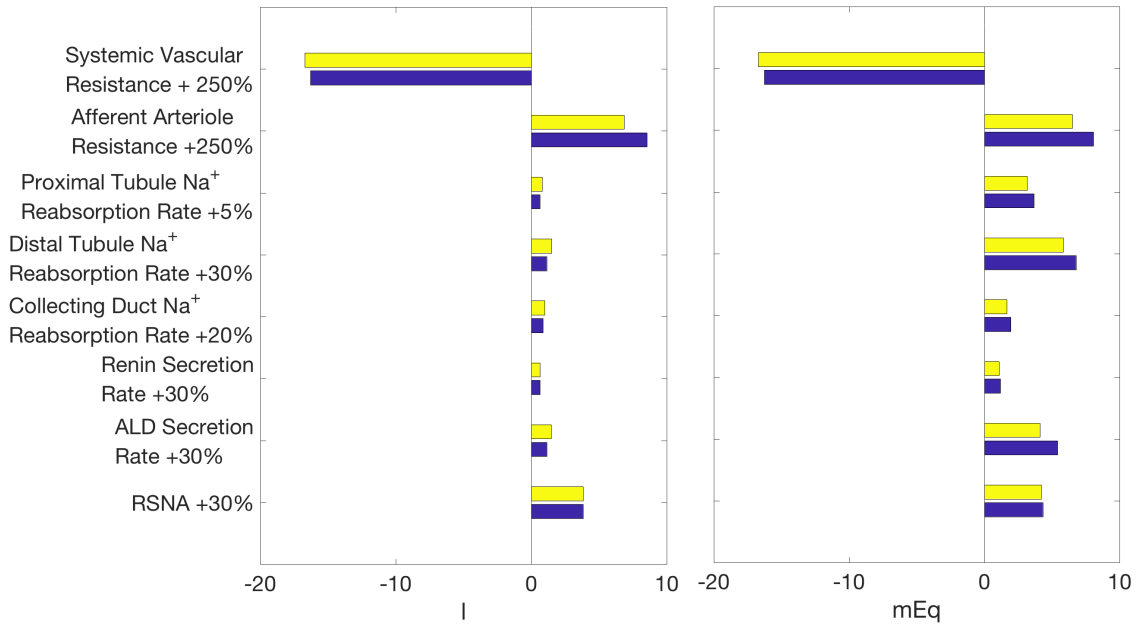


Figure 3.4: Change in selected variables from various causes of hypertension. The chosen increase in afferent arteriole resistance yields the largest rise in mean arterial pressure (MAP).

resistance leads to similar increases in Na^+ amount as other causes of hypertension. Instead, the increase in MAP stems from water retention as extracellular fluid volume increases by double that of the next largest cause of hypertension, RSNA (Fig. 3.4b).

3.3.3 Explaining sex differences in response to hypertensive stimulus

In the next set of simulations, we seek to explain men's higher susceptibility to hypertension, compared to women, in response to increased afferent arteriole resistance. In our models, afferent arteriole resistance is controlled through multiple feedback systems, including RSNA, AT1R-bound Ang II, and AT2R-bound Ang II — all of which exhibit sex differences. When baseline afferent arteriole resistance is elevated, each feedback system reacts to keep the effective afferent arteriole resistance near normotensive levels. Consequently, male afferent arteriole resistance increases from 32.2 mmHg to 52.4 mmHg (a 62.6% increase) while female afferent arteriole resistance only increases from 32.1 mmHg to 48.2 mmHg (a 50.2% increase). Thus, despite the same increase in the baseline afferent arteriole resistance parameter, the female model exhibits a significantly smaller increase in afferent arteriole resistance. This sex difference can be attributed primarily to the stronger RSNA-mediated feedback mechanisms in females: RSNA stimulation of afferent arteriole resistance drops by 51.2% percent in the female model, but only by 47.8% in the male model. Compared to RSNA, the two other (RAS-mediated) feedback systems show a much smaller male-female difference in response to changes in baseline afferent arteriole resistance. Thus we hypothesize that RSNA is the main cause of female resistance to developing hypertension.

To test this hypothesis, we conduct model simulations using the male model with

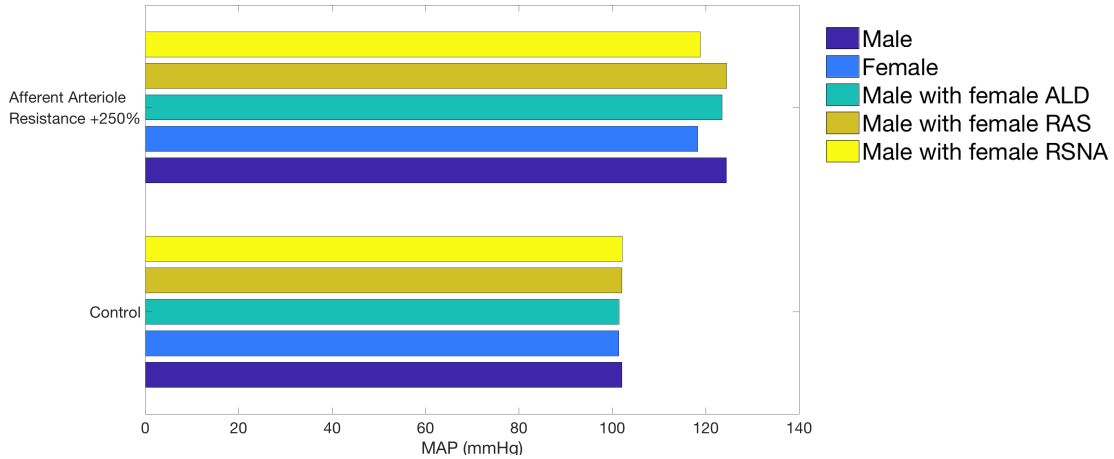


Figure 3.5: Predicted blood pressure in baseline male and female (two blues) and three instances of male model with one trait set to female value (green and two yellows). Blood pressure was obtained for control conditions (lower) and hypertensive conditions induced by elevation in afferent arteriole resistance (upper).

one trait set to the corresponding female value at a time (Fig. 3.5). Specifically, we induce hypertension in three variants of the male model by increasing afferent arteriole resistance by 250%. The three variants are: one with baseline ALD level replaced by the female value (e.g., 69.2 ng/l instead of 85 ng/l), one with female RAS parameters, and another with the female effects of RSNA (Eq. 3.24). Each of these traits were described previously. The variant of the male model that yields blood pressure most similar to the female model will have the female trait that may best explain the sex difference in response to increased afferent arteriole resistance. Results are shown in Fig. 3.5.

The male models with female ALD level or RAS parameters behave similarly to the baseline male model, in the sense that the higher afferent arteriole resistance yields similar increases in MAP. In contrast, the male model with female RSNA acts similarly to the female model. Thus, we conclude that in our models, female protection against increased afferent arteriole resistance is due, in large part, to sex differences in RSNA sensitivity.

3.3.4 Hypertensive drug treatments

In the next set of simulations, we investigate the sex-specific responses to two classes of hypertensive therapies that target the RAS. We focus on renal hypertension, which is caused by the narrowing of the afferent arterioles, modeled by a higher baseline afferent arteriole resistance. We consider two types of anti-hypertensive drugs. The first, ACEI, block ACE from converting Ang I into Ang II. To simulate their effects, we reduce c_{ACE} by a target level κ_{ACE} :

$$c_{ACE} = c_{ACE}^0 \times (1 - \kappa_{ACE}) \quad (3.25)$$

where $0 \leq \kappa_{ACE} \leq 1$. To determine the value of κ_{ACE} , we compare our model to experimental data. Nussberger et al. found that with ACEI administration, Ang II levels in normotensive men dropped by 63% [168]. To achieve this reduction in [Ang II] in our normotensive male model requires a $\kappa_{ACE} = 0.78$. This κ_{ACE} is used in all simulations.

The second class of hypertensive drugs considered are ARB, which stop Ang II from attaching to the AT1R. To simulate their effects, we reduce c_{AT1R} by a target level κ_{ARB} :

$$c_{AT1R} = c_{AT1R}^0 \times (1 - \kappa_{ARB}) \quad (3.26)$$

where $0 \leq \kappa_{ARB} \leq 1$. To determine the level of ARB, we again compare with experimental results. Tsutamoto et al. found that with ARB, Ang II rose by 90% in humans with mild to moderate congestive heart failure [230]. As their patients had normal blood pressure, we compare this to the normotensive male model, which requires $\kappa_{ARB} = 0.67$ to reproduce the experimental rise in Ang II. This κ_{ARB} is used in all simulations.

The effects of ACEI and ARB on MAP in men and women are summarized in Fig. 3.6. These results indicate that ACEI and ARB induce a similar reduction in MAP in men, whereas ARB yield a significantly larger MAP decrease in women than ACEI (Fig 3.6).

We hypothesize that the above difference may be attributable to the dilatory effects of AT2R-bound Ang II on renal vascular resistance, which is present only in the female model (Eqs. 3.14 and 3.15). When this effect is eliminated, then the sex difference in MAP response is much attenuated. (Fig. 3.6). These results suggest that the vasodilatory effects of AT2R-bound Ang II are essential for explaining the significantly stronger MAP-lowering effect of ARB over ACEI seen in women but not in men.

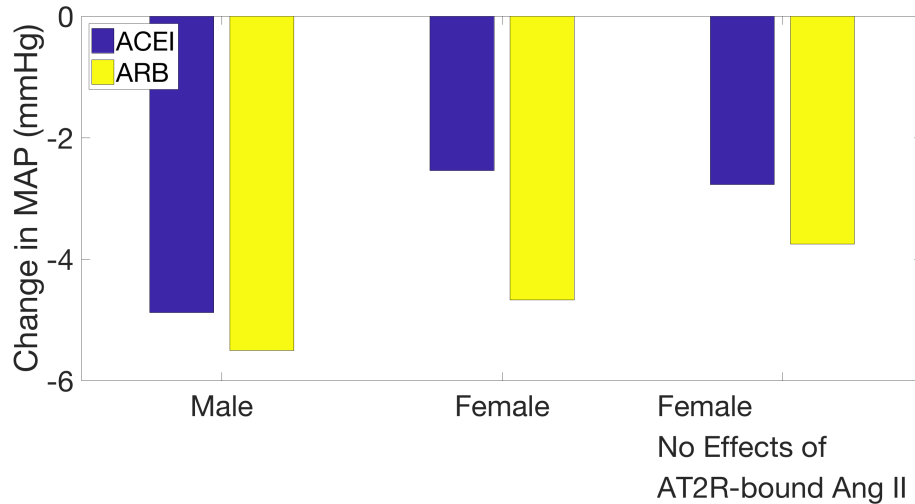


Figure 3.6: Change in MAP following ACEI (blue) and ARB (yellow) administration on hypertensive male model (first group) and on hypertensive female models with and without the vasodilatory effect of [AT2R-bound Ang II] (second and third groups, respectively).

3.4 Discussion

Despite known sex differences in responses to some anti-hypertensive therapies, male and female hypertensive patients are typically treated with the same therapeutic approach. The objective of this study is to apply sex-specific computational models of blood pressure regulation to reveal the contribution of different pathways and systems to the sexual dimorphism in the pathophysiology of hypertension and in the efficacy of commonly prescribed anti-hypertensive therapies, ACEI and ARB. Our models represent physiological systems responsible for long term blood pressure regulation, including the cardiovascular system and the kidney [78], as well as the RAS [80] and RSNA [103]. Major novel aspects of these models include sex specific descriptions of RSNA sensitivity (Eq. 3.24), the RAS (Table 3.2), ALD concentration, and the effects of AT2R-bound Ang II on renal vascular resistance (Eqs. 3.14 and 3.15).

Model simulations indicate a stronger response, measured by increases in MAP, in men compared to women to a number of hypertensive stimuli, including Ang II infusion (Fig. 3.3f) and increased afferent arteriole resistance (Fig. 3.4a). This difference in responses can be attributed to the sex difference in the reaction rate constants of the RAS, to female-specific vasodilatory benefits of AT2R-bound Ang II, and to the RSNA, which is more excitable in the male (Fig. 3.5).

Men’s stronger responses to ACEI and ABR relative to women. The same factors that heighten men’s sensitivity to hypertensive stimuli also enhance their response to anti-hypertensive treatments that target the RAS. For instance, ACEI are predicted to yield a significantly larger decrease in MAP in men (4.88 mmHg) compared to women (2.54 mmHg, Fig. 3.6). This result is consistent with a study by Falconnet et al., who found that chronic ACEI decreased both systolic and diastolic blood pressure in hypertensive men more than women (18.9/13.3 mmHg decrease for

men, vs 11.5/7.8 mmHg decrease for women) [52]. One discrepancy between the simulation and clinical studies is that the model predicts in both sexes significantly smaller absolute MAP reductions than those reported in Ref. [52]. That discrepancy could be due to the effects of ACEI beyond the RAS, such as its inhibition of the degradation of bradykinin, an inflammatory mediator [218]. The build up of bradykinin causes blood vessels to dilate, thereby reducing blood pressure. Bradykinin may also contribute to the enhanced effectiveness of ACEI in men; bradykinin signaling causes nitric oxide release, which reduces oxidative stress [218, 202, 71, 169]. While it is ambiguous if men or women have greater levels of oxidative stress, it has been shown that increasing oxidative stress in male SHR increases blood pressure and vice versa, whereas the same is not true in female SHR [203]. While important, these effects are beyond the scope of the model.

Furthermore, model simulations yield a slightly smaller decrease in MAP due to ARB in the female model (4.67 mmHg) as compared to the male model (5.50 mmHg, Fig. 3.6). This small difference is consistent with the findings that hydrochlorothiazide and ARB treatment together resulted in only a 3 mmHg greater average decrease in the female population than in the male population [204]. In contrast, in a study of ARB treatment in patients with essential hypertension, after 6 weeks of treatment ARB was found to be more effective in women (23 mmHg decrease in systolic pressure) compared to men (15 mmHg) [22]. The above differing, and sometimes contrasting, observations and model predictions are a consequence of the multiple origins of hypertension.

ARB are more effective than ACEI in women, but that difference vanishes in men. Our models predict that ARB reduce blood pressure more than ACEI in females (4.67 versus 2.54 mmHg drop, respectively, Figure 3.6). This result is

consistent with the findings of a study of chronic heart failure patients treated with either ACEI or ARB, which indicate that ARB reduced patient morbidity more than ACEI in females [94]. No difference in patient morbidity was found in males. It is noteworthy that our model only produces this result when the vasodilatory effects of AT2R-bound Ang II are included in the female model; more below.

In contrast, our model predicts no significant difference in MAP reductions in the male model following ACEI or ARB treatment (Figure 3.6). Direct comparison of our model's prediction with clinical or experimental data is difficult, inasmuch as most studies failed to divide blood pressure measurements by sex. A number of studies have shown ARBs and ACEIs to induce similar reductions in blood pressure [66, 41, 97, 54]. In contrast, Mogensen et al. found ARB reduced systolic blood pressure more than ACEI [158] whereas Azizi et al. and Morgan et al. reported the opposite findings [8, 160]. However, as previously noted, none of these studies divided the results by sex. Most studies had a much larger participation from men than women (approximately two thirds male) [66, 97, 54, 158, 8] or were almost completely male [160].

A key contribution of the present study is the explanation of why ARB leads to a larger blood pressure reduction than ACEI in females, but that benefit is not seen in men. Both ACEI and ARB lower MAP by reducing [AT1R-bound Ang II]. In the present model, the only difference between ACEI and ARB is the direction of change of [AT2R-bound Ang II]: ACEI cause a *decrease* in [AT2R-bound Ang II], while ARB cause an *increase*. This opposite effect is the reason why the introduction of the vasodilatory effects of AT2R-bound Ang II into the model is necessary to replicating the differences in reaction to ACEI and ARB in women. Given the observation that AT2R have been reported to be absent or nearly so in the kidney of the adult rat [215], we incorporate the model assumption that AT2R-bound Ang II causes the afferent

and efferent arterioles to dilate in the female kidney (Eqs. 3.14 and 3.15). The novel representation of AT2R-bound Ang II effects leads to a cardiovascular benefit that is specific to ARB and females: while both ACEI and ARB lowers MAP by reducing [AT1R-bound Ang II], in females ARB, but not ACEI, also lowers MAP by reducing arteriolar resistance (via elevating [AT2R-bound Ang II]). The MAP-lowering effect from the reduction in afferent arteriole resistance is then compounded by the RSNA response in female which is more easily repressed compared to men.

The potential importance of sexual dimorphism in the regulation of afferent arteriole resistance is consistent with other model predictions. In their model of pressure-diuresis and naturesis, Beard and Mescam found that the differential regulation of afferent and efferent arteriole resistance was sufficient to explain the observed differences between normotensive and hypertensive Dahl salt-sensitive rats [10].

In summary, the cardiovascular advantages of ARB over ACEI are stronger in women than in men because of (1) the higher AT2R expression in women especially in the afferent and efferent arterioles and (2) a less excitable and more easily repressed RSNA in women.

Model limitations and future extensions. This study presents the first sex-specific computational models of whole-body long-term blood pressure regulation. While comprehensive, the representation of some regulatory processes, especially those concerning renal tubular transport and autoregulation, is relatively simplistic. For example, the renal autoregulatory components, such as the tubuloglomerular feedback and the myogenic response, can be replaced by more comprehensive models (e.g., Refs. [118, 129, 130, 208, 209]) with sex-specific responses incorporated [87]. Also, if one wishes to simulate and compare the actions of different drugs (e.g., diuretics) that target the nephron directly, one may replace the relatively simple re-

nal transport components (orange nodes in Fig. 3.1) by a more detailed epithelial transport model (e.g., Refs. [46, 134, 133, 124, 132, 122, 131]), with known sexual dimorphism in renal transporter expression [199, 234] incorporated as done in Ref. [92, 139]. With the inclusion of a detailed epithelial transport model, the drug's effect on specific transporters can be simulated, with the influence on, e.g., Na^+ transport predicted (rather than specified *a priori*).

Chapter 4

Triple Whammy AKI

4.1 Introduction

¹With cardiovascular disease being the leading cause of death in adults worldwide, prescribing safe and effective antihypertensive therapies is of great concern. However, a common combination of renin-angiotensin system (RAS) inhibitors, such as angiotensin converting enzyme inhibitors (ACEI) or angiotensin receptor blockers (ARB), with diuretics and easily accessible over the counter non-steroidal anti-inflammatory drugs (NSAIDs) can cause kidney damage. This triple therapy, known as “triple whammy,” was associated with a 31% increased risk for acute kidney injury (AKI), compared to patients treated with diuretic and ACEI/ARB only (95% confidence interval 1.12–1.53)[117]. Triple whammy AKI occurs in 0.88% - 22% of triple treatment patients [117, 19]. AKI may be a serious health condition and has major economic impact. For instance, AKI accounts for 5% of hospital budget [34, 233] and 1% of overall health expenditure [109]. Mortality among AKI patients can be as high as 50-80% of cases in specific populations, such as critically ill patients. Understanding how each of these drugs affect renal autoregulation individually and in combination can help medical providers avoid prescribing dangerous combinations in at risk individuals and administer them with confidence to low risk patients, especially to those who may benefit from pain killers for acute or chronic pain relief.

¹This chapter has been submitted for publication as [138]. Francisco J. López-Hernández contributed biological insights and edits. Anita T. Layton contributed with model and simulation design, edits, and revisions.

A goal of this study is to better understand the mechanism by which triple whammy increases the risk of AKI. AKI is marked by higher serum creatinine levels, which indicate a critically low glomerular filtration rate (GFR), according to internationally recognized definitions (i.e. KDIGO) [108] and may be accompanied by low urine flow (less than 400 l/day) [113]. ACEI and diuretics lower blood pressure through increasing urine flow to reduce blood volume. Combined with NSAIDs, these drugs can prevent the body from properly reacting to hypovolemic states, resulting in dangerously low GFR. In fact, RAS inhibitors and NSAIDs interfere with and thus uncouple the renal afferent and efferent arteriole contractility demand generated by diuretic-induced volume loss to maintain GFR, giving rise to a hemodynamic, pre-renal form of AKI [184]. Triple whammy leads to AKI in some patients but not others. Thus, another goal of this study is to identify which individuals may be particularly susceptible to AKI following triple whammy, and which factors may individually render them so.

To achieve these goals, we apply previously published computational models of blood pressure regulation (Chapter 3, [137]). The models were parameterized separately for men and women, and include variables describing circulation, renal function, sodium and water transport through the nephron, and the RAS. The mechanisms affected by ACEI, diuretics, and NSAIDs are included and the model is able to directly predict GFR, which is often difficult to obtain experimentally. To identify risk factors for development of AKI, we simulate single, double, and triple drug treatments for normotensive, hypertensive, male, and female humans. Our simulation results reveal a key role of the myogenic response in determining the risk of AKI. Myogenic response, the mechanism by which afferent arteriole resistance is manipulated to maintain appropriate flow through the nephron, is one of the few regulators of GFR untouched by ACEI, diuretics, and NSAIDs. As such, during triple treatment

the myogenic response plays a larger than usual role in GFR regulation [184]. We hypothesize that individuals with an impaired myogenic response may be particularly susceptible to triple whammy AKI. Additionally, high dosages or low water intake can predispose patients to triple whammy AKI.

4.2 Methods

We applied previously published sex-specific computational models of blood pressure regulation in men and women [137](Fig. 4.1). These models represent the interactions among the cardiovascular system, the renal system, the renal sympathetic nervous system, and the RAS. A large system of coupled nonlinear algebraic differential equations is used to describe how these systems regulate blood pressure and respond to perturbations. For instance, renal blood flow is adjusted, in part, via renal autoregulatory mechanisms [103, 208], according to hormonal and nervous inputs; and renal blood flow, in part, determines Na+ excretion, which in turn impacts blood pressure.

Below we highlight model components that are particularly relevant to the pharmaceutical treatments considered in this study.

4.2.1 Water and sodium intake

Water intake (Φ_{win}) is dependent on the antidiuretic hormone concentration (C_{adh})

$$\Phi_{\text{win}} = \frac{0.0078541}{0.65451 + 18.11 \times C_{\text{adh}}^{-1.607}} - 0.002. \quad (4.1)$$

The parameters were chosen, in part, to ensure that the model can withstand large

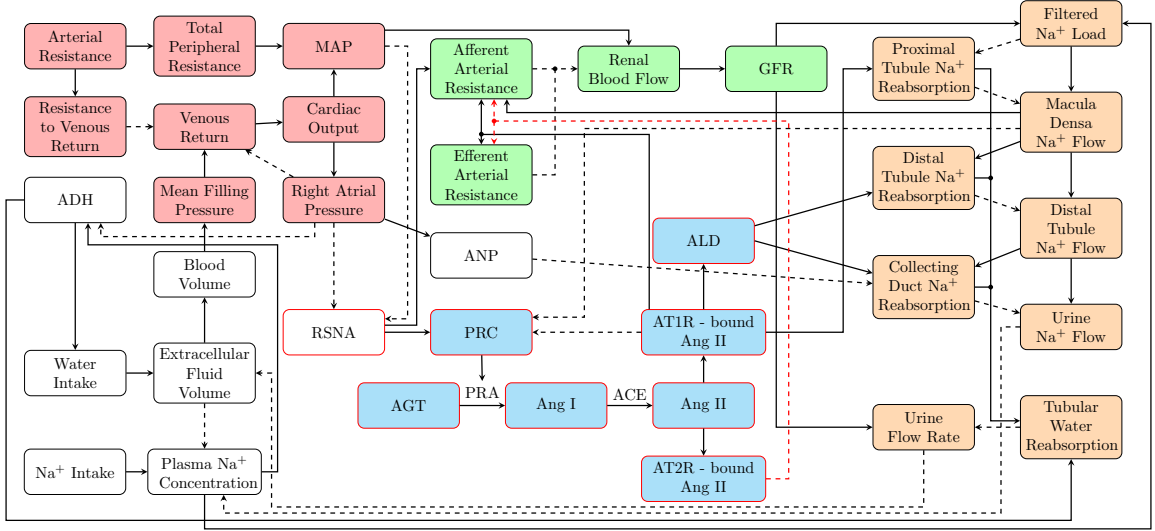


Figure 4.1: Flowchart of the blood pressure regulation model. Red nodes denote variables describing heart function and blood pressure; green nodes, renal function; orange nodes, Na^+ and water reabsorption along a nephron; blue nodes, the renin-angiotensin system (RAS). Red outlines describe sex differences between the male and female models.

increases in urine flow following administration of a diuretic without experiencing extreme hypovolemia.

Low water intake can lead to hypovolemia and low GFR, especially when the mechanisms to enhance renal water retention and to counteract hypovolemia (e.g., via the RAS) are inhibited through drug treatments. As such, in model simulations that consider low water intake, we attenuate the dependence of water intake on the antidiuretic hormone concentration in order to induce hypovolemia and use the following function instead of Eq. 4.1:

$$\Phi_{\text{win}}^{\text{low}} = \frac{0.0177}{3.9271 + 18.22 \times C_{\text{adh}}^{-1.607}} - 0.002. \quad (4.2)$$

Sodium intake (Φ_{sodin}) increases with aldosterone (ALD) concentration (C_{al}).

$$\Phi_{\text{sodin}} = -\frac{0.93}{4.76 + 0.14 \times C_{\text{al}}^{0.765}} + 0.230 \quad (4.3)$$

4.2.2 Renal tubular water reabsorption and urine flow

Previous formulations of this model [80, 103, 137] are limited in that water and Na^+ reabsorption rates are independent of each other. This poses a significant problem when one seeks to understand the impact of inhibiting Na^+ transport (e.g., administration of a diuretic) on urine flow. Thus, to represent the role of transmembrane Na^+ concentration gradient in driving water reabsorption, we introduce the term μ_{Na} in the tubular water reabsorption equation

$$\Phi_{\text{twreab}} = A_{\text{twreab}} - \frac{0.001}{\mu_{\text{adh}}} + (0.8 + 0.08 \tanh(8.5(\mu_{\text{Na}} - 1)))\Phi_{\text{GFR}} \quad (4.4)$$

as

$$\mu_{\text{Na}} = \frac{\Phi_{\text{pt-sodreab}} + \Phi_{\text{dt-sodreab}} + \Phi_{\text{cd-sodreab}}}{\Phi_{\text{pt-sodreab}}^{\text{eq}} + \Phi_{\text{dt-sodreab}}^{\text{eq}} + \Phi_{\text{cd-sodreab}}^{\text{eq}}}. \quad (4.5)$$

The Φ terms in Eq. 4.5 represent predicted Na^+ reabsorption along the three model nephron segments: the “proximal segment (pt)” that includes the proximal tubule and the loop of Henle, the “distal segment (dt)” that includes the distal convoluted tubule and the connecting tubule, and the collecting duct (cd). The superscript “eq” in Eq. 4.5 denotes the equilibrium Na^+ reabsorption values. Model parameters are chosen to increase tubular water reabsorption with enhanced Na^+ reabsorption. A_{twreab} in Eq. 4.4 is chosen separately for each model to yield a baseline value = 0.001 l/min (specifically, male normotensive, $A_{\text{twreab}} = 0.0193$; female

normotensive, 0.0199; male hypertensive, 0.0182; female hypertensive 0.0181).

Urine flow is given by the difference between GFR (Φ_{GFR}) and tubular water reabsorption (Φ_{twreab} , Eq. 4.4).

$$\Phi_{\text{u}} = \Phi_{\text{GFR}} - \Phi_{\text{twreab}} \quad (4.6)$$

Φ_{u} is bounded above 0.06 ml/min during control simulations to maintain a minimal level of metabolic waste excretion, and we use $= 0.027$ ml/min or 389 ml/day (consistent with the definition of oliguria [113]) as a threshold to identify AKI.

4.2.3 Blood volume

Blood volume (V_{b}) is dependent on extracellular fluid volume (V_{ecf}) and is allowed to decrease so that states of extreme loss of extracellular fluid will cause hypovolemia.

$$V_{\text{b}} = 0.35 \times V_{\text{ecf}} \quad (4.7)$$

4.2.4 Macula densa feedback

The macula densa cells sense Na^+ flow entering the distal tubule, and balance SNGFR and thick ascending limb transport capacity via the tubuloglomerular feedback (TGF). When the macula densa cells sense a below-target Na^+ flow, TGF is activated to dilate the afferent arteriole, thereby increasing renal blood flow and SNGFR; and vice versa (Fig. 4.2a). The model afferent arteriole resistance (R_{aa}) is proportional to Σ_{TGF} , which denotes the feedback effect of macula densa Na^+ flow

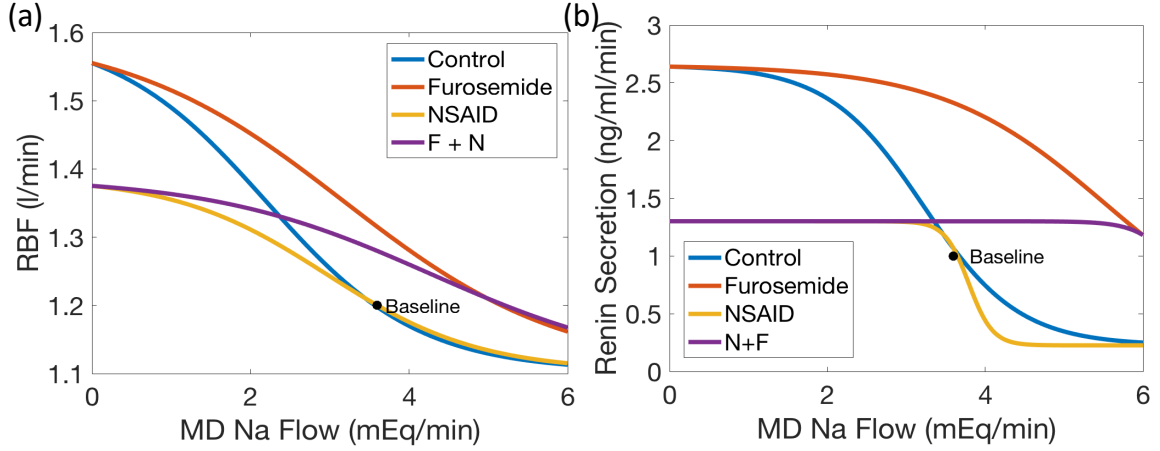


Figure 4.2: Effects of furosemide and NSAIDs on renal blood flow (RBF) and renin secretion. (a) RBF decreases at higher macula densa (MD) Na^+ flow via the tubuloglomerular feedback (TGF), obtained for four treatment conditions: control (no drug), furosemide only, NSAIDs only, and furosemide and NSAIDs (F + N). The effects of furosemide and NSAIDs are represented in the TGF function (Eq. 4.8). (b) Renin secretion decreases at higher MD Na^+ flow. That relation, and how it is affected by the administration of furosemide and NSAIDs, is represented in the feedback function (Eq. 4.9).

($\Phi_{\text{md-sod}}$) (Eq. B.5). TGF is affected by both furosemide and NSAID treatment, represented by the term $\kappa_{f-\text{md}}$ and the indicator function, $\mathbb{I}()$, respectively, in Eq. 4.2. How the effects of these two drugs are fitted is discussed in later sections.

$$\Sigma_{\text{TGF}} = 0.3408 + \mathbb{I}(\text{NSAID}) \times 0.3032 + \frac{3.449 - \mathbb{I}(\text{NSAID}) \times 2.261}{3.88 - \mathbb{I}(\text{NSAID}) \times 1.852 + e^{((1-\kappa_{f-\text{md}})\Phi_{\text{md-sod}} - 3.859 \text{ mEq/min})/(-0.9617 \text{ mEq/min})}} \quad (4.8)$$

Another feedback mechanism is one in which low macula densa Na^+ flow triggers increased renin secretion to activate the RAS and to enhance Na^+ retention, and vice versa (Fig. 4.2b). Renin secretion (R_{sec}) is proportional to $\nu_{\text{md-sod}}$, which is the feedback effect of $\Phi_{\text{md-sod}}$. This feedback effect is changed by both furosemide and NSAID treatment, represented by the term $\kappa_{f-\text{md}}$ and the indicator function, $\mathbb{I}()$,

respectively:

$$\begin{aligned} \nu_{\text{md-sod}} &= 0.2262 \\ &+ \frac{28.04 + \mathbb{I}(\text{NSAID}) \times 55.36}{11.56 + \mathbb{I}(\text{NSAID}) \times 66.04 + e^{((1-\kappa_f-\text{md})\Phi_{\text{md-sod}}-1.637 \text{ mEq/min})/(0.6056 \text{ mEq/min})}} \end{aligned} \quad (4.9)$$

4.2.5 Simulating administration of ACEI

To simulate the effect of ACEI, we reduce the rate at which Ang I is converted to Ang II, denoted c_{ACE} (see Eq. B.77), by a target level κ_{ACEI} :

$$c_{\text{ACE}} = c_{\text{ACE}}^0 \times (1 - \kappa_{\text{ACEI}}) \quad (4.10)$$

where c_{ACE}^0 is the baseline Ang I-to-Ang II conversion rate, and $0 \leq \kappa_{\text{ACEI}} < 1$. To determine the value of κ_{ACEI} , we compared our model to experimental data. Delles et al. [42] found that in hypertensive male patients, ACEI reduced mean arterial pressure (MAP) by 11% and did not change GFR. To replicate this in our model, we use $\kappa_{\text{ACEI}} = 0.76$ for all models.

4.2.6 Simulating administration of furosemide

Furosemide, a loop diuretic, inhibits the $\text{Na}^+\text{-K}^+\text{-Cl}^-$ cotransporter 2 (NKCC2) along the thick ascending limb of the loop of Henle. In our model, this is included in the Na^+ reabsorption of the model proximal segment, which consists of the proximal convoluted tubule, S3 segment, and the loop of Henle. To model the inhibition of NKCC2, we reduce fractional model proximal segment Na^+ reabsorption ($\eta_{\text{pt-dosreab}}$)

by a percentage κ_f , $0 \leq \kappa_f < 1$. As such, Eq. B.18 becomes

$$\eta_{\text{pt-sodreab}} = (1 - \kappa_f) \times \eta_{\eta\text{-pt}} \times \gamma_{\text{filsod}} \times \gamma_{\text{at}} \times \gamma_{\text{rsna}}. \quad (4.11)$$

Furosemide also inhibits the NKCC2 transporters in the macula densa, which interferes with macula densa Na^+ signaling and has implications on TGF signal and renin secretion. We describe the inhibition of Na^+ sensing in the macula densa cells by $\kappa_{f\text{-md}}$, where $0 \leq \kappa_{f\text{-md}} < 1$. By multiplying $\Phi_{\text{md-sod}}$ by $(1 - \kappa_{f\text{-md}})$ in Eqs. 4.8 and 4.9, we model the effect of NKCC2 inhibition by furosemide such that the macula densa cells only sense a fraction of the Na^+ flowing past in the lumen.

Experimental treatment with 40 mg i.v. furosemide results in a 70% increase in ALD [227], while a 0.5 mg/kg per hour i.v. over 30 min caused a 12% decrease in GFR, and a 10-fold increase in urine flow [217]; these studies did not separate men and women. In another study, plasma renin activity (PRA) for men and women were reported to increase by 132% and 117% increase, respectively, when given a 40 mg dose intravenously [102]. While these exact changes could not be matched, $\kappa_f = 0.15$, $\kappa_{f\text{-md}} = 0.4$ were chosen to be used in all models to increase urine flow, ALD, and PRA, as well as decrease GFR.

4.2.7 Simulating administration of NSAIDs

NSAIDs inhibit the COX-1 and COX-2 enzymes, which play a key role in macula densa Na^+ signaling pathway during low Na^+ flow. The mechanisms that are affected by NSAIDs include TGF and a feedback effect on renin secretion.

According to Araujo et al. [4], COX-2 inhibition reduces TGF by 46%. To match this, in Eq. 4.8 with NSAID treatment and during low Na^+ flow, the change in RBF

is reduced by 46% (Fig. 4.2a).

Traynor et al. [228] found that with COX-2 inhibition, the increased renin secretion in response to low lumen sodium flow is eliminated. Thus, with NSAID treatment, Eq. 4.9 is designed to level off during low Na^+ flow, stopping renin secretion from increasing (Fig. 4.2b).

4.2.8 Simulating impaired autoregulation

TGF and myogenic activity accounts for 90% of renal autoregulation [114]. Under double treatment with ACEI and furosemide, the body's ability to defend against hypovolemia through the RAS and renal sympathetic nervous activity (RSNA) is eliminated and regulation of GFR falls to TGF and the myogenic response [184]. Hence, we assess the extent to which patients who have impaired myogenic regulation are at increased risk for double or triple whammy AKI. To investigate this, we describe an impaired myogenic effect using the following formula to link glomerular hydrostatic pressure to afferent arteriole resistance (Eq. B.5):

$$\Sigma_{\text{myo}} = 1.2 + \frac{0.3}{1 + 9e^{-0.1(P_{\text{gh}} - 62 \text{ mmHg})}}. \quad (4.12)$$

Compared to the analogous formula for normal myogenic effect (Eq. B.8), the above formula attenuates the reduction (rise) in afferent arteriole resistance during low (high) levels of glomerular hydrostatic pressure, thereby narrowing the range of blood pressure within which GFR is stable; see Fig. 4.3.

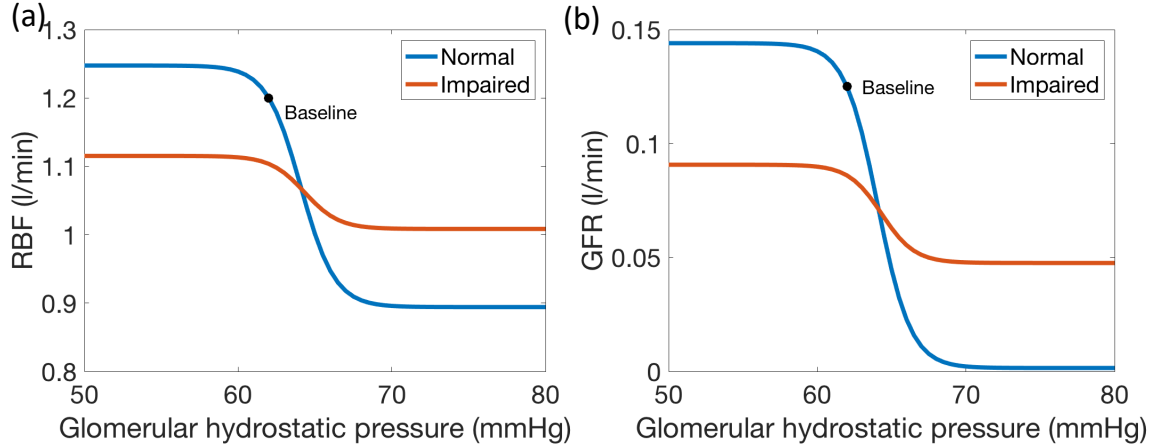


Figure 4.3: The myogenic response. The relationship between glomerular hydrostatic pressure and renal blood flow (a) and between glomerular hydrostatic pressure and GFR (b) due to the myogenic effect, showing both the normal and impaired myogenic effect. Baseline indicates the control steady state values.

4.3 Results

The model is run forward in time for 2 simulated days. To simulate the administration of ACEI or furosemide, the relevant parameters (κ_{ACEI} , κ_f , κ_{f-md}) are gradually increased over the initial 30 minutes from the baseline values to their target values. Average urine flow, GFR, and MAP for each day are then calculated.

Hypertension is a multifaceted disease. The scope of the present study is limited to hypertension that is induced by an over-active RSNA. That is represented by increasing the baseline RSNA parameter (N_{rsna} , see Eq. B.1) by 2.5-fold. This results in constriction of the afferent and efferent arterioles, stimulation of the RAS, and enhanced renal Na^+ reabsorption.

4.3.1 Response to hypertensive stimuli

Key model predictions [urine flow, GFR, MAP, PRA] are shown in Fig. 4.4. The simulations without drug treatment are labelled “Control.” Note that in control sim-

ulations, the MAP increase predicted for the hypertensive female model is lower than the hypertensive male model. Our model includes sex differences in RSNA, in that the female model has less excitable and more easily repressed RSNA [137, 90]. This leads to a smaller actual increase in female RSNA, and thus a smaller increase in MAP (Fig, 4.4a).

In our model, a higher MAP raises GFR in control simulations (Fig. 4.4). Specifically, the 51.8 and 39.2 mmHg increases in MAP predicted in the male and female hypertensive models are associated, respectively, with 11.1% and 9.4% increases in GFR. In contrast in population studies, higher daytime diastolic blood pressure is correlated with lower GFR [147]. This paradoxical effect may be attributable to the renal damage caused by elevated blood pressure, which is not captured in our hypertensive models.

4.3.2 Response to drug treatments

Key model predictions for single drug treatments are shown in Fig. 4.4, labelled “ACEI”, “Furosemide,” and “NSAIDs.” ACEI and, to a larger extent, furosemide lower MAP and GFR, and those decreases are larger in hypertensive models more than in normotensive models. For both normotensive and hypertensive models, all single drug treatment simulations yield urine flow substantially above threshold for AKI, with the exception of NSAID single treatment in normotensive models.

Experimentally, NSAID treatment causes little or no increase in MAP in normotensive patients, whereas an increase in MAP has been reported in hypertensive patients (3.32 mmHg [181]; 5mmHg [175, 99]). However, that increase in MAP does not come through water and Na^+ retention [99] but rather through an increase in arterial pressure and peripheral resistance and possible decline in cardiac output [166].

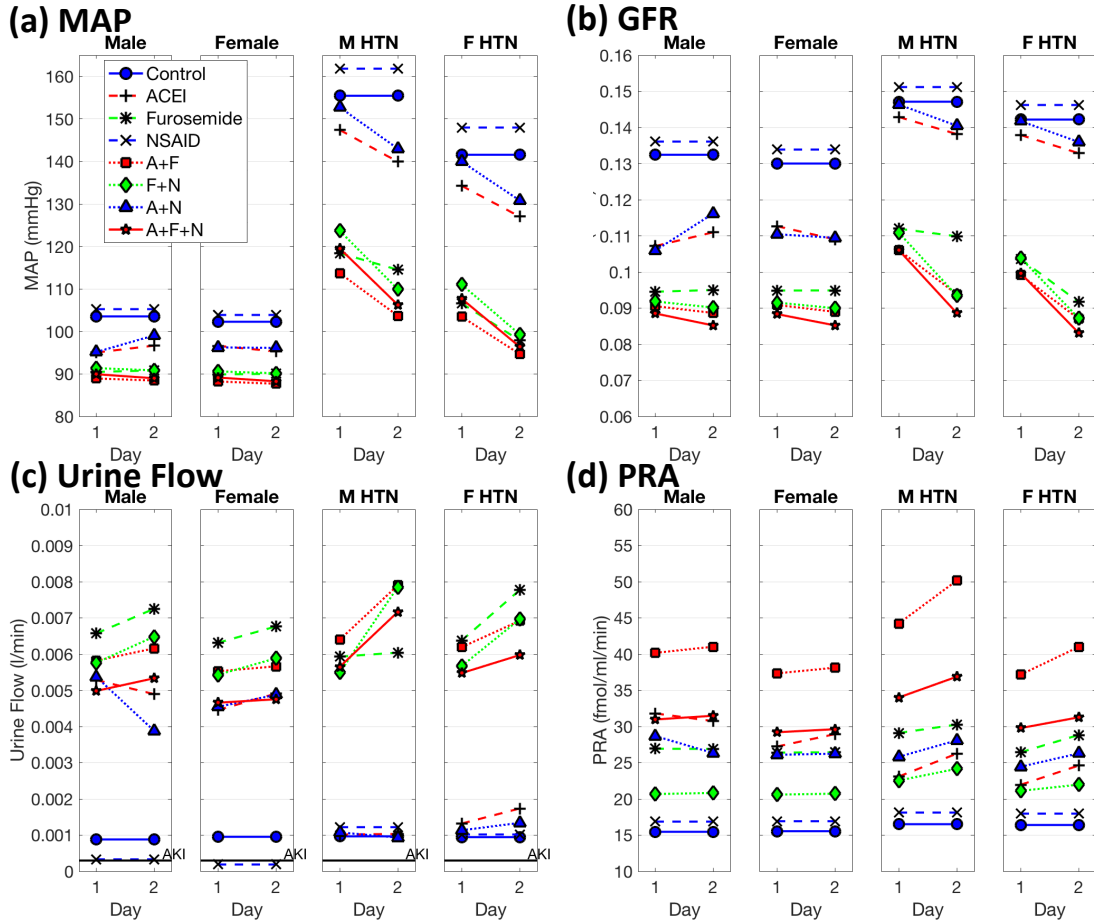


Figure 4.4: Effect of drug treatments on renal and cardiovascular function. Shown are key model predictions for male normotensive (“Male”), female normotensive (“Female”), male hypertensive (“M HTN”), and female hypertensive (“F HTN”) models, obtained under control conditions (i.e., no drug) and following single, double, and triple drug treatments. (a) mean arterial pressure (MAP); (b) glomerular filtration rate (GFR); (c) urine flow; (d), plasma renin activity (PRA). Two data points are computed for each case, corresponding to key variables averaged over days 1 and 2. Triple treatment yields the lowest GFR (c), albeit not to a level indicative of acute kidney injury.

NSAIDs has also been observed to lead to reductions in PRA and ALD [175]. While the present models do not predict the drop in PRA (Fig. 4.4d) or ALD (results not shown), they do predict a slight increase in MAP following NSAID treatment alone (Fig. 4.4a).

We then consider combination treatments involving pairs of drugs. Key results are shown in Fig. 4.4. ACEI and furosemide together create a stronger MAP lowering effect in all models compared to either single treatment. In contrast, the addition of NSAIDs does not have a significant effect on MAP lowering effect of furosemide in any model. None of the double treatments reduces urine flow below the AKI threshold.

Triple treatment involving ACEI, furosemide, and NSAIDs results in MAP levels similar to double treatment with ACEI and furosemide. All simulations are above the urine threshold for AKI (Fig. 4.4c). A larger decrease in GFR is predicted for the hypertensive models (39.8% and 41.5% in male and female, respectively) than the normotensive models (35.7% and 34.5% in male and female, respectively), stemming from a larger drop in MAP in the hypertensive models. However, GFR drops to slightly lower levels in the female hypertensive model. Taken together, none of the models predict critically low GFR following triple treatment. This result may not be unexpected, given that only a fraction (0.8%-22%) of patients subjected to triple treatment actually suffer pre-renal azotemia stemming from low GFR [117, 19]. As such, a hypertensive patient without additional autoregulatory problems is unlikely to suffer from AKI following triple treatment.

4.3.3 Risk factors for AKI

We conduct simulations to assess the effects of key risk factors on the predicted response to double and triple treatments. The risk factors considered are impaired renal

autoregulation, low water intake, and high drug dosages. Impaired renal autoregulation is simulated by attenuating the myogenic response (Fig. 4.3). Low water intake is simulated by attenuating the response of water intake to ADH concentration (Eq. 4.2). High dosages are simulated by increasing the parameters associated with ACEI and furosemide: $\kappa_{\text{ACEI}} = 0.9$, $\kappa_f = 0.3$, $\kappa_{f\text{-md}} = 0.5$ (compared to standard dosage values of 0.76, 0.15, and 0.4, respectively), and we further assume that NSAIDs completely inhibit TGF. Predicted MAP, GFR, and urine flow values at the end of the second day are shown in Fig. 4.5 for the male and female hypertensive models.

Recall that in the absence of these risk factors, ACEI and furosemide together lower GFR (by 36.2% and 38.8% in hypertensive male and female models, respectively) further than single treatments or double treatments with NSAIDs (Fig. 4.4b). When the effect of ACEI and furosemide is not counteracted by a robust myogenic response, GFR is further reduced (by 38.7% and 39.7%). When further aggravated by low water intake, GFR drops even lower (by 52.1% and 50.7%). It is noteworthy that in the presence of a robust myogenic mechanism, low water intake significantly lowers GFR.

Somewhat surprisingly, high dosages do not lead to further drops in MAP in the case of furosemide + NSAID or triple treatment. However, a higher dose of ACEI + NSAID or ACEI + furosemide does increase the MAP lowering effect. Triple treatment at high dosage is predicted to lower GFR to 0.0704 and 0.0699 l/min in male and female hypertensive models, respectively, which correspond to 21% and 16% reduction from normal conditions (i.e., triple treatment at regular dosage). Excessive dosages of drugs may lead to increased risk for AKI, this is especially important as many dosages are only based on clinical trials including men, rather than finding appropriate dosages for women separately.

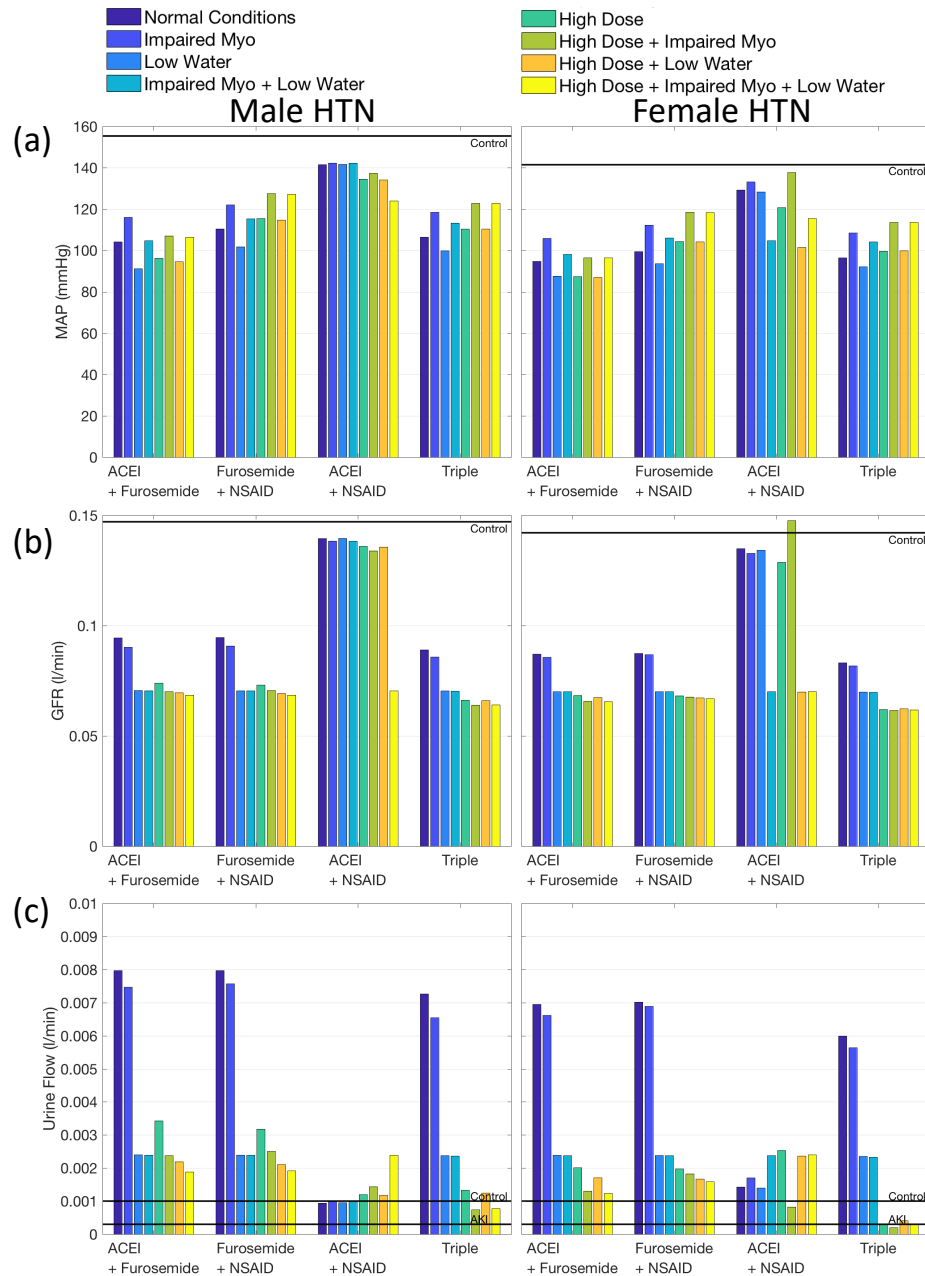


Figure 4.5: Effect of selected drug combinations on renal and cardiovascular function of the male and female hypertensive models, obtained under differing aggravating conditions. (a) mean arterial pressure (MAP) value at the end of the second day following treatment; (b) glomerular filtration rate (GFR); (c) urine flow. Triple treatment yields the lowest GFR, albeit not to a level indicative of acute kidney injury. Solid lines labelled “Control” indicates values without drug treatment. Triple treatment administered at high dosage yield urine flow indicative of acute kidney injury (c).

4.4 Discussion

AKI is typically associated with elevated serum creatinine levels and a severe drop in urine output. The present study is concerned with “pre-renal AKI,” which results from altered renal hemodynamics leading to critically lowered GFR. (“Renal AKI” is caused by drug or ischemia-induced parenchymal injury, whereas “post-AKI” is a result of urinary tract obstruction.) Pre-renal AKI may develop as a result of hypotension, dehydration, heart failure, renal microangiopathy, or following the administration of certain drug treatments. Triple treatment with ACEI, diuretics, and NSAIDs is known to increase the rate of AKI [117]. However, the factors that predispose some patients to the development of triple whammy AKI are incompletely characterized. Our study has identified dehydration as a key contributing factor to the development of triple whammy AKI.

To maintain normal kidney function, GFR is kept within a narrow range and exhibits a wide plateau for renal perfusion pressures 80–180 mmHg [23]. A key autoregulatory mechanism is the myogenic response, which is a property of the preglomerular vasculature wherein a rise in intravascular pressure elicits constriction that generates a compensatory increase in vascular resistance. Another autoregulatory mechanism is TGF, which is a negative feedback response that balances glomerular filtration with tubular reabsorptive capacity. Both mechanisms operate via regulation of the contractility of the afferent arteriole smooth muscle cells.

In TGF, the macula densa cells located at the end of the cortical thick ascending limb act as the salt sensor. Tubular salt sensing by the macula densa involves apical NaCl transport mechanisms, including the furosemide-sensitive $\text{Na}^+\text{-K}^+\text{-2Cl}^-$ cotransporter (NKCC2), which is the primary NaCl entry mechanism. When tubular fluid $[\text{Na}^+]$ and $[\text{Cl}^-]$ at the macula densa exceed their respective target values, the

macula densa cells signals to constrict the afferent arteriole, and vice versa. Among the mediators produced by the macula densa cells are the vasodilator prostaglandins, which are derived from the COX-2 pathway and are critical in the TGF mechanism and renin signaling cascade. Renin activates the systemic and renal RAS, which increase blood pressure and GFR.

RSNA regulates blood pressure via the natriuresis-diuresis-driven volumic response, and GFR via afferent and efferent arteriolar tone as well as proximal Na^+ reabsorption. Specifically, the RSNA-mediated responses include the (i) release of ADH, which increases GFR by inducing afferent vasodilation and efferent vasoconstriction, (ii) renin secretion, which activates RAS and raises blood pressure, and (iii) enhanced Na^+ reabsorption, leading to volume expansion and blood pressure increases [43, 98, 116].

Yet another factor in the interplay between blood pressure and GFR is blood volume. Perturbations in blood volume stimulate the stretch/distension receptors located on the right auricle and central veins, and induce responses aimed at stabilizing blood pressure. An increase in blood volume gives rise to atrial stretch and activates the release of atrial natriuretic peptide from cardiomyocytes. Atrial natriuretic peptide induces afferent vasodilation and efferent vasoconstriction; consequently, GFR increases, followed by natriuresis and diuresis.

The individual effect on GFR and blood pressure of each of the above mechanisms is well characterized. However, how they interact, especially under drug-induced alterations, is not completely understood in an integrated sense. Diuretics, for instance, lowers extracellular fluid volume by inhibiting tubular solute and water reabsorption and inducing natriuresis and diuresis. Taken in isolation, the reduction in extracellular fluid volume leads to reduction in blood volume and blood pressure, especially in hypertensive patients (Fig. 4.4a). ACEI inhibit the synthesis of Ang II, a potent

vasoconstrictor and anti-natriuretic peptide that promotes blood pressure elevation. Another commonly prescribed RAS inhibitor is the ARB, which impedes the binding of Ang II to Ang II type I receptor (AT1R), which is implicated in vasoconstriction, ALD secretion, and enhanced tubular salt and water reabsorption. ACEI and ARB lower blood pressure, especially in hypertensive patients (Fig. 4.4a), but alone do not significantly alter GFR (Fig. 4.4b). NSAIDs inhibit the production of prostaglandins, which, under hypovolemic conditions, may have an adverse effect on salt and water retention, and GFR regulation.

As previously noted, a number of blood pressure compensatory mechanisms are activated following the administration of diuretics (e.g., RSNA and RAS). The effects of these mechanisms are significantly attenuated by the concurrent administration of an ACEI (or ARB). As a result, model simulations predict that the combined administration of ACEI and furosemide slightly lower blood pressure and GFR, compared to furosemide alone, in normotensive populations; the predicted blood pressure and GFR reductions are more significant in hypertensive populations (Figs. 4.4a and 4.4b). The competing effects of lower GFR and lower tubular Na^+ and water reabsorption results in the attenuation by ACEI of the diuretic effect (i.e., urine output) of furosemide in normotensive models and the female hypertensive model but increase the diuretic effect of furosemide in male hypertensive model (Fig. 4.4c). Some experimental findings have revealed that ACEI attenuate the diuretic effect of furosemide in normotensive humans [227] and normotensive Sprague-Dawley rats [226] while others have found that in chronic heart failure patients ACEI and furosemide double treatment increased urine flow in comparison to furosemide only treatment [65]. Thunhorst and Johnson [226] found the dosage of ACEI to be the determining factor: low dosage of captopril was found to increase urine flow, whereas a high dose decreased urine flow, possibly due to the RAS being a mediator of water ingestion.

This may suggest that dosing needs to be tailored to the individual in order to achieve the intended diuretic effect and properly reduce blood pressure or to avoid problematic side effects.

NSAIDs have been consistently found to attenuate the diuretic and RAS activating effect of furosemide in normotensive and hypertensive humans [175, 226, 213] and normotensive Sprague-Dawley rats [101]. Simulation results are in general agreement with these findings. In the models, urine flow is predicted to be attenuated with NSAID and furosemide double treatment compared to furosemide single treatment, with the exception of the male hypertensive model where it increases with double treatment (Fig. 4.4c). The increase in PRA from furosemide is also attenuated with NSAID treatment (Fig. 4.4d). These attenuations of renin and urine flow stems from NSAIDs inhibition of macula densa sodium signaling. Diuretic attenuation occurs due to the decrease of GFR from TGF (Fig. 4.2A), while RAS attenuation occurs to the inhibition of macula densa signaling of renin secretion (Fig. 4.2B). As such, this double treatment may put patients at risk for AKI as the RAS' ability to respond to a hypovolemic state may be impaired.

ACEI and NSAIDs together have been shown to not decrease blood pressure and GFR in normotensive individuals [214] and to have no effect on RBF and GFR in ACEI treated hypertensive patients with controlled blood pressure [185]. However, the renin increase due to ACEI is attenuated with COX-2 inhibition [33]. While our models predict a decrease in MAP in response to ACEI single treatment, the addition of NSAIDs slightly weakens that response (Fig. 4.4a). Model predictions differ from experimental results in that the renin increase from ACEI is somewhat enhanced with NSAIDs (by 18%) in the hypertensive models (Fig. 4.4d). In a retrospective cohort study, Lapi et al. [117], found that double treatment with ACEI and NSAIDs is not associated with an increased risk of AKI. Consistent with that observation, model

simulations predict a slight increase in the hypertensive as well as similar urine flow levels in all models (Fig. 4.4c). Thus, no indication of an elevated risk for AKI is predicted following the combination therapy of ACEI and NSAIDs, in the absence of additional risk factors.

In triple treatment with ACEI, diuretics, and NSAIDs, critical blood pressure and GFR regulatory mechanisms are simultaneously interrupted. As previously noted, diuretics decreases extracellular fluid volume and blood pressure. The renal autoregulatory mechanisms that maintain GFR via TGF- and RAS-mediated compensation are inhibited through ACEI and NSAID. Consequently, triple therapy has been reported to increase the rate of AKI [117, 221, 142, 59]. Perhaps not unexpectedly, model simulations indicate that triple treatment reduces GFR more than single or double treatments in all individuals (Fig. 4.4b). However, under triple treatment, urine flow and GFR have not been predicted to fall sufficiently far to indicate AKI. This result is consistent with the fact that only a fraction of individuals develop AKI following triple treatment. Thus, we expect individuals who may be hypertensive but are otherwise healthy to be able to withstand triple treatment—in the absence of other aggravating factors.

One aggravating factor explored in the present study is dosage differences, which, perhaps not unexpectedly, can substantially lower GFR and urine flow (Fig. 4.5). Similarly, differences in pharmacokinetics and metabolism can also affect the drug concentrations at target sites and increase the risk for AKI in some individuals.

We also considered the effect of an impaired myogenic response, as seen in cardiovascular and renal diseases [14, 15]. As previously noted, GFR normally exhibits a wide plateau for a range of renal perfusion pressure values. That plateau can be attributed, in large part, to the myogenic response; by comparison the contribution of TGF is significant only for a narrow range of pressure values around the base-

line [209]. When renal autoregulation is impaired (Fig. 4.3), GFR becomes more sensitive to variations in renal perfusion pressure, which drops following the administration of diuretics and ACEI. An excessive reduction in GFR may result in AKI. Normally, GFR needs to decrease beyond 60% for plasma creatinine to significantly increase, and thus for AKI to ensue, due to the increased creatinine secretion that generates a creatinine-blind window for the detection of GFR decline [86]. Indeed, our model predicts that with an impaired myogenic response GFR exhibits a slightly larger decrease with all treatments involving furosemide, and a significant decrease when given high dosages (Fig. 4.5b). The excessive decrease in GFR may lead to a corresponding decrease in urine flow. Indeed, when myogenic response is impaired, urine flow is predicted to drop to the AKI level following the triple treatment at high dosage (Fig. 4.5c).

Hydration status is also a key factor in heightening the risk of AKI (Fig. 4.5). Other factors not considered in the present study includes alterations in the glomerular ultrafiltration coefficient (e.g., in mesangial contraction [45]), reduction in oncotic filtration pressure (e.g., in proteinuria [107]), TGF resetting [225], and the presence of certain other drugs.

A major contributing factor to triple whammy AKI that isn't considered in the present study is nephron loss, often a consequence of hypertension. The kidney adapts to a reduction in nephron population and can, up to some critical nephron loss, maintain GFR at the normal level [53, 122]. Nonetheless, subcritical nephron loss likely elevates the risk for triple whammy AKI. To simulate kidney function under differing physiological and pathophysiological conditions, a more detailed representation of the kidney may be incorporated (e.g., for nephron function [124, 133, 131] and for renal autoregulation [130, 118, 28, 48]).

Finally, hypertension is simulated by assuming an overactive RSNA. However,

hypertension is typically a result of a variety of changes in the body, including, but not limited to, increases in systemic vascular resistance, preglomerular resistance, afferent arteriole resistance, Na^+ retention, renin or ALD secretion, or nephron loss. Results of the present simulations will probably extend to other causes of hypertension, inasmuch as RSNA stimulates many of the other causes of hypertension, such as afferent arteriole resistance, renin secretion, and ALD secretion.

Chapter 5

Potassium Homeostasis

5.1 Introduction

The majority of this dissertation pertains to the regulation of blood pressure through the effects of the kidney on water and sodium homeostasis; however, sodium is not the only solute with a major impact on blood pressure. Epidemiological studies have repeatedly indicated a major role for K^+ in blood pressure control. Specifically, a high dietary K^+ -to- Na^+ ratio appears to be inversely related to blood pressure [84, 111, 196, 242]. Even independent of Na^+ and aside from blood pressure considerations, regulation of K^+ is important to understand, as disorders affecting plasma K^+ concentration can be rapidly fatal and are associated with pathophysiologic processes such as progress of cardiac and kidney diseases [76].

Approximately 2% of total body K^+ is located in the extracellular fluid, while the remaining 98% is stored within cells [35]. Plasma K^+ concentration is tightly controlled, as maintaining a small extracellular and high intracellular concentration is necessary for providing membrane potential to drive action potentials, control muscle contractility, and power ion transporters [151]. This balance may have been determined by the K^+ rich and Na^+ poor environment humans evolved in [170].

5.1.1 Overview of K^+ regulation

Plasma K^+ concentration is regulated through both feedforward and feedback controls, as well as through quick responses and slower responses. These control mech-

anisms are described below.

Kidney function In the long term, the kidney is the principal defense against chronic K^+ imbalance [70]. K^+ is freely filtered through the glomerulus and into the renal tubular lumen. As the luminal fluid passes through the nephron, various regulatory processes control how much K^+ is secreted or reabsorbed. The proximal tubules and loops of Henle together consistently reabsorb about 90% of the filtered K^+ , leaving the fine tuning to the distal tubules and collecting ducts [70].

The distal tubule has the ability to secrete or reabsorb K^+ , depending on the state of the body. During normal or high K^+ intake, the distal tubule secretes 10% to 50% of filtered K^+ . Secretion rate is controlled by ALD, which increases the luminal permeability of the distal tubule [239]. However, during low K^+ intake, the distal tubule can only reabsorb up to 3% of filtered K^+ [70], meaning that in times of drastically low K^+ intake, it is up to the collecting duct to conserve K^+ .

The cortical collecting duct and outer medullary collecting duct consist of two types of cells responsible for K^+ regulation: principal cells and intercalated cells, responsible for K^+ secretion and reabsorption, respectively. Principal cells comprise approximately 70 to 75% of collecting duct cells. These cells use the electrochemical gradient established by Na^+ entry into the cell to drive K^+ secretion. The rate of K^+ secretion is regulated by dietary K^+ intake, intracellular K^+ level, Na^+ delivery to the cells, urine flow rate, and hormones, such as ALD and Ang II [70]. ENaC and ROMK-like small conductance K channels in principal cells are sensitive to Ang II through AT1R binding [177, 238], while ALD stimulates secretion by increasing the driving force for K movement through apical channels [174]. As such, principle cells are targets for ARB and ALD receptor antagonists. During K^+ depletion, intercalated cells upregulate expression of luminal H,K-ATPases to enhance potassium

reabsorption [44]. Through these mechanisms, the outer medullary collecting duct can reabsorb up to 10% of filtered K^+ .

Internal K^+ balance While the kidney determines overall K^+ conservation and loss, it takes time to have an effect – urinary excretion of a potassium load occurs over 24-48 hours [79]. In the event of large K^+ intake, such as a meal, the low plasma K^+ concentration must be maintained before renal regulation can fully take effect. The excess K^+ is taken up into liver and skeletal muscle cells. This quick storage of excess K^+ allows the body to maintain an appropriately low plasma K^+ concentration, and then to slowly release K^+ back into the blood as kidney function takes effect. The rate of cellular uptake is regulated by insulin and ALD. In the presence of either signal, the uptake of K^+ into cells is increased, causing the excess K^+ to enter the cells.

Feedback control Feedback controls respond to changes in plasma K^+ concentration to maintain K^+ homeostasis. In the face of high plasma K^+ concentration, more K^+ is filtered through the glomeruli, which, taken in isolation, would lead to higher urinary K^+ excretion. High plasma K^+ concentration also increases ALD secretion, which stimulates the activity and synthesis of $Na^+-K^+-ATPase$ and luminal K^+ channels in the collecting duct principal cells, increasing K^+ secretion into the tubular fluid and eventual urinary K^+ excretion [237]. ALD also increases the abundance of $Na^+-K^+-ATPase$ in muscle cells, increasing the cellular uptake of K^+ [180].

Conversely, low plasma K^+ concentration suppresses ALD production, reducing K^+ secretion in the collecting duct and urinary K^+ excretion, thereby allowing intracellular K^+ in the muscles to leak back into the extracellular fluid.

Feedforward control Feedforward control refers to a pathway that reacts to an environmental input in a predetermined way, without reference to the value being controlled. Increased dietary K^+ intake activates a feedforward control in which K^+ secretion is stimulated in the distal tubule before changes in plasma K^+ [18] or ALD [188] can be observed. This effect has been repeatedly shown in sheep [188], rats [21, 212], and humans [18].

Identifying all the mechanisms whereby K^+ is regulated is an open area of research [151, 35, 50].

One hypothesized mechanism is muscle-kidney cross talk, whereby intracellular K^+ concentration of muscle cells can directly affect urine K^+ excretion without first causing changes in extracellular K^+ concentration. This hypothesis is gaining support [29, 6, 235], but details remain lacking. This mechanism would facilitate the return of cellular K^+ levels to baseline after perturbations needed to maintain the extracellular K^+ concentration.

For example, during K^+ loading, cells quickly take up the excess K^+ to maintain a safe extracellular concentration. After the loading ends, that excess intracellular K^+ needs to be removed; however, urine K^+ excretion is dependent on the extracellular concentration and ALD (secretion of which is dependent on extracellular concentration). The feedforward effect does promote urine K^+ flow, but only when there is K^+ in the gut to begin the signaling pathway; depending on the amount of excess K^+ , continued excretion after digestion may be necessary. In this situation, where the extracellular concentration has been maintained by an increase in the intracellular concentration and the feedforward effect is not sufficient in expelling the excess K^+ , then, according to our current understanding, muscle-kidney cross talk may be the mechanism whereby the intracellular concentration is restored to baseline. Similarly,

under low K^+ intake, muscle cells release K^+ to buffer the extracellular concentration. Urine K^+ flow drops to conserve K^+ , due to lack of stimulation from the feedforward effect, lower ALD (stemming from low extracellular K^+), and less K^+ filtered through the glomerulus. However, when extracellular K^+ is stabilized and intake returns to normal, according our current understanding, muscle-kidney cross talk may be the solution to continue low urine K^+ if needed to restore the intracellular concentration.

In this chapter, we present a model of K^+ homeostasis consistent in format with the models presented in chapters 3 and 4 to investigate how feedback and feedforward control each contributes to the regulation of plasma K^+ concentration. We also investigate how muscle-kidney cross talk may affect recovery from K^+ loading and depletion when controlling K^+ transport in the distal tubule or collecting duct.

5.2 Methods

The model described here represents a simple model of K^+ homeostasis including dietary intake, intra- and extracellular K^+ storage, renal function, the feedforward effect of dietary intake on renal function, and ALD's feedback control. It is fitted for men, and variables describing water and Na^+ regulation (extra- and intracellular fluid volume, GFR, Na^+ concentration) are considered constant for simplicity. A flowchart depicting the system is shown in Fig. 5.1.

5.2.1 Internal K^+ balance

K^+ intake is treated as an independent variable. While computing a steady state solution we model K^+ intake (Φ_{Kin}) as a constant throughout the day:

$$\Phi_{Kin}^{ss} = 0.083\text{mEq}/\text{min} \quad (5.1)$$

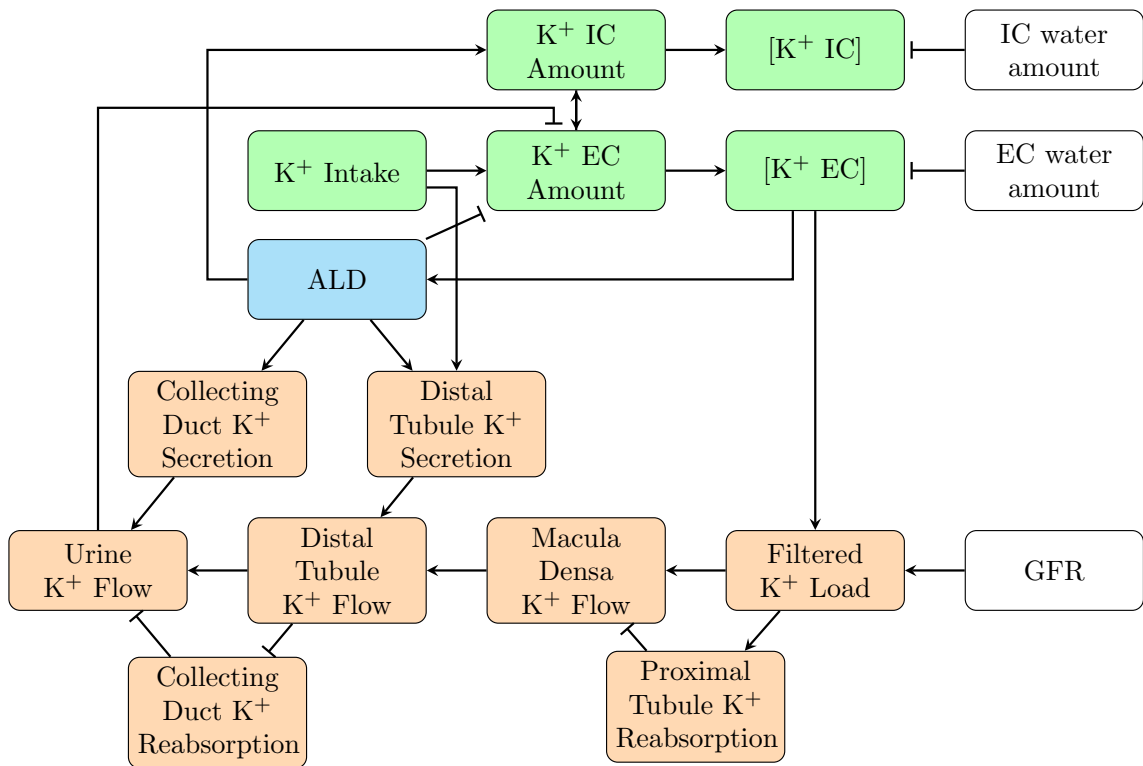


Figure 5.1: Flowchart depicting K⁺ homeostasis model. Green nodes represent internal K⁺ balance; orange, kidney function; blue, Aldosterone (ALD); and white, constants.

However, realistically, K^+ intake varies throughout the day, with periods of high intake (meals) and periods of no intake (between meals). The K^+ intake for each time dependent simulation will be described as each simulation is introduced.

The extracellular K^+ amount (M_{Kec}) increases with dietary intake (Φ_{Kin}) and decreases with urine K^+ flow (Φ_{uK}). Also affecting M_{Kec} is the exchange of K^+ between the extracellular and intracellular compartments. Flow from extracellular to intracellular (Φ_{ECtoIC}) is driven by Na^+ - K^+ -ATPase pumps while flow from intracellular to extracellular (Φ_{ICtoEC}) is by diffusion.

$$\frac{dM_{Kec}}{dt} = \Phi_{Kin} - \Phi_{uK} - \Phi_{ECtoIC} + \Phi_{ICtoEC} \quad (5.2)$$

$$\frac{dM_{Kic}}{dt} = \Phi_{ECtoIC} - \Phi_{ICtoEC} \quad (5.3)$$

The K^+ concentration ($[K_{EC}^+]$, $[K_{IC}^+]$) is the amount of K^+ divided by the amount of water for either the intra (IC) or extracellular (EC) compartment. The extracellular fluid volume (V_{ecf}) is considered a constant at 15 L. The intracellular fluid volume is also constant ($V_{icf} = 28$ L).

$$[K_{EC}^+] = M_{Kec}/V_{ecf} \quad (5.4)$$

$$[K_{IC}^+] = M_{Kic}/V_{icf} \quad (5.5)$$

Flow from extra- to intracellular compartments (Φ_{ECtoIC}) due to Na^+ - K^+ -ATPase activity is modeled with Michaelis-Menten kinetics, with a maximum rate of V_{max} equal to 134 mEq/min [32] and a half maximal activation level of $K_m = 0.8$ mEq/l. The value for K_m was chosen to be in the range of 0.8 to 1.5 mEq/L as given in [32]. ALD leads to a modest increase in Na^+ - K^+ -ATPase abundance (mathematically an increase in V_{max}), and thus higher flux [173, 32].

$$\Phi_{\text{ECtoIC}} = \frac{\rho_{\text{al}} \times V_{\text{max}} \times [K_{\text{EC}}^+]}{K_{\text{m}} + [K_{\text{EC}}^+]} \quad (5.6)$$

where ρ_{al} represents the effect of ALD. Phakdeekitcharoen et al. [180] measured how ALD levels affect $\text{Na}^+\text{-K}^+\text{-ATPase}$ pump activity. Using their data, we fit ρ_{al} as shown below.

$$\rho_{\text{al}} = \frac{66.4 \text{ nmol/mg protein/h} + 0.237 \times C_{\text{al}}}{89.605 \text{ nmol/mg protein/h}} \quad (5.7)$$

Flow from intra- to extracellular compartments (Φ_{ICtoEC}) is driven by diffusion through a permeable membrane. To fit the permeability constant (P), we use the knowledge that at steady state, the flow into and out of cells should be equal, meaning we set Eqs. 5.6 and 5.8 equal, use the baseline values for $[K_{\text{EC}}^+]$ and $[K_{\text{IC}}^+]$ and solve for P .

$$\Phi_{\text{ICtoEC}} = P \times ([K_{\text{IC}}^+] - [K_{\text{EC}}^+]) \quad (5.8)$$

5.2.2 Kidney function

The kidney is modeled as a single nephron, split into three model segments: the “proximal segment (pt)” that includes the proximal tubule and the loop of Henle, the “distal segment (dt)” that includes the distal convoluted tubule and the connecting tubule, and the collecting duct (cd).

K^+ is freely filtered at the glomulerus; as such, the filtered potassium load (Φ_{filK}) is GFR (Φ_{GFR}) multiplied by the extracellular potassium concentration ($[K_{\text{EC}}^+]$). In

this model, GFR is held constant.

$$\Phi_{\text{filK}} = \Phi_{\text{GFR}} \times [K_{\text{EC}}^+] \quad (5.9)$$

Proximal tubule K^+ reabsorption ($\Phi_{\text{pt-Kreab}}$) is a fraction of the filtered K^+ load. Fractional proximal tubule K^+ reabsorption ($\eta_{\text{pt-Kreab}}$) has a baseline of 90%. Macula densa K^+ flow (Φ_{mdK}) is the filtered K^+ load minus proximal tubule reabsorption.

$$\Phi_{\text{pt-Kreab}} = \Phi_{\text{filK}} \times \eta_{\text{pt-Kreab}} \quad (5.10)$$

$$\eta_{\text{pt-Kreab}} = 0.9 \quad (5.11)$$

$$\Phi_{\text{mdK}} = \Phi_{\text{filK}} - \Phi_{\text{pt-Kreab}} \quad (5.12)$$

The macula densa marks the beginning of the distal tubule. K^+ is secreted into the distal tubular lumen, and that amount is independent of the K^+ delivered to the distal tubule. Distal tubule K^+ secretion ($\Phi_{\text{dt-Ksec}}$) has a baseline value of $\Phi_{\text{dt-Ksec}}^{\text{eq}} = 0.0291$ mEq/min. This baseline value is fitted to yield a urinary K^+ flow of 0.0873 mEq/min at steady state. The regulatory effect on distal tubule K^+ secretion ($\eta_{\text{dt-Ksec}}$) is dependent on the combined effect of ALD concentration (γ_{al}) and the feedforward effect (γ_{Kin}); see Eq. 5.14. Distal tubule K^+ outflow (Φ_{dtK}) is given by the macula densa K^+ flow (input) plus distal tubule K^+ secretion (Eq. 5.15).

$$\Phi_{\text{dt-Ksec}} = \Phi_{\text{dt-Ksec}}^{eq} \times \eta_{\text{dt-Ksec}} \quad (5.13)$$

$$\eta_{\text{dt-Ksec}} = \gamma_{\text{al}} \times \gamma_{\text{Kin}} \quad (5.14)$$

$$\Phi_{\text{dtK}} = \Phi_{\text{mdK}} + \Phi_{\text{dt-Ksec}} \quad (5.15)$$

Distal tubule K^+ secretion increases with ALD level. Field et al. found that in adult male Sprague-Dawley rats an increase in plasma ALD concentration from 4.4 ng/dl to 55.8 ng/dl caused distal tubule secretion to increase by 83% [55]. Our (human) model has a baseline $C_{\text{al}} = 85$ ng/l, so we fit the equation so that the same percentage increase from our ALD baseline causes the same percentage increase in secretion.

$$\gamma_{\text{al}} = 0.3475 * C_{\text{al}}^{0.23792} \quad (5.16)$$

It is noteworthy that findings in a separate study by Rabinowitz et al. may disagree with the steep slope near baseline, as these authors found that an increase in ALD concentration at sufficiently high levels raises K^+ secretion, but not when ALD concentration is within its normal physiological range [187].

In a feedforward effect, distal tubule K^+ secretion increases with higher K^+ intake. The scaling constant A_{Kin} was fitted along with collecting duct reabsorption parameters ($A_{\text{cd-Kreab}}, B_{\text{cd-Kreab}}$ Eq. 5.22) to reproduce the behavior seen in Preston et al. [183] due to the lack of direct experimental data. This process of parameter fitting, including target model behavior and chosen values, is described in Section 5.3.1.

$$\gamma_{\text{Kin}} = A_{\text{Kin}} \times \Phi_{\text{Kin}} \quad (5.17)$$

The collecting duct has the ability to both secrete and reabsorb K^+ through the function of principal and intercalated cells, respectively. Collecting duct K^+ secretion ($\Phi_{\text{cd-Ksec}}$) has a baseline value of $\Phi_{\text{cd-Ksec}}^{eq} = 0.0053 \text{ mEq/min}$. Collecting duct K^+ secretion is regulated ($\eta_{\text{cd-Ksec}}$) by the ALD concentration ($\lambda_{\text{al}}, C_{\text{al}}$). Schwartz et al. [206] measured K^+ flux in the cortical collecting ducts of rabbits at various plasma ALD levels. Using this data, we fit the curve connecting ALD levels to collecting duct K^+ secretion.

$$\Phi_{\text{cd-Ksec}} = \Phi_{\text{cd-Ksec}}^{eq} \times \eta_{\text{cd-Ksec}} \quad (5.18)$$

$$\eta_{\text{cd-Ksec}} = \lambda_{\text{al}} \quad (5.19)$$

$$\lambda_{\text{al}} = 0.4361 * C_{\text{al}}^{0.206} \quad (5.20)$$

Collecting duct K^+ reabsorption is modeled separately from secretion, as they are mediated by different types of cells in the collecting duct. Collecting duct K^+ reabsorption ($\Phi_{\text{cd-Kreab}}$) is a fraction of distal tubule K^+ outflow. Fractional collecting duct K^+ reabsorption ($\eta_{\text{cd-Kreab}}$) is dependent on distal tubule K^+ outflow. How the fitting parameters $A_{\text{cd-Kreab}}$ and $B_{\text{cd-Kreab}}$ are chosen is described later (Section 5.3.1).

$$\Phi_{\text{cd-Kreab}} = \Phi_{\text{dtK}} \times \eta_{\text{cd-Kreab}} \quad (5.21)$$

$$\eta_{\text{cd-Kreab}} = \frac{1}{1 + e^{A_{\text{cd-Kreab}}(\Phi_{\text{dtK}} - B_{\text{cd-Kreab}})}} \quad (5.22)$$

Finally, urinary K^+ excretion (Φ_{uK}) is given by the distal tubule K^+ outflow (Φ_{dtK}) plus collecting duct K^+ secretion ($\Phi_{cd-Ksec}$) minus collecting duct K^+ reabsorption ($\Phi_{cd-Kreab}$).

$$\Phi_{uK} = \Phi_{dtK} + \Phi_{cd-Ksec} - \Phi_{cd-Kreab} \quad (5.23)$$

5.2.3 Aldosterone

ALD concentration (C_{al}) is modeled as the normalized ALD concentration (N_{al}) multiplied by the baseline concentration (85 ng/l). N_{al} increases with ALD secretion (N_{als}) and decays with a half life of T_{al} . N_{als} is affected by the extracellular potassium and sodium concentrations (C_{sod}), MAP, and AT1R-bound Ang II. In this limited model, MAP and AT1R-bound Ang II are held constant and so not listed here (Eqs. B.65-B.68). We keep the effect of the K^+ concentration and Na^+ concentration ($\xi_{k/sod}$) the same as it was in Karaaslaan et al. [103], but with a gentler slope.

$$C_{al} = N_{al} \times 85\text{ng/l} \quad (5.24)$$

$$\frac{dN_{al}}{dt} = \frac{1}{T_{al}}(N_{als} - N_{al}) \quad (5.25)$$

$$N_{als} = \xi_{k/sod} \quad (5.26)$$

$$\xi_{k/sod} = \frac{[K_{EC}^+]/C_{sod}}{0.0072917} - 3 \quad (5.27)$$

Table 5.1: Parameter values for K^+ model equations. Model is fitted to represent a man.

Parameter	Description	Value	Unit
$\Phi_{dt-Ksec}^{eq}$	baseline distal tubule K^+ secretion	0.0291	mEq/min
$\Phi_{cd-Ksec}^{eq}$	baseline collecting duct K^+ secretion	0.0053	mEq/min
Φ_{Kin}^{ss}	K^+ intake for steady state solution	0.083	mEq/min
Φ_{GFR}	glomerular filtration rate	0.125	L/min
A_{Kin}	fitting constant for γ_{Kin}	11.455	min/mEq
$A_{cd-Kreab}$	fitting constant for $\eta_{cd-Kreab}$	-160.4	min/mEq
$B_{cd-Kreab}$	fitting constant for $\eta_{cd-Kreab}$	0.046105	mEq/min
C_{sod}	Na^+ concentration	144	mEq/L
P	cell permeability constant	0.82887	min^{-1}
K_m	half maximal activation	0.8	mEq/L
T_{al}	ALD half life	30	min
V_{ecf}	extracellular fluid volume	15	L
V_{icf}	intracellular fluid volume	28	L
V_{max}	maximum K^+ flow into cells	134	mEq/min

Table 5.2: Variable values for K^+ model equations at steady state. Model is fitted to represent a man.

Variable	Description	Value	Unit
γ_{al}	effect of ALD on distal tubule K^+ secretion	1	
γ_{Kin}	effect of K^+ intake on distal tubule K^+ secretion	1	
$\xi_{k/sod}$	effect of $K^+ : Na^+$ ratio on ALD secretion	1	
$\eta_{dt-Ksec}$	regulation of distal tubule K^+ secretion	1	

Table 5.2: Variable values for K^+ model equations at steady state. Model is fitted to represent a male human.

Variable	Description	Value	Unit
$\eta_{cd-Kreab}$	fractional collecting duct K^+ reabsorption	0	
$\eta_{cd-Ksec}$	regulation of collecting duct K^+ secretion	1	
$\eta_{pt-Kreab}$	fractional proximal tubule K^+ reabsorption	0.9	
λ_{al}	effect of ALD on collecting duct K^+ secretion	1	
ρ_{al}	effect of ALD on cellular K^+ uptake	1	
Φ_{dtK}	distal tubule K^+ outflow	0.0820	mEq/min
$\Phi_{dt-Ksec}$	distal tubule K^+ secretion	0.0291	mEq/min
$\Phi_{cd-Ksec}$	collecting duct K^+ secretion	0.0053	mEq/min
$\Phi_{cd-Kreab}$	collecting duct K^+ reabsorption	0	mEq/min
Φ_{ECtoIC}	K^+ flow into cells	112.56	mEq/min
Φ_{filK}	filtered K^+ load	0.525	mEq/min
Φ_{ICtoEC}	K^+ flow out of cells	112.56	mEq/min
Φ_{mdK}	macula densa K^+ flow	0.0529	mEq/min
$\Phi_{pt-Kreab}$	proximal tubule K^+ reabsorption	0.4763	mEq/min
Φ_{uK}	urine K^+ flow	0.087	mEq/min
C_{al}	ALD concentration	85	ng/L
$[K_{EC}^+]$	extracellular K^+ concentration	4.2	mEq/L
$[K_{IC}^+]$	intracellular K^+ concentration	140	mEq/L
M_{Kec}	extracellular K^+ amount	32	mEq
M_{Kic}	intracellular K^+ amount	3920	mEq
N_{al}	normalized ALD concentration	1	
N_{als}	normalized ALD secretion	1	

5.3 Results

5.3.1 Acute response to K^+ intake

K^+ loading was simulated by varying K^+ intake as the independent variable. It started at the value of 0.0873 mEq/min (recommended daily intake of 120mEq a day spread evenly over 24 hours) and continued for 100 min, before decreasing to 0 mEq/min and staying at 0 mEq/min for 3 hours. The bolus does of 35 mEq was achieved by linearly increasing Φ_{Kin} for 30 min to a level of 0.10606 mEq/min, where it stayed for 5 hours before linearly decreasing over 30 min back down to 0 mEq/min. Figure 5.2 shows the fitted response due to K^+ intake observed by Preston et al. [183]. The magnitude of the feedforward effect ($A_{Kin} = 11.455$) and collecting duct reabsorption ($A_{cd-Kreab} = -160.4$ and $B_{cd-Kreab} = 0.046105$) were chosen to reproduce a steady state value of $[K_{EC}^+] = 4.2$ mmEq/l, $\Phi_{uK} = 0.0423$ mEq/min during no K^+ intake in the time before the meal, and a maximum of at least $\Phi_{uK} = 0.08$ mEq/min during digestion of the meal. These parameters cause urine K^+ flow to decrease between meals and increase during a meal, allowing $[K_{EC}^+]$ to remain unperturbed.

5.3.2 Response to K^+ loading

To investigate the potential of muscle-kidney cross talk, we introduce a link (ω_{Kic}) between intracellular K^+ concentration and various parts of the nephron. When the cross talk affects distal tubule secretion, collecting duct secretion, or collecting duct reabsorption, the Eqs. 5.14, 5.19, 5.22, respectively are multiplied by ω_{Kic} . We investigate the strength of cross talk needed to elicit a response in urine K^+ by considering slopes (m_{Kic}) of 0.1, 0.01, and 0 (no cross talk). In the case of collecting

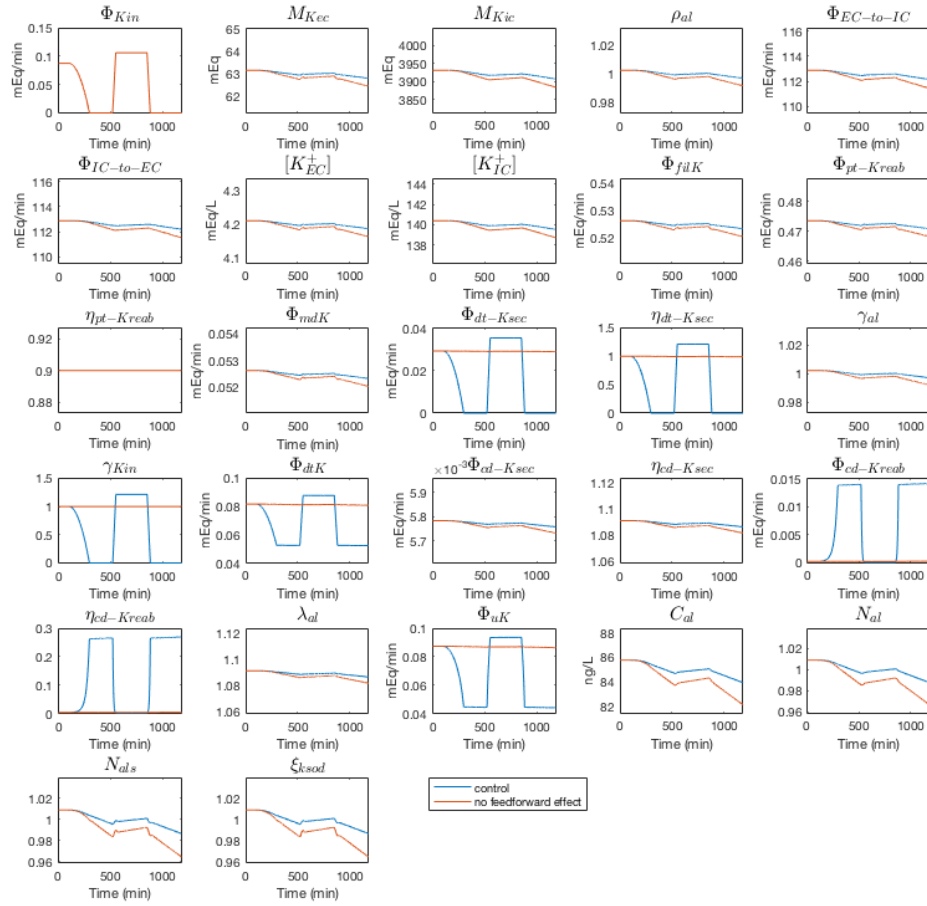


Figure 5.2: Variable values before and while digesting a 35mEq K^+ meal. Blue lines denote the entire model, red the model without the feedforward effect.

duct reabsorption where we use $m_{\text{Kic}} = -0.1, -0.01, \text{ and } 0$. When $[K_{IC}^+]$ is at the baseline value of 140 mEq/l, the function has a value of 1, causing no change.

$$\omega_{\text{Kic}} = \max(0, m_{\text{Kic}}([K_{IC}^+] - 140) + 1) \quad (5.28)$$

We simulate the experiment performed in Rabelink et al. [186] by simulating a normal K^+ intake (120 mEq/day) for two days, a high K^+ intake (400 mEq/day) for four days, then returning to a normal K^+ intake for four days. K^+ intake is split evenly into four meals 6 hours apart, and digestion of each meal is assumed to take 6 hours. As such, K^+ intake is modeled as a downward facing parabola with zeros at the start of the meal and the end of digestion, as shown in Eq. 5.29 where $M_{\text{day}K^+}$ is the daily K^+ amount, t_0 is the start of the meal, and t_1 is the end of digestion 6 hours later. Key model predictions are shown in Figure 5.3.

$$\Phi_{\text{Kin}} = \frac{-3}{2 \times 6^3} M_{\text{day}K^+} (t - t_0)(t - t_1) \quad (5.29)$$

When muscle extracellular K^+ concentration is able to affect distal tubule secretion (Fig. 5.3a, urine K^+ flow increases to a higher level during K^+ loading, and takes longer to return to baseline after loading ends. This results in a slightly lower intracellular concentration at the end of loading, and a faster return to baseline after loading. The extracellular K^+ concentration rises to the same level with or without cross talk, but returns to baseline faster with strong cross talk.

Having cross talk affect collecting duct secretion (Fig. 5.3b) or reabsorption (Fig. 5.3c) has a minimal effect on urine K^+ flow, intra- or extracellular concentration.

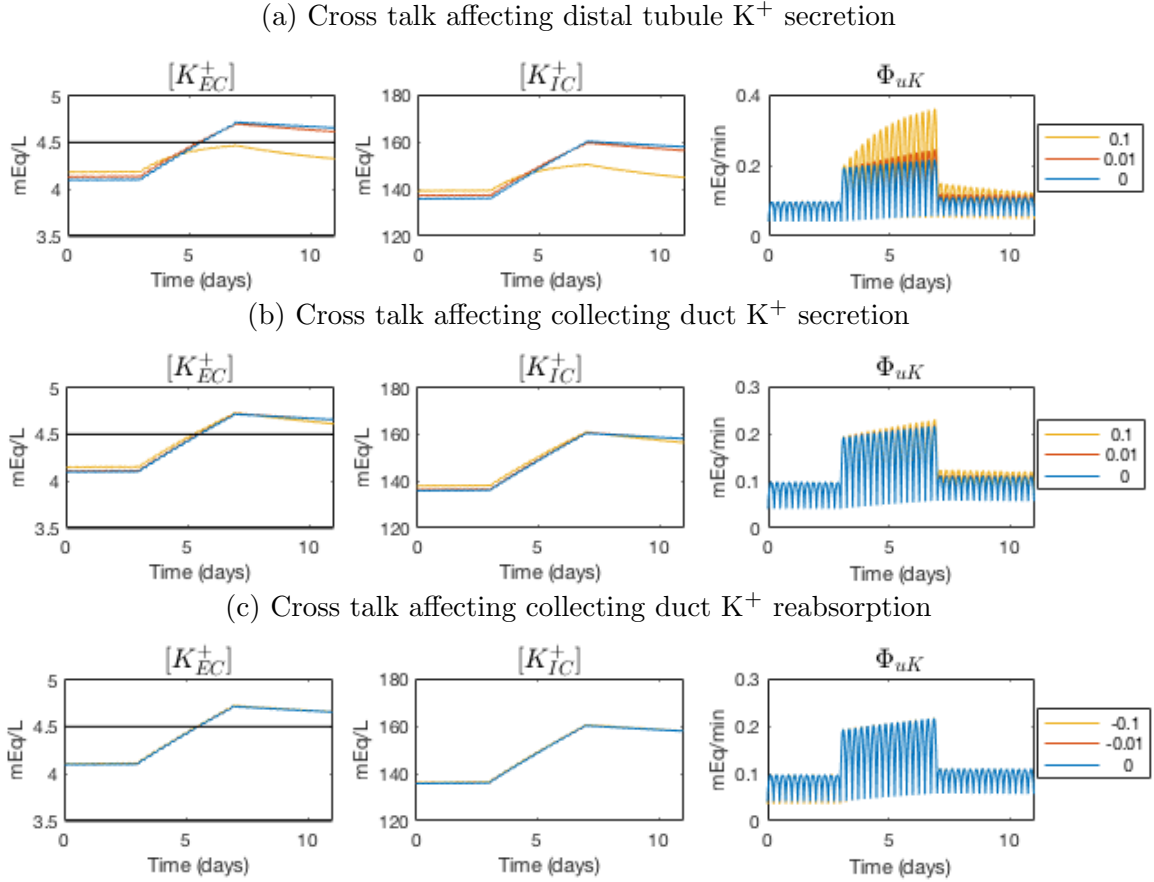


Figure 5.3: Model response to K^+ loading with muscle-kidney cross talk affecting (a) distal tubule K^+ secretion, (b) collecting duct K^+ secretion, or (c) collecting duct K^+ reabsorption. Color legend reports the slope of Eq. 5.28.

5.3.3 Response to K^+ depletion

We simulate K^+ depletion by limiting the daily K^+ intake to 10 mEq a day using Eq. 5.29 for 30 days, inducing hypokalemia (extracellular K^+ concentration < 3.5 mEq/L), then returning K^+ intake to normal levels (120 mEq/day) for 4 days. Again, we include muscle-kidney cross talk with distal tubule K^+ secretion, collecting duct K^+ secretion, and collecting duct K^+ reabsorption with slopes with two slopes (Eq. 5.28, $m_{Kic} = 0.1, 0.01$) and compare with no cross talk ($m_{Kic} = 0$). Key model results are shown in Fig. 5.4.

A strong effect of intracellular K^+ concentration on distal tubule K^+ secretion

results in less severe hypokalemia after 41 days (i.e., $[K_{EC}^+]$ and $[K_{EC}^+]$ do not drop as low as control) and a steeper incline in $[K_{EC}^+]$ and $[K_{EC}^+]$ when K^+ intake resumes. This is due to a lower urine K^+ flow after intake returns to normal (Fig. 5.4a).

In the collecting duct, having intracellular K^+ concentration affect secretion or reabsorption causes the model to retain K^+ during the depletion period, but does not increase the slope of intracellular K^+ during the recovery period (Figs. 5.4b and 5.4c). This is especially true in the case of affecting collecting duct K^+ reabsorption, where the urine K^+ flow is able to decrease further during the depletion period, causing the model to completely avoid hypokalemia (marked by the horizontal black line).

5.4 Discussion

Potassium regulation is necessary for proper cell function and is linked to blood pressure regulation. Disorders affecting plasma K^+ concentration increase the risk and severity of cardiovascular and renal diseases. Presented here is a model of K^+ regulation incorporating both feedback and feedforward controls of internal K^+ balance and renal K^+ handling. The model can serve as a tool for investigating new mechanisms of K^+ regulation.

The model reproduces a stable extracellular K^+ concentration between and during meals typical in a healthy diet as well as increased urine K^+ flow during digestion of a meal (Fig. 5.2). Preston et al. [183] found that during a meal, urine K^+ flow increased rapidly and remained elevated while serum K^+ concentration remained stable during the 5 hour study period. In our model, urine K^+ flow is driven by the feedforward effect, and without that feedforward effect, there is no change in urine flow during digestion and a loss of K^+ between meals (Fig. 5.2, red line). This suggests that the feedforward effect linking dietary K^+ intake to distal tubule K^+ secretion is necessary

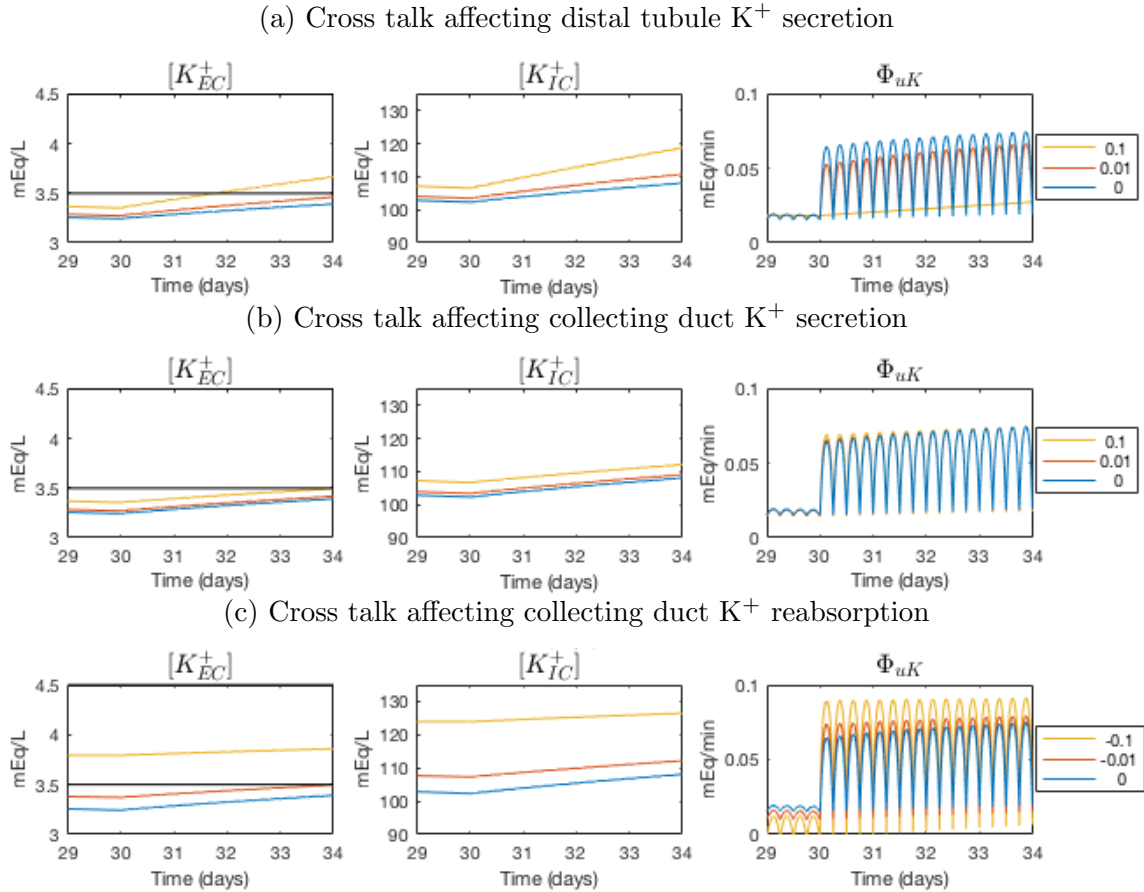


Figure 5.4: Model response to K^+ depletion with muscle-kidney cross talk affecting (a) distal tubule K^+ secretion, (b) collecting duct K^+ secretion, or (c) collecting duct K^+ reabsorption. Color legend reports the slope of Eq. 5.28. Black lines mark the threshold for hypokalemia.

for quick excretion of K^+ in the urine in response to elevated K^+ intake.

In contrast to a single meal, we investigate how the model would respond to repeated K^+ loading. Rabelink et al. found that after a period of K^+ loading, serum K^+ concentration returned to normal almost immediately after discontinuation of high K^+ intake, with a slightly negative K^+ balance only during the first 24 hours after discontinuation [186]. Our model instead takes many days to return extracellular K^+ concentration ($[K_{EC}^+]$) to baseline, despite rising to similar levels during K^+ loading (Fig. 5.3, blue line). The speed of recovery is increased when muscle-kidney cross

talk causes distal tubule K^+ secretion to increase when $[K_{EC}^+]$ is high. This allows model urine K^+ flow to be somewhat elevated after discontinuation of K^+ loading in comparison to before K^+ loading (Fig. 5.3a), matching the negative K^+ balance found by Rabelink et al. [186].

In a study of 29 patients with hypokalemic paralysis, Garg et al. found the average recovery time when treated with 80–100 mEq/day K^+ was 34.7 hours, or within two days [63]. When simulating K^+ depletion, the model extracellular concentration slowly drops; as such, we chose to simulate K^+ depletion for 30 days to replicate moderate hypokalemia (between 2.5 and 3.5 mEq/L). When returned to normal K^+ intake, the model without muscle-kidney cross talk takes at least 4 days for $[K_{EC}^+]$ to recover to 3.5 mEq/L and even longer to return to model baseline (4.2 mEq/L, Fig. 5.3, blue line). When the model represents muscle-kidney cross talk that causes distal tubule K^+ secretion to decrease as $[K_{EC}^+]$ decreases, the recovery time is significantly shortened (Fig. 5.3a). Given a sufficiently strong muscle-kidney cross-talk effect (slope of 0.1, yellow line) the model reached the upper threshold for moderate hypokalemia in 2 days.

Results of the K^+ loading and depletion simulations suggest that, without the representation of muscle-kidney cross talk, our model is unable to quickly recover from substantial perturbations in extracellular K^+ concentration. The inclusion of muscle-kidney cross talk significantly improves recovery times, especially in depletion cases; however, in loading cases still takes longer to for $[K_{EC}^+]$ to return to baseline than recorded in clinical studies. Potential reasons for this discrepancy include (1) adaptations to chronic changes to intake not included in the model and (2) other regulatory mechanisms not included in the model.

During chronic K^+ restriction, changes occur in regulation of both internal K^+ balance and renal excretion [70, 29]. When not severe enough to cause hypokalemia,

insulin-stimulated clearance of K^+ from the plasma is blunted [29] but Na^+ - K^+ -ATPase activity remains normal. When K^+ restriction is severe enough to cause hypokalemia, Na^+ - K^+ -ATPase pumps are less numerous and less active in the skeletal muscle [70]. Renal adaptations include lower urinary K^+ excretion achieved through adjustments in transporter activity and abundance [70]. Our model does not account for modifications in response to chronic changes in K^+ intake.

Other mechanisms for K^+ regulation not represented in the present model include circadian rhythms, interaction of Na^+ and K^+ in renal membrane transporters, metabolic control of internal K^+ balance [70], and insulin's effect on internal balance [151].

Circadian rhythms may provide a “predictive control” of extracellular K^+ , where K^+ excretion is increased during times of expected K^+ intake [151]. Recent studies have found evidence that clock genes control these rhythms in K^+ excretion [75, 76]. These circadian rhythms in K^+ excretion may partially come from circadian rhythms of ALD, as evidence of circadian rhythms of glucocorticoid synthesis and secretion has been found in the adrenal gland [173]. More in depth reviews of the circadian rhythm in K^+ regulation are available [76, 75, 159].

Potassium regulation is linked to Na^+ regulation, both in regard to internal K^+ balance and renal K^+ excretion. The high intracellular and low extracellular K^+ concentrations are dependent on Na^+ - K^+ -ATPase activity, causing the converse Na^+ transmembrane concentration gradient across the cell membrane. Similarly, transporters acting on both Na^+ and K^+ (e.g. Na^+ - K^+ - $2Cl^-$ cotransporter [173]), or acting on one but dependent on the gradient of the other (e.g. K^+ secretion through the distal ROMK channel is driven by Na^+ gradient [173]), are found along the distal convoluted tubule, the connecting tubule and the collecting duct. This link between Na^+ and K^+ due to transporter activity is the subject of a number of re-

views [151, 173, 106]. Finally, linking this model of K^+ regulation with one of Na^+ regulation may provide greater insights into the relationship between Na^+ , K^+ , and blood pressure regulation. Indeed, this model has been proposed with the intent to incorporate it into the model presented in chapter 4.

Chapter 6

Conclusion

This dissertation presents ordinary and algebraic differential equations based computational models to understand sex differences in blood pressure regulation and anti-hypertensive treatments. Model components include the cardiovascular system, renal sympathetic nervous system (RSNA), renal hemodynamics [207, 27, ?], nephron water and solute transport [39, ?, 126], the renin-angiotensin system (RAS), and water, sodium, and potassium homeostasis.

The first part of this dissertation presents a model of the RAS fitted for four groups of rats: male normotensive, female normotensive, male hypertensive, and female hypertensive rats. We investigate the mechanisms that drive the translation of physiological sex differences into sex differences in the efficacy of angiotensin converting enzyme inhibitors (ACEI) and angiotensin receptor blockers (ARB) in treating hypertension. We propose that female rats either have (1) a stronger feedback effect of AT1R-bound Ang II on renin secretion, or (2) stronger effects of AT2R-bound Ang II on the rest of body.

We further investigate the mechanisms behind sex differences in drug treatment efficacy by fitting the RAS submodel to male and female humans and incorporating the resulting submodel into a larger circulation model inspired by Refs. [78, 103, 80]. We integrate sex differences in RSNA and the effects of the RAS on the body. We identify the source of female protection against hypertension caused by increased afferent arteriole resistance as their less excitable RSNA. We also identify the advantage of ARB over ACEI in the female model as stemming from the effects of AT2R-bound

Ang II on renal arteriole resistance.

We then expand the scope of our blood pressure regulation model to investigate risk factors for “triple whammy” acute kidney injury. We refine the description of water reabsorption in the nephron to allow for proper simulation of loop diuretics. We identify low water intake (or another blood volume reducing event), an impaired myogenic response, and higher dosages as possible risk factors for triple whammy acute kidney injury.

Lastly, we present a model of potassium homeostasis. The model includes both feedforward and feedback controls involved in potassium regulation. We investigate the feasibility of muscle-kidney cross talk to stabilize variations in intracellular potassium concentration and conclude that to replicate the recovery from potassium loading or depletion muscle kidney cross talk likely controls distal tubule potassium secretion. While currently a stand-alone model, the potassium homeostasis is formulated to allow future incorporation into the blood pressure regulation model.

While the models described here have proven useful in answering questions relating to sex differences in blood pressure regulation and safety while treating hypertension, they are limited in a number of ways. In order to simulate kidney function under differing physiological and pathophysiological conditions, more detailed representation is needed (e.g., for nephron function [124, 133, 131] and for renal autoregulation [130, 118, 28, 48, 208, 209]). In order to simulate the molecular mechanisms of drugs a more detailed description of epithelial transport is needed [46, 134, 133, 124, 132, 122, 131]).

6.1 Future directions

In the future, we plan on combining the K^+ homeostasis model (chapter 5) with the blood pressure regulation model (chapter 4) and including the effects of renal Na^+ transport on renal K^+ transport and vice versa. This will allow us to (1) investigate the mechanisms behind how a high K^+ to Na^+ intake ratio can reduce blood pressure [151], (2) investigate how RAS inhibitors increase the risk of hyperkalemia [220], and (3) evaluate the efficacy of loop diuretics as a treatment for acute hyperkalemia [35]. We can also investigate the discrepancy noted in studies looking at high and low K^+ diets in chronic kidney disease patients. Currently, the suggested course of action is a low K^+ diet, but some studies have observed that high K^+ diets were associated with a lower risk of death or progression of kidney disease [35].

There are still many unknowns about how sex influences the development and treatment of hypertension, and the models presented here have the potential to be extended in ways to become tools to study these. Known sex differences in renal transporter expression [199, 234] can be included as done in Ref. [139]. We could also incorporate direct tracking of sex hormones and their effect on various model component – including the RAS, ALD, renal transport – which would allow us to look at changes that occur during the transition to menopause or better identify appropriate treatments for individuals based on hormone levels. These models can also be used to investigate sex differences in response to other anti-hypertensive treatments, such as the natriuretic effect of thiazide diuretics [60] and the safety of direct renin inhibitors [67]. These models can be used to investigate why there is a difference in RSNA activity levels in men and women, but renal denervation has the same anti-hypertensive effect in male and female SHR [96].

Appendix A

Determining Sex-specific Human RAS Parameters

To identify sex-specific RAS model parameters, we apply RAS hormone peptide levels from the literature (see Table 3.1 and description below) and solve for sex-specific RAS reaction rate constants as done in Chapter 2. The goal is to determine the reaction rates in Eqs. 3.1–3.11. To that end, we first set the RAS hormone peptide levels to values gleaned from literature. The values and references are found in Table 3.1 and further discussed below.

Human male concentrations are taken from Ref. [141, 104, 168, 26, 167]. Female hormone concentrations are estimated from these male values using the male-to-female ratios reported in the references given in Table 3.1, column labelled “Female”.

With the hormone concentrations specified, the 12 unknowns are (i) [PRC], (ii) PRA, (iii) AGT production rate (k_{AGT}) (iv) seven reaction rate constants (c_i), (v) [Ang IV], and (vi) [AT1R-bound Ang II].

The unknowns are computed by applying the steady-state formulation of the model equations (Eqs. 3.1–3.10), and the steady-state conservation equation.

$$\begin{aligned}
0 = & k_{\text{AGT}} - \frac{\ln(2)}{h_{\text{AGT}}}[\text{AGT}] - \frac{\ln(2)}{h_{\text{Ang I}}}[\text{Ang I}] - \frac{\ln(2)}{h_{\text{Ang II}}}[\text{Ang II}] \\
& - \frac{\ln(2)}{h_{\text{Ang (1-7)}}}[\text{Ang (1-7)}] - \frac{\ln(2)}{h_{\text{Ang IV}}}[\text{Ang IV}] \\
& - \frac{\ln(2)}{h_{\text{AT1R}}}[\text{AT1R-bound Ang II}] - \frac{\ln(2)}{h_{\text{AT2R}}}[\text{AT2R - bound Ang II}]
\end{aligned}$$

With 12 unknowns and 9 equations, we need 3 additional constraints. To that end, we impose the (i) ratio of AT1R-to-AT2R receptors (i.e., the associated reaction rate constants), (ii) ratio of NEP-to-ACE2, and (iii) ratio of ACE-to-Chymase. Sex-specified ratios are available for AT1R-to-AT2R receptors [210], but not the other ratios. See Table A.1.

Table A.1: Sex-specific RAS reaction rate constant ratios.

Ratio	Male	Female
ACE-to-Chymase	9.5	9.5
AT1R-to-AT2R	2.59[210]	0.7[210]
NEP-to-ACE2	8.78[195]	8.78[195]

Appendix B

Full Model Equations

B.1 Renal hemodynamics

RSNA Renal sympathetic nervous activity (RSNA) is the nervous system control of kidney function. RSNA is affected by mean arterial pressure (MAP) and right atrial pressure (P_{ra}). Mathematically, RSNA is the baseline level ($N_{rsna} = 1$) multiplied by the effects of MAP (α_{map}) and the effects of P_{ra} (α_{rap}). Eq. B.2 describes the sex differences in RSNA, namely that females have less excitable and more easily repressed RSNA [90]. Eqs. B.3 and B.4 are taken from Ref. [103].

$$rsna_0 = N_{rsna} \times \alpha_{map} \times \alpha_{rap} \quad (B.1)$$

$$rsna = \begin{cases} rsna_0^{\frac{1}{rsna_0}} & \text{in females} \\ rsna_0 & \text{in males} \end{cases} \quad (B.2)$$

$$\alpha_{map} = 0.5 + \frac{1}{1 + e^{(P_{ma} - 100 \text{ mmHg})/15}} \quad (B.3)$$

$$\alpha_{rap} = 1 - 0.008 \text{mmHg}^{-1} P_{ra} \quad (B.4)$$

Renal Resistance Renal vascular resistance (R_r) is the sum of afferent arteriole resistance (R_{aa}) and efferent arteriole resistance (R_{ea}). Afferent arteriole resistance (R_{aa}) is the baseline resistance ($R_{aa-ss} = 31.67 \text{ mmHg min L}^{-1}$) multiplied by the effects of RSNA (β_{RSNA}), tubuloglomerular feedback (Σ_{TGF}), the myogenic effect

(Σ_{myo}), AT1R-bound Ang II ($\Psi_{\text{AT1R-AA}}$), and AT2R-bound Ang II ($\Psi_{\text{AT1R-AA}}$).

The myogenic effect (Eq. B.8) is signalling stimulated by glomerular hydrostatic pressure (P_{gh}) meant to protect the delicate capillaries of the glomerulus from excessively high or low pressure.

Tubuloglomerular feedback is where sodium (Na^+) flow inside the nephron at the macula densa stimulates a signalling pathway which controls resistance at the afferent arteriole to maintain a safe level of luminal flow through the nephron. We model Tubuloglomerular feedback (Σ_{TGF}) as a function of macula densa Na^+ flow ($\Phi_{\text{md-sod}}$) [103].

Efferent arteriole resistance (R_{ea}) is the baseline resistance ($R_{\text{ea-ss}} = 51.66 \text{ mmHg min l}^{-1}$) multiplied by the effects of AT1R-bound Ang II ($\Psi_{\text{AT1R-EA}}$) [80] and AT2R-bound Ang II ($\Psi_{\text{AT2R-EA}}$). β_{RSNA} and Σ_{TGF} are given by Karaaslan et al. [103] while $\Psi_{\text{AT1R-AA}}$ and $\Psi_{\text{AT1R-EA}}$ are given by Hallow et al. [80].

$$R_{\text{aa}} = R_{\text{aa-ss}} \times \beta_{\text{rsna}} \times \Sigma_{\text{TGF}} \times \Sigma_{\text{myo}} \times \Psi_{\text{AT1R-AA}} \times \Psi_{\text{AT2R-AA}} \quad (\text{B.5})$$

$$R_{\text{ea}} = R_{\text{ea-ss}} \times \Psi_{\text{AT1R-EA}} \times \Psi_{\text{AT2R-EA}} \quad (\text{B.6})$$

$$\beta_{\text{rsna}} = 1.5(\text{rsna} - 1) + 1 \quad (\text{B.7})$$

$$\Sigma_{\text{myo}} = 0.9 + \frac{1}{1 + 9e^{-0.9(P_{\text{gh}}-62)}} \quad (\text{B.8})$$

$$\Sigma_{\text{TGF}} = 0.3408 + \frac{3.449}{3.88 + e^{(\Phi_{\text{md-sod}}-3.859)/-0.9617}} \quad (\text{B.9})$$

Renal blood flow Renal blood flow (Φ_{rb}) is mean arterial pressure (P_{ma}) divided by total renal resistance (R_{r}).

$$\Phi_{\text{rb}} = P_{\text{ma}}/R_{\text{r}} \quad (\text{B.10})$$

Glomerular filtration rate The glomerular filtration rate (Φ_{GFR}) is the product of the net filtration pressure (P_f) and the constant glomerular capillary filtration coefficient (C_{gcf}). The net filtration pressure is the difference between the glomerular hydrostatic pressure (P_{gh}) and the sum of the Bowman hydrostatic pressure (P_B) and the glomerular osmotic pressure (P_{go}), both of which are considered constant. The glomerular hydrostatic pressure (P_{gh}) is the difference between the mean arterial pressure (P_{ma}) and the mean afferent arteriole pressure, which is represented as the product of the renal blood flow (Φ_{rb}) and the afferent arteriole resistance (R_{aa}).

$$\Phi_{\text{GFR}} = P_f \times C_{\text{gcf}} \quad (\text{B.11})$$

$$P_f = P_{\text{gh}} - (P_B + P_{\text{go}}) \quad (\text{B.12})$$

$$P_{\text{gh}} = P_{\text{ma}} - \Phi_{\text{rb}} \times R_{\text{aa}} \quad (\text{B.13})$$

B.2 Sodium

Sodium intake Na^+ appetite is regulated by many things, including aldosterone (ALD), Ang II, brain osmolarity, arterial and venous baroreceptors, Na^+ concentration of blood plasma and cerebrospinal fluid, neuromodulators, and signals from the gut [64]. Here, Na^+ intake ($\Phi_{\text{sod-in}}$) is modeled to subtly vary with ALD concentration ($C_{\text{al}}^{0.765}$).

$$\Phi_{\text{sod-in}} = \frac{-0.93}{4.76 + 0.14C_{\text{al}}^{0.765}} + 0.230 \quad (\text{B.14})$$

Sodium amount and concentration The total Na^+ amount (M_{sod}) increases with Na^+ intake ($\Phi_{\text{sod-in}}$) and decreases with urine Na^+ flow ($\Phi_{\text{u-sod}}$). At baseline

the total Na^+ amount is 2160mEq.

$$\frac{dM_{\text{sod}}}{dt} = \Phi_{\text{sod-in}} - \Phi_{\text{u-sod}} \quad (\text{B.15})$$

The Na^+ concentration (C_{sod}) is equal to the total Na^+ amount (M_{sod}) divided by the extracellular fluid volume (V_{ecf}).

$$C_{\text{sod}} = M_{\text{sod}}/V_{\text{ecf}} \quad (\text{B.16})$$

Filtered sodium load The filtered Na^+ load is the rate at which Na^+ is freely filtered through the glomerulus. As such, the filtered Na^+ load (Φ_{filsod}) is the glomerular filtration rate (Φ_{GFR}) multiplied by the plasma Na^+ concentration (C_{sod}).

$$\Phi_{\text{filsod}} = \Phi_{\text{GFR}} \times C_{\text{sod}} \quad (\text{B.17})$$

Proximal tubule sodium transport The proximal model segment (pt) includes the proximal tubule and the loop of Henle and ends at the macula densa. Here, the amount of Na^+ reabsorbed depends on RSNA and bound angiotensin type one receptors ([AT1R-bound Ang II]). Proximal tubule Na^+ reabsorption ($\Phi_{\text{pt-sodreab}}$) is the fractional proximal tubule Na^+ reabsorption ($\eta_{\text{pt-sodreab}}$) multiplied by the filtered Na^+ load (Φ_{filsod}). Fractional proximal tubule Na^+ reabsorption ($\eta_{\text{pt-sodreab}}$) is a baseline amount ($\eta_{\eta-pt}$) multiplied by the effects of the filtered Na^+ load (γ_{filsod}), AT1R-bound Ang II (γ_{at}), and RSNA (γ_{rsna}). γ_{filsod} , γ_{rsna} , and γ_{at} are taken from [103] with some adjustments in γ_{at} to account for a different baseline [AT1R-bound Ang II] ($[\text{AT1R} - \text{boundAngII}]_{\text{eq}}$).

$$\Phi_{\text{pt-sodreab}} = \Phi_{\text{filsod}} \times \eta_{\text{pt-sodreab}} \quad (\text{B.18})$$

$$\eta_{\text{pt-sodreab}} = \eta_{\eta\text{-pt}} \times \gamma_{\text{filsod}} \times \gamma_{\text{at}} \times \gamma_{\text{rsna}} \quad (\text{B.19})$$

$$\gamma_{\text{filsod}} = 0.85 + \frac{0.3}{1 + e^{(\Phi_{\text{filsod}} - 18)/138}} \quad (\text{B.20})$$

$$\gamma_{\text{at}} = 0.95 + \frac{0.12}{1 + e^{2.6 - 2.3418[\text{AT1R-boundAngII}]/[\text{AT1R-boundAngII}]_{\text{eq}}}} \quad (\text{B.21})$$

$$\gamma_{\text{rsna}} = 0.72 + \frac{0.56}{1 + e^{(1 - \text{rsna})/2.18}} \quad (\text{B.22})$$

Macula densa Na^+ flow ($\Phi_{\text{md-sod}}$) is the filtered Na^+ load (Φ_{filsod}) less what was reabsorbed in the proximal tubule ($\Phi_{\text{pt-sodreab}}$).

$$\Phi_{\text{md-sod}} = \Phi_{\text{filsod}} - \Phi_{\text{pt-sodreab}} \quad (\text{B.23})$$

Distal tubule sodium transport The distal segment (dt) of our model includes the distal convoluted tubule and the connecting tubule. Here, Na^+ reabsorption is dependent on the ALD concentration (C_{al}). Distal tubule Na^+ reabsorption ($\Phi_{\text{dt-sodreab}}$) is the fractional distal tubule Na^+ reabsorption ($\eta_{\text{dt-sodreab}}$) multiplied by the macula densa Na^+ flow ($\Phi_{\text{md-sod}}$). Fractional distal tubule Na^+ reabsorption ($\eta_{\text{dt-sodreab}}$) is a baseline amount ($\eta_{\eta\text{-dt}}$) multiplied by the effect of ALD (ψ_{al}). ψ_{al} is taken from [103].

$$\Phi_{\text{dt-sodreab}} = \Phi_{\text{md-sod}} \times \eta_{\text{dt-sodreab}} \quad (\text{B.24})$$

$$\eta_{\text{dt-sodreab}} = \eta_{\eta\text{-dt}} \times \psi_{\text{al}} \quad (\text{B.25})$$

$$\psi_{\text{al}} = 0.17 + \frac{0.94}{1 + e^{(0.48 - 1.2 \log_{10}(C_{\text{al}}))/0.88}} \quad (\text{B.26})$$

Distal tubule Na^+ outflow ($\Phi_{\text{dt-sod}}$) is the macula densa Na^+ flow ($\Phi_{\text{md-sod}}$) minus

distal tubule Na^+ reabsorption ($\Phi_{\text{dt-sodreab}}$).

$$\Phi_{\text{dt-sod}} = \Phi_{\text{md-sod}} - \Phi_{\text{dt-sodreab}} \quad (\text{B.27})$$

Collecting duct sodium transport The collecting duct is the final part of the nephron where Na^+ reabsorption is affected by distal tubule Na^+ outflow ($\Phi_{\text{dt-sod}}$), atrial natriuretic peptide concentration (C_{anp}), and the ALD concentration (C_{al}). Collecting duct Na^+ reabsorption ($\Phi_{\text{cd-sodreab}}$) is equal to the distal tubule Na^+ outflow ($\Phi_{\text{dt-sod}}$) multiplied by the fractional collecting duct Na^+ reabsorption ($\eta_{\text{cd-sodreab}}$). The fractional collecting duct Na^+ reabsorption ($\eta_{\text{cd-sodreab}}$) is the baseline value ($\eta_{\eta\text{-cd}}$) multiplied by the effects of distal tubule Na^+ outflow (λ_{dt} , [103]), atrial natriuretic peptide (λ_{anp} , [103]), and ALD (λ_{al} , [80]).

$$\Phi_{\text{cd-sodreab}} = \Phi_{\text{dt-sod}} \times \eta_{\text{cd-sodreab}} \quad (\text{B.28})$$

$$\eta_{\text{cd-sodreab}} = \eta_{\eta\text{-cd}} \times \lambda_{\text{dt}} \times \lambda_{\text{anp}} \quad (\text{B.29})$$

$$\lambda_{\text{dt}} = 0.82 + \frac{0.39}{1 + e^{(\Phi_{\text{dt-sod}} - 1.7625)/0.375}} \quad (\text{B.30})$$

$$\lambda_{\text{anp}} = -0.1 \times \hat{C}_{\text{anp}} + 1.1 \quad (\text{B.31})$$

$$\lambda_{\text{al}} = \frac{1}{0.76} C_{\text{al}}^{0.06} \quad (\text{B.32})$$

Urine Na^+ flow ($\Phi_{\text{u-sod}}$) is distal tubule Na^+ outflow ($\Phi_{\text{dt-sod}}$) minus collecting duct Na^+ reabsorption ($\Phi_{\text{cd-sodreab}}$).

$$\Phi_{\text{u-sod}} = \Phi_{\text{dt-sod}} - \Phi_{\text{cd-sodreab}} \quad (\text{B.33})$$

B.3 Water

Water intake The rate of water intake (Φ_{win}) is dependent on the antidiuretic hormone concentration (C_{adh}) [103].

$$\Phi_{\text{win}} = \max\left(0, \frac{0.0078541}{0.65451 + 18.22(C_{\text{adh}})^{-1.607}} - 0.002\right) \quad (\text{B.34})$$

Fluid volume The rate of change in extracellular fluid volume (V_{ecf}) is the water intake (Φ_{win}) minus the urine flow rate (Φ_{u}). The steady state value for V_{ecf} is 15L.

$$\frac{dV_{\text{ecf}}}{dt} = \Phi_{\text{win}} - \Phi_{\text{u}} \quad (\text{B.35})$$

Blood volume (V_{b}) is represented as a function of extracellular fluid volume (V_{ecf}). We differ from Karaaslaan [103] and Guyton [78] in that we allow V_{b} to decrease with V_{ecf} rather than levelling off. This is necessary in order for the model to experience hypovolemia.

$$V_{\text{b}} = 0.325 \times V_{\text{ecf}} \quad (\text{B.36})$$

Urine production Water resorption along the nephron is driven by the antidiuretic hormone concentration (C_{adh}) as well as the osmotic gradient produced through Na^+ transport. As such, tubular water reabsorption ($\Phi_{\text{t-wreab}}$) is modeled as a minimum amount (A_{twreab}) minus some amount due to antidiuretic hormone (μ_{adh}) plus a fraction of the glomerular filtration rate (Φ_{GFR}) determined by the ratio of the total Na^+ reabsorption to baseline (μ_{Na}). This includes Na^+ reabsorption in the proximal

tubule ($\Phi_{\text{pt-sodreab}}$), distal tubule ($\Phi_{\text{dt-sodreab}}$), and collecting duct ($\Phi_{\text{cd-sodreab}}$).

$$\Phi_{\text{t-wreab}} = A_{\text{twreab}} - \frac{0.001}{\mu_{\text{adh}}} + (0.8 + 0.08 * \tanh(8.5(\mu_{\text{Na}} - 1)))\Phi_{\text{GFR}} \quad (\text{B.37})$$

$$\mu_{\text{Na}} = \frac{\Phi_{\text{pt-sodreab}} + \Phi_{\text{dt-sodreab}} + \Phi_{\text{cd-sodreab}}}{\Phi_{\text{pt-sdoreab}}^{eq} + \Phi_{\text{dt-sdoreab}}^{eq} + \Phi_{\text{cd-sdoreab}}^{eq}} \quad (\text{B.38})$$

$$\mu_{\text{adh}} = 0.3313 + \frac{0.8}{1 + e^{0.6 - 3.7 \log_{10}(C_{\text{adh}})}} \quad (\text{B.39})$$

$$(\text{B.40})$$

Urine flow (Φ_{u}) is equal to the glomerular filtration rate (Φ_{GFR}) minus tubular water reabsorption ($\Phi_{\text{t-wreab}}$).

$$\Phi_{\text{u}} = \Phi_{\text{GFR}} - \Phi_{\text{t-wreab}} \quad (\text{B.41})$$

B.4 The cardiovascular system

Mean filling pressure Mean filling pressure (P_{mf}) is the weighted average of pressure in all segments of the circulation system [78]. The compliance of all segments of the circulation is affected by the autonomous nervous system, represented here by the autonomic multiplier effect (ϵ_{aum}). Thus, mean filling pressure (P_{mf}) is a function of both blood volume (V_{b}) and the autonomic multiplier effect (ϵ_{aum}) [103].

$$P_{\text{mf}} = (7.436 \text{ mmHg/L} \times V_{\text{b}} - 30.18 \text{ mmHg}) \times \epsilon_{\text{aum}} \quad (\text{B.42})$$

Heart function The venous return (Φ_{vr}), which is blood flow into the heart, is the mean filling pressure (P_{mf}) minus the right atrial pressure (P_{ra}) and divided by the

resistance to venous return (R_{vr}),

$$\Phi_{vr} = \frac{P_{mf} - P_{ra}}{R_{vr}} \quad (\text{B.43})$$

The cardiac output (Φ_{co}) is taken equal to the venous return (Φ_{vr}), as at steady state, the input to and the output from the heart must be equal.

$$\Phi_{co} = \Phi_{vr} \quad (\text{B.44})$$

According to the Frank-Starling Law, the right atrial pressure (P_{ra}) is a function of the cardiac output (Φ_{co}) [78]. We subtract a constant (P_{ra-eq}) at the end so that P_{ra} is equal to zero at steady state.

$$P_{ra} = 0.2787 \text{ mmHg} \times e^{\Phi_{co} \times (0.2281 \text{ min/L})} - P_{ra-eq} \quad (\text{B.45})$$

Blood vessel growth Vascularity (vas) is a representation of the average measure of the number and diameter of blood vessels in the body. During long periods of excess blood flow in the circulatory system, the diameter and number of tissue vessels slowly increase. Similarly, the “vascularity” decreases slowly during times of too little flow. As such, we model the rate of change in vascularity as the difference between the vascularity formation rate (vas_f) and the vascularity destruction rate (vas_d). The vascular formation rate is modeled as a function of cardiac output (Φ_{co}) while the vascular destruction is a constant fraction ($K_{vd} = 0.00001$) of vascularity.

The equations for both vascular formation and destruction are taken from [103].

$$\frac{d\text{vas}}{dt} = \text{vas}_f - \text{vas}_d \quad (\text{B.46})$$

$$\text{vas}_f = \frac{11.312 \times e^{-\Phi_{co} \times (0.4799 \text{ min/L})}}{100000} \quad (\text{B.47})$$

$$\text{vas}_d = \text{vas} \times K_{vd} \quad (\text{B.48})$$

Arterial resistance The arterial resistance (R_a) is the basic arterial resistance (R_{ba}) multiplied by the autonomic multiplier effect (ϵ_{aum}). The basic arterial resistance (R_{ba}) is inversely proportional to vascularity (vas) with a constant of proportionality $K_{bar} = 16.6 \text{ mmHg min/mL}$ [103].

$$R_a = R_{ba} \times \epsilon_{aum} \quad (\text{B.49})$$

$$R_{ba} = K_{bar}/\text{vas} \quad (\text{B.50})$$

$$(\text{B.51})$$

Guyton et al. [78] describes the resistance to venous return (R_{vr}) as a weighted sum of a constant basic venous resistance (R_{bv}) and the arterial resistance (R_a).

$$R_{vr} = (8R_{bv} + R_a)/31 \quad (\text{B.52})$$

The total peripheral resistance (R_{tp}) is equal to the sum of the arterial resistance (R_a) and the basic venous resistance (R_{bv}).

$$R_{tp} = R_a + R_{bv} \quad (\text{B.53})$$

Mean arterial pressure Mean arterial pressure (P_{ma}) is equal to the cardiac output (Φ_{co}) multiplied by the total peripheral resistance (R_{tp}).

$$P_{\text{ma}} = \Phi_{\text{co}} \times R_{\text{tp}} \quad (\text{B.54})$$

B.5 Feedback systems

Autonomous nervous system As done in Guyton et al. [78], the effects of the autonomous nervous system is represented as a normalized variable, the autonomic multiplier effect (ϵ_{aum}). It is composed of chemoreceptor (a_{chemo}) and baroreceptor (a_{baro}) activities, which are functions of the mean arterial pressure (P_{ma}). a_{auto} is an intermediate variable. Eq. B.58 includes adaptation behavior where $0.0000667 \text{ min}^{-1}$ is the inverse of the adaptation time constant.

$$\epsilon_{\text{aum}} = a_{\text{chemo}} + a_{\text{baro}} \quad (\text{B.55})$$

$$a_{\text{auto}} = 3.0042e^{-P_{\text{ma}} \times 0.0011 \text{ mmHg}^{-1}} \quad (\text{B.56})$$

$$a_{\text{chemo}} = \frac{1}{4}a_{\text{auto}} \quad (\text{B.57})$$

$$\frac{da_{\text{baro}}}{dt} = \frac{3}{4} \left(\frac{da_{\text{auto}}}{dt} - (0.0000667 \text{ min}^{-1}) \times (a_{\text{baro}} - 1) \right) \quad (\text{B.58})$$

Antidiuretic hormone The antidiuretic hormone concentration (C_{adh}) is modeled as the product of the normalized antidiuretic hormone concentration (N_{adh}) times its baseline value (4 milli-units/L). Eq. B.60 models the regulation mechanisms, whereby the normalized antidiuretic hormone concentration (N_{adh}) is regulated to the normalized antidiuretic hormone secretion rate (N_{adhs}) as done in [103]. The time constant T_{adh} is taken as 6 min, the baseline value of N_{adh} is taken as 1. The normalized antidiuretic secretion rate (N_{adhs}) is dependent on the Na^+ concentration (C_{sod}) when

it is above 141 mEq/L, the autonomic multiplier effect (ϵ_{aum}) when it is greater than 1, and the effect of right atrial pressure (δ_{ra}). Eqs. B.61 and B.62 are taken from [103].

$$C_{\text{adh}} = 4 \text{ milli-units/L} \times N_{\text{adh}} \quad (\text{B.59})$$

$$\frac{dN_{\text{adh}}}{dt} = \frac{1}{T_{\text{adh}}} (N_{\text{adhs}} - N_{\text{adh}}) \quad (\text{B.60})$$

$$N_{\text{adhs}} = (\max(141, C_{\text{sod}}) - 141 + \max(1, \epsilon_{\text{aum}}) - 1 - \delta_{\text{ra}}) / 3 \quad (\text{B.61})$$

$$\frac{d\delta_{\text{ra}}}{dt} = 0.2P_{\text{ra}} - 0.0007\delta_{\text{ra}} \quad (\text{B.62})$$

Aldosterone The ALD concentration (C_{al}) is the normalized ALD concentration (N_{al}) multiplied by the baseline ALD concentration ($C_{\text{al}}^{\text{eq}}$). The rate of change in the normalized ALD concentration is dependent on normalized ALD secretion (N_{als}) and decay. The time constant T_{al} governing the regulation of ALD concentration is taken as 60 min, as used by Guyton et al. [78]. Normalized ALD secretion is affected by the potassium to Na^+ ratio ($\xi_{\text{k/sod}}$), MAP (ξ_{map}), and AT1R-bound Ang II (ξ_{at}). $\xi_{\text{k/sod}}$ is taken from [103]. ξ_{map} represents the direct stimulation of ALD that may be present in cases of hypotension, as done by [78]. ξ_{at} is taken from [103] with some

adjustments for our baseline value of AT1R-bound Ang II ($[AT1R - boundAngII]_{EQ}$).

$$C_{al} = N_{al} \times C_{al}^{eq} \quad (B.63)$$

$$\frac{dN_{al}}{dt} = \frac{1}{T_{al}} (N_{als} - N_{al}) \quad (B.64)$$

$$N_{als} = \xi_{k/sod} \times \xi_{map} \times \xi_{at} \quad (B.65)$$

$$\xi_{k/sod} = \frac{C_K/C_{sod}}{0.00496} - 6 \quad (B.66)$$

$$\xi_{map} = \begin{cases} 70.1054e^{-(0.0425) \times P_{ma}} & P_{ma} \leq 100 \text{ mmHg} \\ 1 & P_{ma} > 100 \text{ mmHg} \end{cases} \quad (B.67)$$

$$\xi_{at} = 0.47 + \frac{2.4}{1 + e^{(2.82 - 1.9515[AT1R - boundAngII]/[AT1R - boundAngII]_{EQ})/0.8}} \quad (B.68)$$

Atrial natriuretic peptide Atrial natriuretic peptide is the main component of a pathway whereby right artial pressure influences renal Na^+ excretion. The normalized atrial natriuretic peptide concentration (\hat{C}_{anp}) is a function of right atrial pressure (P_{ra}) in accordance with Lohmeier et al. [143].

$$\hat{C}_{anp} = 7.4052 - \frac{6.554}{1 + e^{(P_{ra} - 3.762 \text{ mmHg})/(1 \text{ mmHg})}} \quad (B.69)$$

B.6 Renin-angiotensin system model

AGT is catalytically cleaved by plasma renin activity (PRA) to produce Ang I. The rate of change of $[AGT]$ is given by the production rate k_{AGT} , its conversion to Ang I, and the decay based on its half life h_{AGT} .

$$\frac{d[AGT]}{dt} = k_{AGT} - PRA - \frac{\ln(2)}{h_{AGT}} [AGT] \quad (B.70)$$

Renin is secreted at the rate R_{sec} . It has a baseline rate of N_{rs} and is dependent on the feedback from [AT1R-bound Ang II] (ν_{AT1} [80]).

$$R_{sec} = N_{rs} \times \nu_{md-sod} \times \nu_{rsna} \times \nu_{AT1} \quad (\text{B.71})$$

$$\nu_{md-sod} = 0.2262 + \frac{28.04}{11.56 + e^{(\Phi_{md-sod} - A_{nu-mdsod})/(0.6056 \text{ mEq/min})}} \quad (\text{B.72})$$

$$\nu_{rsna} = 1.822 - \frac{2.056}{1.358 + e^{rsna-0.8667}} \quad (\text{B.73})$$

$$\nu_{AT1} = 10^{0.0102 - 0.95 \times \log_{10} \left(\frac{[\text{AT1R-bound Ang II}]}{[\text{AT1R-bound Ang II}]_{EQ}} \right)} \quad (\text{B.74})$$

The plasma renin concentration (PRC) is dependent on R_{sec} and decays with a half life of h_{renin} . PRA is related to [PRC] by a fixed constant of $X_{PRC-PRA}$ which was determined by [80] from the ratio of PRA to PRC in normotensive subjects in the absence of RAS-blocking therapies.

$$\frac{d[\text{PRC}]}{dt} = R_{sec} - \frac{\ln(2)}{h_{renin}} [\text{PRC}] \quad (\text{B.75})$$

$$\text{PRA} = [\text{PRC}] \times X_{PRC-PRA} \quad (\text{B.76})$$

Ang I is converted into other forms through angiotensin converting enzyme (ACE), chymase, and neutral endopeptidase (NEP) activity; the respective reaction rate constants are denoted c_{ACE} , c_{chym} , and c_{NEP} . The half life of Ang I is denoted $h_{Ang I}$.

$$\frac{d[\text{Ang I}]}{dt} = \text{PRA} - (c_{ACE} + c_{chym} + c_{NEP})[\text{Ang I}] - \frac{\ln(2)}{h_{Ang I}} [\text{Ang I}] \quad (\text{B.77})$$

Ang II is converted from Ang I through ACE and chymase and then converted into Ang (1-7) through ACE2 at the rate c_{ACE2} . Ang II also binds to the AT1R

and AT2R at rates c_{AT1R} and c_{AT2R} , respectively. We assume that Ang II, AT1R-bound Ang II, and AT2R-bound Ang II have half lives $h_{Ang II}$, h_{AT1R} , and h_{AT2R} , respectively.

$$\begin{aligned} \frac{d[Ang II]}{dt} &= (c_{ACE} + c_{chym})[Ang I] - (c_{ACE2} + c_{Ang II=Ang IV} + c_{AT1R} + c_{AT2R}) \\ &\quad \times [Ang II] - \frac{\ln(2)}{h_{Ang II}}[Ang II] \end{aligned} \quad (B.78)$$

$$\frac{d[AT1R-bound Ang II]}{dt} = c_{AT1R}[Ang II] - \frac{\ln(2)}{h_{AT1R}}[AT1R-bound Ang II] \quad (B.79)$$

$$\frac{d[AT2R-bound Ang II]}{dt} = c_{AT2R}[Ang II] - \frac{\ln(2)}{h_{AT2R}}[AT2R-bound Ang II] \quad (B.80)$$

Ang (1-7) is converted by NEP from Ang I and by ACE2 from Ang II, and it decays with a half life of $h_{Ang (1-7)}$.

$$\frac{d[Ang (1-7)]}{dt} = c_{NEP}[Ang I] + c_{ACE2}[Ang II] - \frac{\ln(2)}{h_{Ang (1-7)}}[Ang (1-7)] \quad (B.81)$$

Ang IV is converted from Ang II at the rate $c_{Ang II=Ang IV}$ and decays with a half life of $h_{Ang IV}$.

$$\frac{d[Ang IV]}{dt} = c_{Ang II=Ang IV}[Ang II] - \frac{\ln(2)}{h_{Ang IV}}[Ang IV] \quad (B.82)$$

Table B.1: Parameter values for model equations. Values for the female model are only listed when they differ from the male model.

Parameter	Unit	Male	Female
$\eta_{\eta\text{-cd}}$		0.93	
$\eta_{\eta\text{-dt}}$		0.5	
$\eta_{\eta\text{-pt}}$		0.93	
$\Phi_{\text{cd-sdoreab}}^{eq}$	mEq/min	1.6909	
$\Phi_{\text{dt-sdoreab}}^{eq}$	mEq/min	1.5859	
$\Phi_{\text{pt-sdoreab}}^{eq}$	mEq/min	13.909	
$[\text{AT1R-bound Ang II}]_{\text{eq}}$	fmol/mL	13.99	3.78
$[\text{AT2R-bound Ang II}]_{\text{eq}}$	fmol/mL	5.0854	5.0854
$A_{\nu\text{-mdsod}}$		1.73	1.637
A_{Pra}		0.8268	0.8245
A_{sodin}		-0.087	-0.0741
$A_{\text{t-wreab}}$		0.0193	0.0199
B_{sodin}		2.0404	1.7115
C_{al}^{eq}	ng/L	85	69.1775
C_{gcf}		0.00781	
C_{K}	mEq/mL	5	
c_{ACE}	1/min	0.88492	1.4079
c_{ACE2}	1/min	0.0078009	0.0037603
$c_{\text{AngII=AngIV}}$	1/min	0.25056	0.038644
c_{AT1R}	1/min	0.17008	0.027089
c_{AT2R}	1/min	0.065667	0.038699
c_{chym}	1/min	0.09315	0.1482

Table B.1: Parameter values for model equations. Values for the female model are only listed when they differ from the male model.

Parameter	Unit	Male	Female
c_{NEP}	1/min	0.038189	0.060759
h_{AGT}	min	600	
h_{AngI}	min	0.5	
h_{AngII}	min	0.66	
h_{AngIV}	min	0.5	
$h_{\text{Ang}(1-7)}$	min	30	
h_{AT1R}	min	12	
h_{AT2R}	min	12	
h_{renin}	min	12	
K_{vd}		0.01	
K_{bar}	mmHg min/mL	16.6	
k_{AGT}	1/min	577.04	610.39
N_{rs}	mg/mL/min	1	
N_{rsna}		1	
P_{B}	mmHg	18	
P_{go}	mmHg	28	
$R_{\text{aa-ss}}$	mmHg min l ⁻¹	31.67	
R_{bv}	mmHg min /mL	3.4	
$R_{\text{ea-ss}}$	mmHg min l ⁻¹	51.66	
T_{adh}	min	6	
T_{al}	min	60	
$X_{\text{PRC-PRA}}$	fmol/min/pg	1.01666	

Table B.2: Variable values at steady state.

Variable	Unit	Male	Female
α_{map}		0.9412	0.9619
α_{rap}		1	1
β_{rsna}		0.9072	0.9376
γ_{at}		0.9928	0.9931
γ_{filsod}		1	1
γ_{rsna}		0.9962	0.9975
δ_{ra}		0	0
ϵ_{aum}		1.2404	1.2438
$\eta_{\text{cd-sodreab}}$		0.9294	0.9277
$\eta_{\text{dt-sodreab}}$		0.5530	0.5523
$\eta_{\text{pt-sodreab}}$		0.7908	0.79215
λ_{anp}		0.9999	0.9999
λ_{al}		0.9890	0.9769
λ_{dt}		1.0106	1.0212
μ_{adh}		0.9940	0.9978
μ_{Na}		1.0998	1.0800
ν_{AT1}		1.1839	1.1781
$\nu_{\text{md-sod}}$		0.7591	0.7611
ν_{rsna}		0.9777	0.9850
ξ_{at}		0.9328	0.9369
ξ_{map}		1	1
$\xi_{\text{k/sod}}$		1.0165	1.0137
Σ_{TGF}		1.0652	1.0513

Table B.2: Variable values at steady state.

Variable	Unit	Male	Female
Σ_{myo}		1.1083	1.0659
$\Phi_{\text{cd-sodreab}}$	mEq/min	1.6539	1.6131
Φ_{co}	L/min	4.7964	4.7727
$\Phi_{\text{dt-sod}}$	mEq/min	1.7795	1.7387
$\Phi_{\text{dt-sodreab}}$	mEq/min	2.2012	2.1451
Φ_{filsod}	mEq/min	19.0269	18.6855
Φ_{GFR}	L/min	0.1324	0.1300
$\Phi_{\text{md-sod}}$	mEq/min	3.9808	3.8839
$\Phi_{\text{pt-sodreab}}$	mEq/min	15.0461	14.8017
Φ_{rb}	L/min	1.2351	1.2178
Φ_{sodin}	mEq/min	0.1256	0.1256
$\Phi_{\text{t-wreab}}$	L/min	0.1316	0.1291
Φ_{u}	L/min	0.00088	0.00096
$\Phi_{\text{u-sod}}$	mEq/min	0.1256	0.1256
Φ_{vr}	L/min	4.7964	4.7727
Φ_{win}	L/min	0.00088	0.00096
$\Psi_{\text{AT1R-AA}}$		0.9688	0.9698
$\Psi_{\text{AT1R-EA}}$		0.9867	0.9872
$\Psi_{\text{AT2R-AA}}$		1	1.0088
$\Psi_{\text{AT2R-EA}}$		1	1.0088
ψ_{al}		1.1059	1.1046
[AGT]	fmol/mL	486107	514908
[Ang I]	fmol/mL	6.4376	5.1760

Table B.2: Variable values at steady state.

Variable	Unit	Male	Female
[Ang II]	fmol/mL	4.0771	6.9529
[Ang IV]	fmol/mL	0.7369	0.1938
[Ang (1-7)]	fmol/mL	12.0170	14.7429
[AT1R-bound Ang II]	fmol/mL	12.0051	3.2607
[AT2R-bound Ang II]	fmol/mL	4.6351	4.6583
a_{auto}		0.9617	0.9752
a_{baro}		1	1
a_{chemo}		0.2404	0.2438
C_{al}	ng/L	80.60	65.70
C_{adh}	munits/L	3.8688	3.9504
\hat{C}_{anp}		1.0008	1.0005
C_{sod}	mEq/L	143.66	143.72
M_{sod}	mEq	2130.86	2127.90
N_{adh}		0.96719	0.9876
N_{adhs}		0.96719	0.9876
N_{al}		0.9482	0.9497
N_{als}		0.9482	0.9497
P_{f}	mmHg	16.958	16.647
P_{gh}	mmHg	62.958	62.647
P_{ma}	mmHg	103.55	102.29
P_{mf}	mmHg	7.0281	6.9671
P_{ra}	mmHg	0.0055	0.0033
PRA	fmol/mL/min	15.467	15.544

Table B.2: Variable values at steady state.

Variable	Unit	Male	Female
[PRC]	pg/mL	15.213	15.290
R_a	mmHg min/L	18.188	18.0317
R_{aa}	mmHg min/L	32.863	32.552
R_{ba}	mmHg min/L	14.663	14.497
R_{ea}	mmHg min/L	50.975	51.444
R_r	mmHg min/L	83.839	83.996
R_{sec}		0.8787	0.8832
R_{tp}	mmHg min/L	21.588	21.432
R_{vr}	mmHg min/L	1.4641	1.4591
rsna		0.94112	0.96045
rsna ₀		0.94112	
V_{ecf}	L	14.833	14.806
V_b	L	4.8206	4.8119
vas		1.1321	1.1450
vas _d		0.011321	0.01145
vas _f		0.011321	0.01145

Bibliography

- [1] S. R. ABRAM, B. L. HODNETT, R. L. SUMMERS, T. G. COLEMAN, AND R. L. HESTER, *Quantitative circulatory physiology: an integrative mathematical model of human physiology for medical education*, Advances in Physiology Education, 31 (2007). PMID: 17562912.
- [2] P. J. ADMIRAAL, A. H. DANSER, M. S. JONG, H. PIETERMAN, F. H. DERKX, AND M. A. SCHALEKAMP, *Regional angiotensin ii production in essential hypertension and renal artery stenosis.*, Hypertension, 21 (1993), pp. 173–184.
- [3] S. AHMED, R. HU, J. LEETE, AND A. T. LAYTON, *Understanding sex differences in long-term blood pressure regulation: insights from experimental studies and computational modeling*, American Journal of Physiology-Heart and Circulatory Physiology, 316 (2019), pp. H1113–H1123. PMID: 30875261.
- [4] M. ARAUJO AND W. J. WELCH, *Cyclooxygenase 2 inhibition suppresses tubuloglomerular feedback: roles of thromboxane receptors and nitric oxide*, American Journal of Physiology-Renal Physiology, 296 (2009), pp. F790–F794.
- [5] M. ARAUJO, W. J. WELCH, X. ZHOU, K. SULLIVAN, S. WALSH, A. PASTERNAK, AND C. S. WILCOX, *Inhibition of romk blocks macula densa tubuloglomerular feedback yet causes renal vasoconstriction in anesthetized rats*, American Journal of Physiology-Renal Physiology, 312 (2017), pp. F1120–F1127.
- [6] T. ATANASOVSKA, A. C. PETERSEN, D. M. ROUFFET, F. BILLAUT, I. NG, AND M. J. MCKENNA, *Plasma K^+ dynamics and implications during and following intense rowing exercise*, Journal of Applied Physiology, 117 (2014), pp. 60–68. PMID: 24812644.
- [7] V. A. AVERINA, H. G. OTHMER, G. D. FINK, AND J. W. OSBORN, *A new conceptual paradigm for the haemodynamics of salt-sensitive hypertension: a mathematical modelling approach*, The Journal of Physiology, 590 (2012), pp. 5975–5992.
- [8] M. AZIZI, A. LINHART, J. ALEXANDER, A. GOLDBERG, J. MENTEN, C. SWEET, AND J. MÉNARD, *Pilot study of combined blockade of the renin–angiotensin system in essential hypertensive patients*, Journal of hypertension, 18 (2000), pp. 1139–1147.
- [9] G. BAIARDI, M. MACOVA, I. ARMANDO, H. ANDO, D. TYURMIN, AND J. M. SAAVEDRA, *Estrogen upregulates renal angiotensin ii at1 and at2 receptors in the rat*, Regulatory Peptides, 124 (2005), pp. 7 – 17.

- [10] D. A. BEARD AND M. MESCAM, *Mechanisms of pressure-diuresis and pressure-natriuresis in dahl salt-resistant and dahl salt-sensitive rats*, BMC physiology, 12 (2012), p. 6.
- [11] D. A. BEARD, K. H. PETERSEN, B. E. CARLSON, S. W. OMHOLT, AND S. M. BUGENHAGEN, *A computational analysis of the long-term regulation of arterial pressure*, F1000Research, 2 (2013).
- [12] E. J. BENJAMIN, P. MUNTNER, A. ALONSO, M. S. BITTENCOURT, C. W. CALLAWAY, A. P. CARSON, A. M. CHAMBERLAIN, A. R. CHANG, S. CHENG, S. R. DAS, F. N. DELLING, L. DJOUSSE, M. S. ELKIND, J. F. FERGUSON, M. FORNAGE, L. C. JORDAN, S. S. KHAN, B. M. KISSELA, K. L. KNUTSON, T. W. KWAN, D. T. LACKLAND, T. T. LEWIS, J. H. LICHTMAN, C. T. LONGENECKER, M. S. LOOP, P. L. LUTSEY, S. S. MARTIN, K. MATSUSHITA, A. E. MORAN, M. E. MUSSOLINO, M. O’FLAHERTY, A. PANDEY, A. M. PERAK, W. D. ROSAMOND, G. A. ROTH, U. K. SAMPSON, G. M. SATOU, E. B. SCHROEDER, S. H. SHAH, N. L. SPARTANO, A. STOKES, D. L. TIRSCHWELL, C. W. TSAO, M. P. TURAKHIA, L. B. VANWAGNER, J. T. WILKINS, S. S. WONG, S. S. VIRANI, AND NULL NULL, *Heart disease and stroke statistics—2019 update: A report from the american heart association*, Circulation, 139 (2019), pp. e56–e528.
- [13] G. BIANCHI, U. FOX, G. DI FRANCESCO, A. GIOVANETTI, AND D. PAGETTI, *Blood pressure changes produced by kidney cross-transplantation between spontaneously hypertensive rats and normotensive rats*, Clinical Science, 47 (1974), pp. 435–448.
- [14] A. K. BIDANI, K. A. GRIFFIN, G. WILLIAMSON, X. WANG, AND R. LOUTZENHISER, *Protective importance of the myogenic response in the renal circulation*, Hypertension, 54 (2009), pp. 393–398.
- [15] A. K. BIDANI, A. J. POLICHNOWSKI, R. LOUTZENHISER, AND K. A. GRIFFIN, *Renal microvascular dysfunction, hypertension and ckd progression*, Current opinion in nephrology and hypertension, 22 (2013), p. 1.
- [16] K. J. BUBB, R. S. KHAMBATA, AND A. AHLUWALIA, *Sexual dimorphism in rodent models of hypertension and atherosclerosis*, Br. J. Pharmacol., 167 (2012), pp. 298–312.
- [17] S. M. BUGENHAGEN, A. W. COWLEY, AND D. A. BEARD, *Identifying physiological origins of baroreflex dysfunction in salt-sensitive hypertension in the dahl ss rat*, Physiological genomics, 42 (2010), pp. 23–41.
- [18] L. CALO, A. BORSATTI, S. FAVARO, AND L. RABINOWITZ, *Kaliuresis in normal subjects following oral potassium citrate intake without increased plasma potassium concentration*, Nephron, 69 (1995), pp. 253–258.

- [19] R. M. G. CAMIN, M. COLS, J. L. CHEVARRIA, R. G. OSUNA, M. CARRERAS, J. M. LISBONA, AND J. CODERCH, *Acute kidney injury secondary to a combination of renin-angiotensin system inhibitors, diuretics and nsaid: "the triple whammy"*, *Nefrología (English Edition)*, 35 (2015), pp. 197–206.
- [20] D. J. CAMPBELL, A. C. LAWRENCE, A. TOWRIE, A. KLADIS, AND A. J. VALENTIJN, *Differential regulation of angiotensin peptide levels in plasma and kidney of the rat.*, *Hypertension*, 18 (1991), pp. 763–773.
- [21] T. J. CAMPEN, D. A. VAUGHN, AND D. D. FANESTIL, *Mineralo- and glucocorticoid effects on renal excretion of electrolytes*, *Pflügers Archiv*, 399 (1983), pp. 93–101.
- [22] V. J. CANZANELLO, E. BARANCO-PRYOR, F. RAHBARI-OSKOU, G. L. SCHWARTZ, E. BOERWINKLE, S. T. TURNER, AND A. B. CHAPMAN, *Predictors of blood pressure response to the angiotensin receptor blocker candesartan in essential hypertension*, *American Journal of Hypertension*, 21 (2008), pp. 61–66.
- [23] M. CARLSTRÖM, C. S. WILCOX, AND W. J. ARENDSHORST, *Renal autoregulation in health and disease*, *Physiological reviews*, 95 (2015), pp. 405–511.
- [24] M. C. CHAPPELL, *Nonclassical Renin-Angiotensin System and Renal Function*, John Wiley & Sons, Inc., 2012.
- [25] M. C. CHAPPELL, A. C. MARSHALL, E. M. ALZAYADNEH, H. A. SHALTOU, AND D. I. DIZ, *Update on the angiotensin converting enzyme 2-angiotensin (1-7)-mas receptor axis: fetal programming, sex differences, and intracellular pathways*, *Front Endocrinol (Lausanne)*, 4 (2014), pp. 201–201.
- [26] M. C. CHAPPELL, N. T. PIRRO, A. SYKES, AND C. M. FERRARIO, *Metabolism of angiotensin-(1-7) by angiotensin-converting enzyme*, *Hypertension*, 31 (1998), pp. 362–367.
- [27] J. CHEN, A. EDWARDS, AND A. T. LAYTON, *Effects of ph and medullary blood flow on oxygen transport and sodium reabsorption in the rat outer medulla*, *American Journal of Physiology-Renal Physiology*, 298 (2010), pp. F1369–F1383.
- [28] J. CHEN, I. SGOURALIS, L. C. MOORE, H. E. LAYTON, AND A. T. LAYTON, *A mathematical model of the myogenic response to systolic pressure in the afferent arteriole*, *American Journal of Physiology-Renal Physiology*, 300 (2010), pp. F669–F681.
- [29] P. CHEN, J. P. GUZMAN, P. K. K. LEONG, L. E. YANG, A. PERIANAYAGAM, E. BABILONIA, J. S. HO, J. H. YOUN, W. H. WANG, AND

- A. A. McDONOUGH, *Modest dietary K^+ restriction provokes insulin resistance of cellular K^+ uptake and phosphorylation of renal outer medulla K^+ channel without fall in plasma K^+ concentration*, *American Journal of Physiology-Cell Physiology*, 290 (2006), pp. C1355–C1363. PMID: 16354756.
- [30] Y. CHEN, J. C. SULLIVAN, A. EDWARDS, AND A. T. LAYTON, *Sex-specific computational models of the spontaneously hypertensive rat kidneys: factors affecting nitric oxide bioavailability*, *American Journal of Physiology-Renal Physiology*, 313 (2017), pp. F174–F183.
- [31] Y.-F. CHEN AND Q.-C. MENG, *Sexual dimorphism of blood pressure in spontaneously hypertensive rats is androgen dependent*, *Life Sciences*, 48 (1991), pp. 85 – 96.
- [32] C.-J. CHENG, E. KUO, AND C.-L. HUANG, *Extracellular potassium homeostasis: Insights from hypokalemic periodic paralysis*, *Seminars in Nephrology*, 33 (2013), pp. 237 – 247. Potassium Homeostasis in Humans.
- [33] H.-F. CHENG, J.-L. WANG, M.-Z. ZHANG, Y. MIYAZAKI, I. ICHIKAWA, J. A. MCKANNA, AND R. C. HARRIS, *Angiotensin ii attenuates renal cortical cyclooxygenase-2 expression*, *The Journal of clinical investigation*, 103 (1999), pp. 953–961.
- [34] G. M. CHERTOW, E. BURDICK, M. HONOUR, J. V. BONVENTRE, AND D. W. BATES, *Acute kidney injury, mortality, length of stay, and costs in hospitalized patients*, *Journal of the American Society of Nephrology*, 16 (2005), pp. 3365–3370.
- [35] C. M. CLASE, J.-J. CARRERO, D. H. ELLISON, M. E. GRAMS, B. R. HEMMELGARN, M. J. JARDINE, C. P. KOVESDY, G. A. KLINE, G. LINDNER, G. T. OBRADOR, B. F. PALMER, M. CHEUNG, D. C. WHEELER, W. C. WINKELMAYER, R. PECOITS-FILHO, G. E. ASHUNTANTANG, S. J. BAKKER, G. L. BAKRIS, S. BHANDARI, E. A. BURDMANN, K. L. CAMPBELL, D. M. CHARYTAN, D. J. CLEGG, L. CUPPARI, D. GOLDSMITH, S. I. HALLAN, J. HE, C. A. HERZOG, M. P. HOENIG, E. J. HOORN, J. G. LEIPZIGER, A. K. LEONBERG-YOO, E. V. LERMA, J. E. LOPEZ-ALMARAZ, J. MALYSZKO, J. F. MANN, M. MARKLUND, A. A. McDONOUGH, M. NAGAHAMA, S. D. NAVANEETHAN, B. PITT, O. M. POCHYNYUK, T. P. DE MORAES, Z. RAFIQUE, B. M. ROBINSON, S. D. ROGER, P. ROSSIGNOL, A. J. SINGER, A. SMYTH, M. M. SOOD, M. WALSH, M. R. WEIR, AND C. S. WINGO, *Potassium homeostasis and management of dyskalemia in kidney diseases: conclusions from a kidney disease: Improving global outcomes (KDIGO) controversies conference*, *Kidney International*, 97 (2020), pp. 42 – 61.

- [36] D. H. COHALL, T. SCANTLEBURY-MANNING, S. JAMES, K. HALL, AND C. M. FERRARIO, *Renin-angiotensin-aldosterone system gender differences in an afro-caribbean population*, Journal of the Renin-Angiotensin-Aldosterone System, 16 (2015), pp. 539–546. PMID: 24532825.
- [37] B. P. L. T. T. COLLABORATION ET AL., *Effects of different blood-pressure-lowering regimens on major cardiovascular events: results of prospectively-designed overviews of randomised trials*, The Lancet, 362 (2003), pp. 1527–1535.
- [38] L. K. DAHL AND R. LOVE, *Evidence for relationship between sodium (chloride) intake and human essential hypertension*, AMA archives of internal medicine, 94 (1954), pp. 525–531.
- [39] W. H. DANTZLER, T. L. PANNABECKER, A. LAYTON, AND H. LAYTON, *Urine concentrating mechanism in the inner medulla of the mammalian kidney: role of three-dimensional architecture*, Acta physiologica, 202 (2011), pp. 361–378.
- [40] S. F. DE P. RODRIGUES, R. A. DOS SANTOS, M. M. SILVA-ANTONIALI, C. SCAVONE, D. NIGRO, M. H. C. CARVALHO, R. DE CÁSSIA TOSTES, AND Z. B. FORTES, *Differential effect of losartan in female and male spontaneously hypertensive rats*, Life Sciences, 78 (2006), pp. 2280 – 2285.
- [41] M. DE ROSA, P. CARDACE, M. ROSSI, A. BAIANO, AND A. DE CRISTOFARO, *Comparative effects of chronic ace inhibition and at1 receptor blocked losartan on cardiac hypertrophy and renal function in hypertensive patients*, Journal of human hypertension, 16 (2002), p. 133.
- [42] C. DELLES, J. JACOBI, S. JOHN, I. FLEISCHMANN, AND R. E. SCHMIEDER, *Effects of enalapril and eprosartan on the renal vascular nitric oxide system in human essential hypertension*, Kidney international, 61 (2002), pp. 1462–1468.
- [43] K. M. DENTON, S. E. LUFF, A. SHWETA, AND W. P. ANDERSON, *Differential neural control of glomerular ultrafiltration*, Clinical and experimental pharmacology and physiology, 31 (2004), pp. 380–386.
- [44] T. D. DUBOSE AND L. L. HAMM, *Acid-base and electrolyte disorders: a companion to Brenner & Rector's the kidney*, Elsevier Health Sciences, 2002.
- [45] L. DWORKIN, I. ICHIKAWA, AND B. BRENNER, *Hormonal modulation of glomerular function*, American Journal of Physiology-Renal Physiology, 244 (1983), pp. F95–F104.
- [46] A. EDWARDS, H. CASTROP, K. LAGHMANI, V. VALLON, AND A. T. LAYTON, *Effects of nkcc2 isoform regulation on nacl transport in thick ascending*

- limb and macula densa: a modeling study*, American Journal of Physiology-Renal Physiology, 307 (2014), pp. F137–F146.
- [47] A. EDWARDS AND A. T. LAYTON, *Modulation of outer medullary nacl transport and oxygenation by nitric oxide and superoxide*, American Journal of Physiology-Renal Physiology, 301 (2011), pp. F979–F996.
- [48] —, *Calcium dynamics underlying the myogenic response of the renal afferent arteriole*, American Journal of Physiology-Renal Physiology, 306 (2013), pp. F34–F48.
- [49] A. EDWARDS AND A. T. LAYTON, *Calcium dynamics underlying the myogenic response of the renal afferent arteriole*, American Journal of Physiology - Renal Physiology, 306 (2014), pp. F34–F48.
- [50] D. H. ELLISON, A. S. TERKER, AND G. GAMBA, *Potassium and its discontents: New insight, new treatments*, Journal of the American Society of Nephrology, 27 (2016), pp. 981–989.
- [51] K. E. ELLISON, J. R. INGELFINGER, M. PIVOR, AND V. J. DZAU, *Androgen regulation of rat renal angiotensinogen messenger rna expression.*, The Journal of Clinical Investigation, 83 (1989), pp. 1941–1945.
- [52] C. FALCONNET, M. BOCHUD, P. BOVET, M. MAILLARD, AND M. BURNIER, *Gender difference in the response to an angiotensin-converting enzyme inhibitor and a diuretic in hypertensive patients of african descent*, Journal of Hypertension, 22 (2004).
- [53] H. FATTAH, A. LAYTON, AND V. VALLON, *How do kidneys adapt to a deficit or loss in nephron number?*, Physiology, 34 (2019), pp. 189–197.
- [54] P. FERRARI, H.-P. MARTI, M. PFISTER, AND F. J. FREY, *Additive antiproteinuric effect of combined ace inhibition and angiotensin ii receptor blockade*, Journal of hypertension, 20 (2002), pp. 125–130.
- [55] M. J. FIELD, B. A. STANTON, AND G. H. GIEBISCH, *Differential acute effects of aldosterone, dexamethasone, and hyperkalemia on distal tubular potassium secretion in the rat kidney*, The Journal of Clinical Investigation, 74 (1984), pp. 1792–1802.
- [56] M. FISCHER, A. BAESSLER, AND H. SCHUNKERT, *Renin angiotensin system and gender differences in the cardiovascular system*, Cardiovasc. Res., 53 (2002), pp. 672–677.
- [57] A. N. FORD VERSYPT, G. K. HARRELL, AND A. N. MCPeAK, *A pharmacokinetic/pharmacodynamic model of ACE inhibition of the renin-angiotensin*

system for normal and impaired renal function, Computers & Chemical Engineering, 104 (2017), pp. 311 – 322.

- [58] J.-P. FOURNIER, A. SOMMET, G. DURRIEU, J.-C. POUTRAIN, M. LAPEYRE-MESTRE, AND J.-L. MONTASTRUC, *More on the "triple whammy": Antihypertensive drugs, non-steroidal anti-inflammatory agents and acute kidney injury-a case/non-case study in the french pharmacovigilance database*, Renal failure, 36 (2014), pp. 1–3.
- [59] J.-P. FOURNIER, A. SOMMET, G. DURRIEU, J.-C. POUTRAIN, M. LAPEYRE-MESTRE, J.-L. MONTASTRUC, AND THE FRENCH NETWORK OF REGIONAL PHARMACOVIGILANCE CENTRES, *More on the "triple whammy": antihypertensive drugs, non-steroidal anti-inflammatory agents and acute kidney injury – a case/non-case study in the french pharmacovigilance database*, Renal Failure, 36 (2014), pp. 1166–1168. PMID: 24826803.
- [60] K. L. FRANSON, J. M. KUK, N. P. LAM, AND A. H. LAU, *Gender effect on diuretic response to hydrochlorothiazide and furosemide*, Int J Clin Pharmacol Ther, 34 (1996), pp. 101–105.
- [61] P. E. GALLAGHER, P. LI, J. R. LENHART, M. C. CHAPPELL, AND K. B. BROSNIHAN, *Estrogen regulation of angiotensin-converting enzyme mrna*, Hypertension, 33 (1999), pp. 323–328.
- [62] S. K. GANDHI, J. GAINER, D. KING, AND N. J. BROWN, *Gender affects renal vasoconstrictor response to ang i and ang ii*, Hypertension, 31 (1998), pp. 90–96.
- [63] R. K. GARG, H. S. MALHOTRA, R. VERMA, P. SHARMA, AND M. K. SINGH, *Etiological spectrum of hypokalemic paralysis: A retrospective analysis of 29 patients*, Annals of Indian Academy of Neurology, 16 (2013), pp. 365–370. 24101818[pmid].
- [64] J. C. GEERLING AND A. D. LOEWY, *Central regulation of sodium appetite*, Experimental Physiology, 93 (2008), pp. 177–209.
- [65] J. M. GOOD, A. BRADY, F. H. NOORMOHAMED, C. M. OAKLEY, AND J. CLELAND, *Effect of intense angiotensin ii suppression on the diuretic response to furosemide during chronic ace inhibition.*, Circulation, 90 (1994), pp. 220–224.
- [66] A. H. GRADMAN, K. E. ARCURI, A. I. GOLDBERG, L. S. IKEDA, E. B. NELSON, D. B. SNAVELY, AND C. S. SWEET, *A randomized, placebo-controlled, double-blind, parallel study of various doses of losartan potassium compared with enalapril maleate in patients with essential hypertension*, Hypertension, 25 (1995), pp. 1345–1350.

- [67] A. H. GRADMAN, M. R. WEIR, M. WRIGHT, C. A. BUSH, AND D. L. KEEFE, *Efficacy, safety and tolerability of aliskiren, a direct renin inhibitor, in women with hypertension: a pooled analysis of eight studies*, Journal of Human Hypertension, 24 (2010), pp. 721–729.
- [68] G. GRASSI AND G. MANCIA, *Neurogenic hypertension: is the enigma of its origin near the solution?*, Hypertension, 43 (2004), pp. 154–155.
- [69] G. GRASSI, G. SERAVALLE, AND F. QUARTI-TREVANO, *The ‘neuroadrenergic hypothesis’ in hypertension: current evidence*, Experimental physiology, 95 (2010), pp. 581–586.
- [70] M. GREENLEE, C. S. WINGO, A. A. McDONOUGH, J.-H. YOUN, AND B. C. KONE, *Narrative Review: Evolving Concepts in Potassium Homeostasis and Hypokalemia*, Annals of Internal Medicine, 150 (2009), pp. 619–625.
- [71] R. J. GRYGLEWSKI, W. URACZ, S. CHŁOPICKI, AND E. MARCINKIEWICZ, *Bradykinin as a major endogenous regulator of endothelial function*, Pediatric pathology & molecular medicine, 21 (2002), pp. 279–290.
- [72] Q. GU, V. L. BURT, R. PAULOSE-RAM, AND C. F. DILLON, *Gender differences in hypertension treatment, drug utilization patterns, and blood pressure control among us adults with hypertension: data from the national health and nutrition examination survey 1999–2004*, American journal of hypertension, 21 (2008), pp. 789–798.
- [73] F. GUILLAUD AND P. HANNAERT, *A computational model of the circulating renin-angiotensin system and blood pressure regulation*, Acta Biotheoretica, 58 (2010), pp. 143–170.
- [74] M. L. GUMZ, I. J. LYNCH, M. M. GREENLEE, B. D. CAIN, AND C. S. WINGO, *The renal h⁺-k⁺-atpases: physiology, regulation, and structure*, American Journal of Physiology-Renal Physiology, 298 (2010), pp. F12–F21. PMID: 19640897.
- [75] M. L. GUMZ AND L. RABINOWITZ, *Role of circadian rhythms in potassium homeostasis*, Seminars in Nephrology, 33 (2013), pp. 229 – 236. Potassium Homeostasis in Humans.
- [76] M. L. GUMZ, L. RABINOWITZ, AND C. S. WINGO, *An integrated view of potassium homeostasis*, New England Journal of Medicine, 373 (2015), pp. 60–72. PMID: 26132942.
- [77] A. C. GUYTON, *Renal function curve—a key to understanding the pathogenesis of hypertension.*, Hypertension, 10 (1987), pp. 1–6.

- [78] A. C. GUYTON, T. G. COLEMAN, AND H. J. GRANGER, *Circulation: overall regulation*, *Annu. Rev. Physiol.*, 34 (1972), pp. 13–46.
- [79] N. HADDAD, R. SHIM, AND L. A. HEBERT, *Chapter 22 - nutritional management of water, sodium, potassium, chloride, and magnesium in kidney disease and kidney failure*, in *Nutritional Management of Renal Disease*, J. D. Kopple, S. G. Massry, and K. Kalantar-Zadeh, eds., Academic Press, 2013, pp. 323 – 338.
- [80] K. M. HALLOW, A. LO, J. BEH, M. RODRIGO, S. ERMAKOV, S. FRIEDMAN, H. DE LEON, A. SARKAR, Y. XIONG, R. SARANGAPANI, H. SCHMIDT, R. WEBB, AND A. G. KONDIC, *A model-based approach to investigating the pathophysiological mechanisms of hypertension and response to antihypertensive therapies: extending the guyton model*, *American Journal of Physiology - Regulatory, Integrative and Comparative Physiology*, 306 (2014), pp. R647–R662.
- [81] E. C. HART AND N. CHARKOUDIAN, *Sympathetic neural mechanisms in human blood pressure regulation*, *Current Hypertension Reports*, 13 (2011), pp. 237–243.
- [82] R. HATANO, K. ONOE, M. OBARA, M. MATSUBARA, Y. KANAI, S. MUTO, AND S. ASANO, *Sex hormones induce a gender-related difference in renal expression of a novel prostaglandin transporter, oat-pg, influencing basal pge 2 concentration*, *American Journal of Physiology-Renal Physiology*, 302 (2012), pp. F342–F349.
- [83] M. HAY, *Sex, the brain and hypertension: brain oestrogen receptors and high blood pressure risk factors*, *Clinical Science*, 130 (2016), pp. 9–18.
- [84] S. S. HEDAYATI, A. T. MINHJUDDIN, A. IJAZ, O. W. MOE, E. F. ELSAYED, R. F. REILLY, AND C.-L. HUANG, *Association of urinary sodium/potassium ratio with blood pressure: Sex and racial differences*, *Clinical Journal of the American Society of Nephrology*, 7 (2012), pp. 315–322.
- [85] K. HERMANN, D. GANTEN, T. UNGER, C. BAYER, AND R. E. LANG, *Measurement and characterization of angiotensin peptides in plasma.*, *Clinical Chemistry*, 34 (1988), pp. 1046–1051.
- [86] J. HERRERA AND B. RODRÍGUEZ-ITURBE, *Stimulation of tubular secretion of creatinine in health and in conditions associated with reduced nephron mass. Evidence for a tubular functional reserve.*, *Nephrology Dialysis Transplantation*, 13 (1998), pp. 623–629.
- [87] L. M. HILLIARD, M. NEMATBAKSH, M. M. KETT, E. TEICHMAN, A. K. SAMPSON, R. E. WIDDOP, R. G. EVANS, AND K. M. DENTON, *Gender*

- differences in pressure-natriuresis and renal autoregulation*, Hypertension, 57 (2011), pp. 275–282.
- [88] L. M. HILLIARD, A. K. SAMPSON, R. D. BROWN, AND K. M. DENTON, *The "his and hers" of the renin-angiotensin system*, Curr. Hypertens. Rep., 15 (2013), pp. 71–79.
- [89] L. M. HILLIARD, A. K. SAMPSON, R. D. BROWN, AND K. M. DENTON, *The "his and hers" of the renin-angiotensin system*, Current hypertension reports, 15 (2013), pp. 71–79.
- [90] C. HINOJOSA-LABORDE, I. CHAPA, D. LANGE, AND J. R. HAYWOOD, *Gender differences in sympathetic nervous system regulation*, Clin. Exp. Pharmacol. Physiol., 26 (1999), pp. 122–126.
- [91] Y. HONG, J. DINGEMANSE, AND D. MAGER, *Pharmacokinetic/pharmacodynamic modeling of renin biomarkers in subjects treated with the renin inhibitor aliskiren*, Clinical Pharmacology & Therapeutics, 84 (2008), pp. 136–143.
- [92] R. HU, A. A. MCDONOUGH, AND A. T. LAYTON, *Functional implications of the sex differences in transporter abundance along the rat nephron: modeling and analysis*, American Journal of Physiology-Renal Physiology, 317 (2019), pp. F1462–F1474.
- [93] R. HÜBNER, A. HÖGEMANN, M. SUNZEL, AND J. RIDDELL, *Pharmacokinetics of candesartan after single and repeated doses of candesartan cilexetil in young and elderly healthy volunteers.*, Journal of human hypertension, 11 (1997).
- [94] M. HUDSON, E. RAHME, H. BEHLOULI, R. SHEPPARD, AND L. PILOTE, *Sex differences in the effectiveness of angiotensin receptor blockers and angiotensin converting enzyme inhibitors in patients with congestive heart failure—a population study*, European journal of heart failure, 9 (2007), pp. 602–609.
- [95] N. IKEDA, F. MARUMO, M. SHIRATAKA, AND T. SATO, *A model of overall regulation of body fluids*, Annals of Biomedical Engineering, 7 (1979), pp. 135–166.
- [96] R. ILIESCU, L. L. YANES, W. BELL, T. DWYER, O. C. BALATU, AND J. F. RECKELHOFF, *Role of the renal nerves in blood pressure in male and female shr*, American Journal of Physiology-Regulatory, Integrative and Comparative Physiology, 290 (2006), pp. R341–R344. PMID: 16166211.
- [97] P. JACOBSEN, S. ANDERSEN, B. R. JENSEN, AND H.-H. PARVING, *Additive effect of ace inhibition and angiotensin ii receptor blockade in type i diabetic*

- patients with diabetic nephropathy*, Journal of the American Society of Nephrology, 14 (2003), pp. 992–999.
- [98] E. J. JOHNS, U. C. KOPP, AND G. F. DiBONA, *Neural Control of Renal Function*, American Cancer Society, 2011, pp. 731–767.
- [99] A. G. JOHNSON, T. V. NGUYEN, AND R. O. DAY, *Do nonsteroidal anti-inflammatory drugs affect blood pressure? a meta-analysis*, Annals of internal medicine, 121 (1994), pp. 289–300.
- [100] C. I. JOHNSTON, B. FABRIS, AND K. JANDELEIT, *Intrarenal renin-angiotensin system in renal physiology and pathophysiology.*, Kidney international. Supplement, 42 (1993), pp. S59–63.
- [101] M. C. KAMMERL, R. M. NÜSING, W. RICHTHAMMER, B. K. KRÄMER, AND A. KURTZ, *Inhibition of cox-2 counteracts the effects of diuretics in rats*, Kidney international, 60 (2001), pp. 1684–1691.
- [102] N. M. KAPLAN, D. C. KEM, O. B. HOLLAND, N. J. KRAMER, J. HIGGINS, AND C. GOMEZ-SANCHEZ, *The intravenous furosemide test: a simple way to evaluate renin responsiveness*, Annals of internal medicine, 84 (1976), pp. 639–645.
- [103] F. KARAASLAN, Y. DENIZHAN, A. KAYSERILIOGLU, AND H. O. GULCUR, *Long-term mathematical model involving renal sympathetic nerve activity, arterial pressure, and sodium excretion*, Annals of biomedical engineering, 33 (2005), pp. 1607–1630.
- [104] A. KATSURADA, Y. HAGIWARA, K. MIYASHITA, R. SATOU, K. MIYATA, N. OHASHI, L. G. NAVAR, AND H. KOBORI, *Novel sandwich elisa for human angiotensinogen*, American Journal of Physiology-Renal Physiology, 293 (2007), pp. F956–F960. PMID: 17553939.
- [105] A. KATZ AND F. EPSTEIN, *Relation of glomerular filtration rate and sodium reabsorption to kidney size in compensatory renal hypertrophy.*, The Yale journal of biology and medicine, 40 (1967), p. 222.
- [106] A. I. KATZ, *Renal Na-K-ATPase: its role in tubular sodium and potassium transport*, American Journal of Physiology-Renal Physiology, 242 (1982), pp. F207–F219. PMID: 6278949.
- [107] G. KAYSEN, B. MYERS, W. COUSER, R. RABKIN, AND J. FELTS, *Mechanisms and consequences of proteinuria.*, Laboratory investigation; a journal of technical methods and pathology, 54 (1986), pp. 479–498.

- [108] J. A. KELLUM, N. LAMEIRE, P. ASPELIN, R. S. BARSOUM, E. A. BURDMANN, S. L. GOLDSTEIN, C. A. HERZOG, M. JOANNIDIS, A. KRIBBEN, A. S. LEVEY, ET AL., *Kidney disease: improving global outcomes (KDIGO) acute kidney injury work group. kdigo clinical practice guideline for acute kidney injury*, *Kidney international supplements*, 2 (2012), pp. 1–138.
- [109] M. KERR, M. BEDFORD, B. MATTHEWS, AND D. O’DONOGHUE, *The economic impact of acute kidney injury in england*, *Nephrology Dialysis Transplantation*, 29 (2014), pp. 1362–1368.
- [110] A. A. KHRAIBI, M. LIANG, AND T. J. BERNDT, *Role of gender on renal interstitial hydrostatic pressure and sodium excretion in rats*, *American journal of hypertension*, 14 (2001), pp. 893–896.
- [111] L. M. KIENEKER, R. T. GANSEVOORT, K. J. MUKAMAL, R. A. DE BOER, G. NAVIS, S. J. BAKKER, AND M. M. JOOSTEN, *Urinary potassium excretion and risk of developing hypertension*, *Hypertension*, 64 (2014), pp. 769–776.
- [112] K. KIRIMURA, S. TAKAI, D. JIN, M. MURAMATSU, K. KISHI, K. YOSHIKAWA, M. NAKABAYASHI, Y. MINO, AND M. MIYAZAKI, *Role of chymase-dependent angiotensin II formation in regulating blood pressure in spontaneously hypertensive rats*, *Hypertens. Res.*, 28 (2005), pp. 457–464.
- [113] S. KLAHR AND S. B. MILLER, *Acute oliguria*, *New England Journal of Medicine*, 338 (1998), pp. 671–675. PMID: 9486997.
- [114] N. KLEINSTREUER, T. DAVID, M. J. PLANK, AND Z. ENDRE, *Dynamic myogenic autoregulation in the rat kidney: a whole-organ model*, *American Journal of Physiology-Renal Physiology*, 294 (2008), pp. F1453–F1464.
- [115] K. KOMUKAI, S. MOCHIZUKI, AND M. YOSHIMURA, *Gender and the renin-angiotensin-aldosterone system*, *Fundamental & clinical pharmacology*, 24 (2010), pp. 687–698.
- [116] U. C. KOPP, *Neural control of renal function*, in *Colloquium Series on Integrated Systems Physiology: From Molecule to Function to Disease*, vol. 10, Morgan & Claypool Life Sciences, 2018, pp. i–106.
- [117] F. LAPI, L. AZOULAY, H. YIN, S. J. NESSIM, AND S. SUISSA, *Concurrent use of diuretics, angiotensin converting enzyme inhibitors, and angiotensin receptor blockers with non-steroidal anti-inflammatory drugs and risk of acute kidney injury: nested case-control study*, *Bmj*, 346 (2013), p. e8525.
- [118] A. T. LAYTON, *Feedback-mediated dynamics in a model of a compliant thick ascending limb*, *Mathematical biosciences*, 228 (2010), pp. 185–194.

- [119] —, *Recent advances in renal hypoxia: insights from bench experiments and computer simulations*, American Journal of Physiology-Renal Physiology, 311 (2016), pp. F162–F165.
- [120] A. T. LAYTON AND A. EDWARDS, *Mathematical Modeling in Renal Physiology*, Springer, 2014.
- [121] A. T. LAYTON AND A. EDWARDS, *Predicted effects of nitric oxide and superoxide on the vasoactivity of the afferent arteriole*, American Journal of Physiology - Renal Physiology, 309 (2015), pp. F708–F719.
- [122] A. T. LAYTON, A. EDWARDS, AND V. VALLON, *Adaptive changes in GFR, tubular morphology, and transport in subtotal nephrectomized kidneys: modeling and analysis*, American Journal of Physiology-Renal Physiology, 313 (2017), pp. F199–F209.
- [123] —, *Renal potassium handling in rats with subtotal nephrectomy: modeling and analysis*, American Journal of Physiology-Renal Physiology, 314 (2018), pp. F643–F657.
- [124] A. T. LAYTON, K. LAGHMANI, V. VALLON, AND A. EDWARDS, *Solute transport and oxygen consumption along the nephrons: effects of Na^+ transport inhibitors*, American Journal of Physiology-Renal Physiology, 311 (2016), pp. F1217–F1229.
- [125] A. T. LAYTON AND H. E. LAYTON, *A region-based model framework for the rat urine concentrating mechanism*, Bulletin of mathematical biology, 65 (2003), pp. 859–901.
- [126] —, *Countercurrent multiplication may not explain the axial osmolality gradient in the outer medulla of the rat kidney*, American Journal of Physiology-Renal Physiology, 301 (2011), pp. F1047–F1056.
- [127] —, *A computational model of epithelial solute and water transport along a human nephron*, PLoS computational biology, 15 (2019), p. e1006108.
- [128] A. T. LAYTON, H. E. LAYTON, W. H. DANTZLER, AND T. L. PANNABECKER, *The mammalian urine concentrating mechanism: hypotheses and uncertainties*, Physiology, 24 (2009), pp. 250–256.
- [129] A. T. LAYTON, L. C. MOORE, AND H. E. LAYTON, *Multistability in tubuloglomerular feedback and spectral complexity in spontaneously hypertensive rats*, American Journal of Physiology-Renal Physiology, 291 (2006), pp. F79–F97.
- [130] —, *Multistable dynamics mediated by tubuloglomerular feedback in a model of coupled nephrons*, Bulletin of mathematical biology, 71 (2009), p. 515.

- [131] A. T. LAYTON AND V. VALLON, *Sglt2 inhibition in a kidney with reduced nephron number: modeling and analysis of solute transport and metabolism*, American Journal of Physiology-Renal Physiology, 314 (2018), pp. F969–F984.
- [132] A. T. LAYTON, V. VALLON, AND A. EDWARDS, *Modeling oxygen consumption in the proximal tubule: effects of nhe and sglt2 inhibition*, American Journal of Physiology-Renal Physiology, 308 (2015), pp. F1343–F1357.
- [133] —, *A computational model for simulating solute transport and oxygen consumption along the nephrons*, American Journal of Physiology-Renal Physiology, 311 (2016), pp. F1378–F1390.
- [134] —, *Predicted consequences of diabetes and sglt inhibition on transport and oxygen consumption along a rat nephron*, American Journal of Physiology-Renal Physiology, 310 (2016), pp. F1269–F1283.
- [135] M. LEANING, H. PULLEN, E. CARSON, AND L. FINKELSTEIN, *Modelling a complex biological system: the human cardiovascular system - 1. methodology and model description*, Transactions of the Institute of Measurement and Control, 5 (1983), pp. 71–86.
- [136] J. LEETE, S. GURLEY, AND A. T. LAYTON, *Modeling sex differences in the renin angiotensin system and the efficacy of antihypertensive therapies*, Computers & Chemical Engineering, 112 (2018), pp. 253 – 264.
- [137] J. LEETE AND A. T. LAYTON, *Sex-specific long-term blood pressure regulation: modeling and analysis*, Computers in biology and medicine, 104 (2019), pp. 139–148.
- [138] J. LEETE, F. J. LÓPEZ-HERNÁNDEZ, AND A. T. LAYTON, *Determining risk factors for triple whammy acute kidney injury: sex-specific modeling and analysis*, Submitted, (2020).
- [139] Q. LI, A. A. MCDONOUGH, H. E. LAYTON, AND A. T. LAYTON, *Functional implications of sexual dimorphism of transporter patterns along the rat proximal tubule: Modeling and analysis*, American Journal of Physiology-Renal Physiology, (2018).
- [140] P. LIJNEN, A. AMERY, AND R. FAGARD, *Endogenous angiotensin i concentration in human plasma*, The Journal of laboratory and clinical medicine, 92 (1978), p. 353–362.
- [141] A. LO, J. BEH, H. DE LEON, M. K. HALLOW, R. RAMAKRISHNA, M. RODRIGO, A. SARKAR, R. SARANGAPANI, AND A. GEORGIEVA, *Using a Systems Biology Approach to Explore Hypotheses Underlying Clinical Diversity of the Renin Angiotensin System and the Response to Antihypertensive Therapies*, Springer New York, New York, NY, 2011, pp. 457–482.

- [142] K. K. LOBOZ AND G. M. SHENFIELD, *Drug combinations and impaired renal function—the ‘triple whammy’*, British journal of clinical pharmacology, 59 (2005), pp. 239–243.
- [143] T. E. LOHMEIER, H. L. MIZELLE, G. A. REINHART, AND J.-P. MONTANI, *Influence of angiotensin on the early progression of heart failure*, American Journal of Physiology-Regulatory, Integrative and Comparative Physiology, 278 (2000), pp. R74–R86. PMID: 10644624.
- [144] L. L. MACKAY AND E. M. MACKAY, *Factors which determine renal weight*, American Journal of Physiology-Legacy Content, 83 (1927), pp. 196–201.
- [145] C. MARIC-BILKAN AND M. B. MANIGRASSO, *Sex differences in hypertension: contribution of the renin–angiotensin system*, Gender medicine, 9 (2012), pp. 287–291.
- [146] E. MASSANA, M. BARBANOJ, C. MOROS, A. MORTE, I. GICH, AND F. JANA, *No sex-related pharmacokinetic and pharmacodynamic differences of captopril*, Pharmacological Research, 36 (1997), pp. 41 – 47.
- [147] U. D. MATHISEN, T. MELSOM, O. C. INGEBRETSEN, T. G. JENSSEN, I. NJØLSTAD, M. D. SOLBU, I. TOFT, AND B. O. ERIKSEN, *Ambulatory blood pressure is associated with measured glomerular filtration rate in the general middle-aged population*, Journal of hypertension, 30 (2012), pp. 497–504.
- [148] S. MATSUO, E. IMAI, M. HORIO, Y. YASUDA, K. TOMITA, K. NITTA, K. YAMAGATA, Y. TOMINO, H. YOKOYAMA, AND A. HISHIDA, *Revised equations for estimated gfr from serum creatinine in japan*, American Journal of Kidney Diseases, 53 (2009), pp. 982–992.
- [149] A. A. McDONOUGH, *Isn forefronts symposium 2015: Maintaining balance under pressure—hypertension and the proximal tubule*, Kidney International Reports, 1 (2016), pp. 166–176.
- [150] A. A. McDONOUGH AND M. T. NGUYEN, *Maintaining balance under pressure*, Hypertension, 66 (2015), pp. 450–455.
- [151] A. A. McDONOUGH AND J. H. YOUN, *Potassium homeostasis: The knowns, the unknowns, and the health benefits*, Physiology, 32 (2017), pp. 100–111. PMID: 28202621.
- [152] G. T. MCINNES, *Angiotensin II antagonism in clinical practice: experience with valsartan*, J. Cardiovasc. Pharmacol., 33 Suppl 1 (1999), pp. 29–32.
- [153] M. MCINTYRE, S. CAFFE, R. MICHALAK, AND J. REID, *Losartan, an orally active angiotensin (at1) receptor antagonist: a review of its efficacy and safety*

- in essential hypertension*, Pharmacology & therapeutics, 74 (1997), pp. 181–194.
- [154] C. A. MCKINNEY, C. FATTAH, C. M. LOUGHREY, G. MILLIGAN, AND S. A. NICKLIN, *Angiotensin-(1–7) and angiotensin-(1–9): function in cardiac and vascular remodelling*, Clinical Science, 126 (2014), pp. 815–827.
- [155] J. A. MILLER, L. A. ANACTA, AND D. C. CATTRAN, *Impact of gender on the renal response to angiotensin ii*, Kidney International, 55 (1999), pp. 278 – 285.
- [156] K. M. MIRABITO, L. M. HILLIARD, G. A. HEAD, R. E. WIDDOP, AND K. M. DENTON, *Pressor responsiveness to angiotensin ii in female mice is enhanced with age: role of the angiotensin type 2 receptor*, Biology of sex differences, 5 (2014), p. 13.
- [157] N. MIYATA, F. PARK, X. F. LI, AND A. W. COWLEY, *Distribution of angiotensin at1 and at2 receptor subtypes in the rat kidney*, American Journal of Physiology-Renal Physiology, 277 (1999), pp. F437–F446. PMID: 10484527.
- [158] C. E. MOGENSEN, S. NELDAM, I. TIKKANEN, S. OREN, R. VISKOPER, R. W. WATTS, AND M. E. COOPER, *Randomised controlled trial of dual blockade of renin-angiotensin system in patients with hypertension, microalbuminuria, and non-insulin dependent diabetes: the candesartan and lisinopril microalbuminuria (calm) study*, Bmj, 321 (2000), pp. 1440–1444.
- [159] M. C. MOORE EDE, M. F. BRENNAN, AND M. R. BALL, *Circadian variation of intercompartmental potassium fluxes in man*, Journal of Applied Physiology, 38 (1975), pp. 163–170. PMID: 1110234.
- [160] T. MORGAN, A. ANDERSON, D. BERTRAM, AND R. J. MACINNIS, *Effect of candesartan and lisinopril alone and in combination on blood pressure and microalbuminuria*, Journal of the Renin-Angiotensin-Aldosterone System, 5 (2004), pp. 64–71.
- [161] K. MORITZ, J. CUFFE, L. WILSON, H. DICKINSON, M. WLODEK, D. SIMMONS, AND K. DENTON, *sex specific programming: a critical role for the renal renin-angiotensin system*, Placenta, 31 (2010), pp. S40–S46.
- [162] R. MOSS AND A. T. LAYTON, *Dominant factors that govern pressure natriuresis in diuresis and antidiuresis: a mathematical model*, American Journal of Physiology-Renal Physiology, 306 (2014), pp. F952–F969.
- [163] D. MOZAFFARIAN, E. BENJAMIN, A. GO, D. ARNETT, M. BLAHA, M. CUSHMAN, S. DE FERRANTI, J. DESPRES, H. FULLERTON, V. HOWARD, ET AL., *American heart association statistics c, stroke statistics s: Heart disease*

and stroke statistics—2015 update: a report from the american heart association, Circulation, 131 (2015), pp. e29–322.

- [164] K. MUNGER AND C. BAYLIS, *Sex differences in renal hemodynamics in rats*, American Journal of Physiology-Renal Physiology, 254 (1988), pp. F223–F231. PMID: 3344806.
- [165] A. NIEVES-GONZÁLEZ, C. CLAUSEN, A. T. LAYTON, H. E. LAYTON, AND L. C. MOORE, *Transport efficiency and workload distribution in a mathematical model of the thick ascending limb*, American Journal of Physiology-Renal Physiology, 304 (2013), pp. F653–F664.
- [166] J. NOWAK AND Å. WENNMALM, *Influence of indomethacin and of prostaglandin e1 on total and regional blood flow in man*, Acta physiologica scandinavica, 102 (1978), pp. 484–491.
- [167] J. NUSSBERGER, A. H. GRADMAN, R. E. SCHMIEDER, R. L. LINS, Y. CHIANG, AND M. F. PRESCOTT, *Plasma renin and the antihypertensive effect of the orally active renin inhibitor aliskiren in clinical hypertension*, International Journal of Clinical Practice, 61 (2007), pp. 1461–1468.
- [168] J. NUSSBERGER, G. WUERZNER, C. JENSEN, AND H. R. BRUNNER, *Angiotensin II suppression in humans by the orally active renin inhibitor Aliskiren (SPP100): comparison with enalapril*, Hypertension, 39 (2002), pp. 1–8.
- [169] H. OESEBURG, D. IUSUF, P. VAN DER HARST, W. H. VAN GILST, R. H. HENNING, AND A. J. ROKS, *Bradykinin protects against oxidative stress-induced endothelial cell senescence*, Hypertension, 53 (2009), pp. 417–422.
- [170] W. J. OLIVER, E. L. COHEN, AND J. V. NEEL, *Blood pressure, sodium intake, and sodium related hormones in the yanomamo indians, a "no-salt" culture.*, Circulation, 52 (1975), pp. 146–151.
- [171] Y. OUCHI, L. SHARE, J. T. CROFTON, K. IITAKE, AND D. P. BROOKS, *Sex difference in the development of deoxycorticosterone-salt hypertension in the rat.*, Hypertension, 9 (1987), pp. 172–177.
- [172] R. OZONO, Z.-Q. WANG, A. F. MOORE, T. INAGAMI, H. M. SIRAGY, AND R. M. CAREY, *Expression of the subtype 2 angiotensin ($at_{j\substack{\dot{2} \\ \substack{\dot{2} \\ \substack{\dot{2}}}}}})$ receptor protein in rat kidney*, Hypertension, 30 (1997), pp. 1238–1246.
- [173] B. F. PALMER, *Regulation of potassium homeostasis*, Clinical Journal of the American Society of Nephrology, 10 (2015), pp. 1050–1060.
- [174] L. G. PALMER AND G. FRINDT, *Aldosterone and potassium secretion by the cortical collecting duct*, Kidney International, 57 (2000), pp. 1324 – 1328.

- [175] R. V. PATAK, B. K. MOOKERJEE, C. J. BENTZEL, P. E. HYSERT, M. BABEJ, AND J. B. LEE, *Antagonism of the effects of furosemide by indomethacin in normal and hypertensive man*, Prostaglandins, 10 (1975), pp. 649–659.
- [176] K. D. PENDERGRASS, N. T. PIRRO, B. M. WESTWOOD, C. M. FERRARIO, K. B. BROSNIHAN, AND M. C. CHAPPELL, *Sex differences in circulating and renal angiotensins of hypertensive mren(2).lewis but not normotensive lewis rats*, American Journal of Physiology - Heart and Circulatory Physiology, 295 (2008), pp. H10–H20.
- [177] J. PETI-PETERDI, D. G. WARNOCK, AND P. D. BELL, *Angiotensin II directly stimulates ENaC activity in the cortical collecting duct via AT1 receptors*, Journal of the American Society of Nephrology, 13 (2002), pp. 1131–1135.
- [178] K. H. PETTERSEN, S. M. BUGENHAGEN, J. NAUMAN, D. A. BEARD, AND S. W. OMHOLT, *Arterial stiffening provides sufficient explanation for primary hypertension*, PLoS computational biology, 10 (2014), p. e1003634.
- [179] G. W. PETTIT AND R. L. VICK, *Contribution of pancreatic insulin to extrarenal potassium homeostasis: a two-compartment model*, American Journal of Physiology-Legacy Content, 226 (1974), pp. 319–324.
- [180] B. PHAKDEEKITCHAROEN, W. KITTIKANOKRAT, C. KIJKUNASATHIAN, AND V. CHATSUDTHIPONG, *Aldosterone increases Na^+ - K^+ -ATPase activity in skeletal muscle of patients with conn's syndrome*, Clinical Endocrinology, 74 (2011), pp. 152–159.
- [181] J. E. POPE, J. J. ANDERSON, AND D. T. FELSON, *A meta-analysis of the effects of nonsteroidal anti-inflammatory drugs on blood pressure*, Archives of Internal Medicine, 153 (1993), pp. 477–484.
- [182] P. POURTEYRON, *Etude comparative sur l'anatomie et la pathologie des deux reins*, PhD thesis, 1872.
- [183] R. A. PRESTON, D. AFSHARTOUS, R. RODCO, A. B. ALONSO, AND D. GARG, *Evidence for a gastrointestinal-renal kaliuretic signaling axis in humans*, Kidney International, 88 (2015), pp. 1383–1391.
- [184] L. PRIETO-GARCÍA, M. PERICACHO, S. M. SANCHO-MARTÍNEZ, Á. SÁNCHEZ, C. MARTÍNEZ-SALGADO, J. M. LÓPEZ-NOVOA, AND F. J. LÓPEZ-HERNÁNDEZ, *Mechanisms of triple whammy acute kidney injury*, Pharmacology & therapeutics, 167 (2016), pp. 132–145.
- [185] G. PRITCHARD, D. LYONS, J. WEBSTER, J. PETRIE, AND T. MACDONALD, *Do trandolapril and indomethacin influence renal function and renal functional*

- reserve in hypertensive patients?*, British journal of clinical pharmacology, 44 (1997), pp. 145–149.
- [186] T. J. RABELINK, H. A. KOOMANS, R. J. HENÉ, AND E. J. D. MEES, *Early and late adjustment to potassium loading in humans*, Kidney International, 38 (1990), pp. 942–947.
- [187] L. RABINOWITZ, *Homeostatic regulation of potassium excretion.*, Journal of hypertension, 7 (1989), pp. 433–442.
- [188] L. RABINOWITZ, S. C. DENHAM, AND R. A. GUNTHER, *Aldosterone and postprandial renal excretion of sodium and potassium in sheep*, American Journal of Physiology-Renal Physiology, 233 (1977), pp. F213–F216. PMID: 910916.
- [189] S. RAMUSOVIC AND S. LAEER, *An integrated physiology-based model for the interaction of raa system biomarkers with drugs*, Journal of cardiovascular pharmacology, 60 (2012), pp. 417–428.
- [190] J. F. RECKELHOFF, H. ZHANG, AND K. SRIVASTAVA, *Gender differences in development of hypertension in spontaneously hypertensive rats*, Hypertension, 35 (2000), pp. 480–483.
- [191] V. REGITZ-ZAGROSEK, *Sex and gender differences in cardiovascular disease*, in Sex and gender aspects in clinical medicine, Springer, 2012.
- [192] A. REMUZZI, S. PUNTORIERI, A. MAZZOLENI, AND G. REMUZZI, *Sex related differences in glomerular ultrafiltration and proteinuria in munich-wistar rats*, Kidney International, 34 (1988), pp. 481–486.
- [193] A. REYES-ENGEL, L. MORCILLO, F. J. ARANDA, M. RUIZ, M. J. GAITAN, A. MAYOR-OLEA, P. ARANDA, AND C. M. FERRARIO, *Influence of gender and genetic variability on plasma angiotensin peptides*, J Renin Angiotensin Aldosterone Syst, 7 (2006), pp. 92–97.
- [194] A. REYES-ENGEL, L. MORCILLO, F. J. ARANDA, M. RUIZ, M. J. GAITAN, ÁLVARO MAYOR-OLEA, P. ARANDA, AND C. M. FERRARIO, *Influence of gender and genetic variability on plasma angiotensin peptides*, Journal of the Renin-Angiotensin-Aldosterone System, 7 (2006), pp. 92–97. PMID: 17083063.
- [195] G. I. RICE, A. L. JONES, P. J. GRANT, A. M. CARTER, A. J. TURNER, AND N. M. HOOPER, *Circulating activities of angiotensin-converting enzyme, its homolog, angiotensin-converting enzyme 2, and neprilysin in a family study*, Hypertension, 48 (2006), pp. 914–920.
- [196] S. L. RODRIGUES, M. P. BALDO, R. C. MACHADO, L. FORECHI, M. DEL CARMEM BISI MOLINA, AND J. G. MILL, *High potassium intake blunts the*

effect of elevated sodium intake on blood pressure levels, Journal of the American Society of Hypertension, 8 (2014), pp. 232 – 238.

- [197] V. L. ROGER, A. S. GO, D. M. LLOYD-JONES, R. J. ADAMS, J. D. BERRY, T. M. BROWN, M. R. CARNETHON, S. DAI, G. DE SIMONE, E. S. FORD, ET AL., *Heart disease and stroke statistics—2011 update*, Circulation, 123 (2011), pp. e18–e209.
- [198] I. SABOLIĆ, A. R. ASIF, W. E. BUDACH, C. WANKE, A. BAHN, AND G. BURCKHARDT, *Gender differences in kidney function*, Pflügers Archiv - European Journal of Physiology, 455 (2007), p. 397.
- [199] I. SABOLIĆ, I. VRHOVAC, D. B. EROR, M. GERASIMOVA, M. ROSE, D. BRELJAK, M. LJUBOJEVIĆ, H. BRZICA, A. SEBASTIANI, S. C. THAL, ET AL., *Expression of na^{+} - d -glucose cotransporter *splt2* in rodents is kidney-specific and exhibits sex and species differences*, American Journal of Physiology-Cell Physiology, 302 (2012), pp. C1174–C1188.
- [200] D. SAENZ-CAMPOS, M. BAYES, E. MASANA, S. MARTIN, M. BARBANOJ, AND F. JANE, *Sex-related pharmacokinetic and pharmacodynamic variations of lisinopril.*, Methods and findings in experimental and clinical pharmacology, 18 (1996), pp. 533–538.
- [201] K. SANDBERG AND H. JI, *Sex differences in primary hypertension*, Biology of Sex Differences, 3 (2012), p. 7.
- [202] S. SANGSREE, V. BROVKOVYCH, R. D. MINSHALL, AND R. A. SKIDGEL, *Kininase *i*-type carboxypeptidases enhance nitric oxide production in endothelial cells by generating bradykinin *b1* receptor agonists*, American Journal of Physiology-Heart and Circulatory Physiology, 284 (2003), pp. H1959–H1968.
- [203] J. C. SARTORI-VALINOTTI, R. ILIESCU, L. A. FORTEPIANI, L. L. YANES, AND J. F. RECKELHOFF, *Sex differences in oxidative stress and the impact on blood pressure control and cardiovascular disease*, Clinical and experimental pharmacology and physiology, 34 (2007), pp. 938–945.
- [204] E. SAUNDERS, G. CABLE, AND J. NEUTEL, *Predictors of blood pressure response to angiotensin receptor blocker/diuretic combination therapy: a secondary analysis of the irbesartan/hydrochlorothiazide blood pressure reductions in diverse patient populations (inclusive) study*, The Journal of Clinical Hypertension, 10 (2008), pp. 27–33.
- [205] H. SCHUNKERT, A. J. DANSER, H.-W. HENSE, F. H. DERKX, S. KURZINGER, AND G. A. RIEGGER, *Effects of estrogen replacement therapy on the renin-angiotensin system in postmenopausal women*, Circulation, 95 (1997), pp. 39–45.

- [206] G. J. SCHWARTZ AND M. B. BURG, *Mineralocorticoid effects on cation transport by cortical collecting tubules in vitro*, American Journal of Physiology-Renal Physiology, 235 (1978), pp. F576–F585. PMID: 736142.
- [207] I. SGOURALIS, R. G. EVANS, B. S. GARDINER, J. A. SMITH, B. C. FRY, AND A. T. LAYTON, *Renal hemodynamics, function, and oxygenation during cardiac surgery performed on cardiopulmonary bypass: a modeling study*, Physiological reports, 3 (2015), p. e12260.
- [208] I. SGOURALIS AND A. T. LAYTON, *Autoregulation and conduction of vasomotor responses in a mathematical model of the rat afferent arteriole*, American Journal of Physiology-Renal Physiology, 303 (2012), pp. F229–F239.
- [209] ———, *Theoretical assessment of renal autoregulatory mechanisms*, American Journal of Physiology-Renal Physiology, 306 (2014), pp. F1357–F1371.
- [210] M. M. SILVA-ANTONIALI, R. C. TOSTES, L. FERNANDES, D. R. FIORCHADI, E. H. AKAMINE, M. H. C. CARVALHO, Z. B. FORTES, AND D. NIGRO, *A lower ratio of at1/at2 receptors of angiotensin ii is found in female than in male spontaneously hypertensive rats*, Cardiovascular Research, 62 (2004), pp. 587–593.
- [211] M. A. SPARKS, S. D. CROWLEY, S. B. GURLEY, M. MIROTSOU, AND T. M. COFFMAN, *Classical Renin-Angiotensin System in Kidney Physiology*, John Wiley & Sons, Inc., 2011.
- [212] B. STANTON, L. PAN, H. DEETJEN, V. GUCKIAN, AND G. GIEBISCH, *Independent effects of aldosterone and potassium on induction of potassium adaptation in rat kidney.*, The Journal of Clinical Investigation, 79 (1987), pp. 198–206.
- [213] F. STEINHÄUSLIN, A. MUNAFO, T. BUCLIN, A. MACCIOCCHI, AND J. BIOLLAZ, *Renal effects of nimesulide in furosemide-treated subjects*, Drugs, 46 (1993), pp. 257–262.
- [214] N. STURROCK AND A. STRUTHERS, *Non-steroidal anti-inflammatory drugs and angiotensin converting enzyme inhibitors: a commonly prescribed combination with variable effects on renal function.*, British journal of clinical pharmacology, 35 (1993), pp. 343–348.
- [215] J. C. SULLIVAN, *Sex and the renin-angiotensin system: inequality between the sexes in response to ras stimulation and inhibition*, American Journal of Physiology - Regulatory, Integrative and Comparative Physiology, 294 (2008), pp. R1220–R1226.

- [216] H. SUMINO, S. ICHIKAWA, Y. MIYA, T. SAKAMAKI, AND M. KURABAYASHI, *Angiotensin ii plays an important role in maintaining blood pressure in postmenopausal women receiving hormone replacement therapy**, American Journal of Hypertension, 18 (2005), p. 1340.
- [217] K. SWÄRD, F. VALSSON, J. SELLGREN, AND S.-E. RICKSTEN, *Differential effects of human atrial natriuretic peptide and furosemide on glomerular filtration rate and renal oxygen consumption in humans*, Intensive care medicine, 31 (2005), pp. 79–85.
- [218] S. TADDEI AND L. BORTOLOTTI, *Unraveling the pivotal role of bradykinin in ace inhibitor activity*, American Journal of Cardiovascular Drugs, 16 (2016), pp. 309–321.
- [219] N. TAKAHASHI, J. R. HAGAMAN, H.-S. KIM, AND O. SMITHIES, *Minireview: Computer Simulations of Blood Pressure Regulation by the Renin-Angiotensin System*, Endocrinology, 144 (2003), pp. 2184–2190.
- [220] K. TAKAICHI, F. TAKEMOTO, Y. UBARA, AND Y. MORI, *Analysis of factors causing hyperkalemia*, Internal medicine, 46 (2007), pp. 823–829.
- [221] M. C. THOMAS, *Diuretics, ace inhibitors and nsaid—the triple whammy.*, The Medical Journal of Australia, 172 (2000), pp. 184–185.
- [222] S. R. THOMAS, P. BACONNIER, J. FONTECAVE, J.-P. FRANÇOISE, F. GUILLAUD, P. HANNAERT, A. HERNÁNDEZ, V. LE ROLLE, P. MAZIÈRE, F. TAHI, AND R. J. WHITE, *Saphir: a physiome core model of body fluid homeostasis and blood pressure regulation*, Philosophical Transactions of the Royal Society of London A: Mathematical, Physical and Engineering Sciences, 366 (2008), pp. 3175–3197.
- [223] S. R. THOMAS, A. T. LAYTON, H. E. LAYTON, AND L. C. MOORE, *Kidney modeling: Status and perspectives*, Proceedings of the IEEE, 94 (2006), pp. 740–752.
- [224] J. THOMPSON AND R. A. KHALIL, *Gender differences in the regulation of vascular tone*, Clin. Exp. Pharmacol. Physiol., 30 (2003), pp. 1–15.
- [225] S. C. THOMSON, V. VALLON, AND R. C. BLANTZ, *Resetting protects efficiency of tubuloglomerular feedback*, Kidney International, 54 (1998), pp. S65–S70.
- [226] R. L. THUNHORST AND A. JOHNSON, *Renin-angiotensin, arterial blood pressure, and salt appetite in rats*, American Journal of Physiology-Regulatory, Integrative and Comparative Physiology, 266 (1994), pp. R458–R465.

- [227] C. TOUSSAINT, A. MASSELINK, A. GENTGES, G. WAMBACH, AND G. BÖNNER, *Interference of different ace-inhibitors with the diuretic action of furosemide and hydrochlorothiazide*, *Klinische Wochenschrift*, 67 (1989), pp. 1138–1146.
- [228] T. R. TRAYNOR, A. SMART, J. P. BRIGGS, AND J. SCHNERMANN, *Inhibition of macula densa-stimulated renin secretion by pharmacological blockade of cyclooxygenase-2*, *American Journal of Physiology-Renal Physiology*, 277 (1999), pp. F706–F710.
- [229] ———, *Inhibition of macula densa-stimulated renin secretion by pharmacological blockade of cyclooxygenase-2*, *American Journal of Physiology-Renal Physiology*, 277 (1999), pp. F706–F710.
- [230] T. TSUTAMOTO, A. WADA, K. MAEDA, N. MABUCHI, M. HAYASHI, T. TSUTSUI, M. OHNISHI, M. SAWAKI, M. FUJII, T. MATSUMOTO, ET AL., *Angiotensin ii type 1 receptor antagonist decreases plasma levels of tumor necrosis factor alpha, interleukin-6 and soluble adhesion molecules in patients with chronic heart failure*, *Journal of the American College of Cardiology*, 35 (2000), pp. 714–721.
- [231] F. TURNBULL, M. WOODWARD, B. NEAL, F. BARZI, T. NINOMIYA, J. CHALMERS, V. PERKOVIC, N. LI, S. MACMAHON, AND B. P. L. T. T. COLLABORATION, *Do men and women respond differently to blood pressure-lowering treatment? results of prospectively designed overviews of randomized trials*, *European heart journal*, 29 (2008), pp. 2669–2680.
- [232] M. URSINO AND E. MAGOSSO, *Acute cardiovascular response to isocapnic hypoxia. i. a mathematical model*, *American Journal of Physiology-Heart and Circulatory Physiology*, 279 (2000), pp. H149–H165. PMID: 10899052.
- [233] D. VANDIJCK, S. OEYEN, J. DECRUYENAERE, L. ANNEMANS, AND E. HOSTE, *Acute kidney injury, length of stay, and costs in patients hospitalized in the intensive care unit*, *Acta Clinica Belgica*, 62 (2007), pp. 341–345.
- [234] L. C. VEIRAS, A. C. GIRARDI, J. CURRY, L. PEI, D. L. RALPH, A. TRAN, R. C. CASTELO-BRANCO, N. PASTOR-SOLER, C. T. ARRANZ, A. YU, ET AL., *Sexual dimorphic pattern of renal transporters and electrolyte homeostasis*, *J Am Soc Nephrol*, 28 (2017), pp. 3504–17.
- [235] L. C. VEIRAS, J. HAN, D. L. RALPH, AND A. A. McDONOUGH, *Potassium supplementation prevents sodium chloride cotransporter stimulation during angiotensin II hypertension*, *Hypertension*, 68 (2016), pp. 904–912.

- [236] L. WANG, X. WANG, H. Y. QU, S. JIANG, J. ZHANG, L. FU, J. BUGGS, B. PANG, J. WEI, AND R. LIU, *Role of kidneys in sex differences in angiotensin ii-induced hypertension novelty and significance*, *Hypertension*, 70 (2017), pp. 1219–1227.
- [237] W. WANG, *Regulation of renal K transport by dietary K intake*, *Annual Review of Physiology*, 66 (2004), pp. 547–569. PMID: 14977413.
- [238] Y. WEI, B. ZAVILOWITZ, L. M. SATLIN, AND W.-H. WANG, *Angiotensin II inhibits the ROMK-like small conductance K channel in renal cortical collecting duct during dietary potassium restriction*, *Journal of Biological Chemistry*, 282 (2007), pp. 6455–6462.
- [239] M. WIEDERHOLT, W. SCHOORMANS, F. FISCHER, AND C. BEHN, *Mechanism of action of aldosterone on potassium transfer in the rat kidney*, *Pflügers Archiv*, 345 (1973), pp. 159–178.
- [240] N. WIINBERG, A. HØEGHOLM, H. R. CHRISTENSEN, L. E. BANG, K. L. MIKKELSEN, P. E. NIELSEN, T. L. SVENDSEN, J. P. KAMPMANN, N. H. MADSEN, AND M. W. BENTZON, *24-h ambulatory blood pressure in 352 normal danish subjects, related to age and gender*, *American journal of hypertension*, 8 (1995), pp. 978–986.
- [241] L. L. YANES, D. G. ROMERO, J. W. ILES, R. ILIESCU, C. GOMEZ-SANCHEZ, AND J. F. RECKELHOFF, *Sexual dimorphism in the renin-angiotensin system in aging spontaneously hypertensive rats*, *American Journal of Physiology - Regulatory, Integrative and Comparative Physiology*, 291 (2006), pp. R383–R390.
- [242] Q. YANG, T. LIU, E. V. KUKLINA, W. D. FLANDERS, Y. HONG, C. GILLESPIE, M.-H. CHANG, M. GWINN, N. DOWLING, M. J. KHOURY, AND F. B. HU, *Sodium and Potassium Intake and Mortality Among US Adults: Prospective Data From the Third National Health and Nutrition Examination Survey*, *Archives of Internal Medicine*, 171 (2011), pp. 1183–1191.
- [243] M. A. ZIMMERMAN AND J. C. SULLIVAN, *Hypertension: What's sex got to do with it?*, *Physiology*, 28 (2013), pp. 234–244.

Biography

Jessica Leete earned her bachelors of science at Brigham Young University in 2015, where she was part of the inaugural cohort of the applied and computational math emphasis. There she was awarded the Abrelia C.S. Hinckley scholarship, and the Lloyd Redd scholarship and participated in undergraduate research with Dr. John Dallon. Jessica matriculated at Duke University in the Graduate Program in Computation Biology & Bioinformatics in Fall 2015 and has since been advised by Dr. Anita T. Layton. During this time, she earned an APS abstract travel award at the 2018 APS Cardiovascular, Renal and Metabolic Diseases: Sex-Specific Implications for Physiology Conference.

Jessica has authored or co-authored four manuscripts, including the three that form the core of this dissertation: *Modeling sex differences in the renin angiotensin system and the efficacy of antihypertensive therapies* [136], *Sex-specific long-term blood pressure regulation: modeling and analysis* [137], and *Determining risk factors for triple whammy acute kidney injury: sex-specific modeling and analysis* [138].